

**HUMIC ACID REMOVAL FROM AQUEOUS SOLUTION BY A
HYBRID ELECTRODIALYSIS/ION-EXCHANGE**

CHEN GENTU

(B.Eng., Zhejiang Univ.)

**A THESIS SUBMITTED
FOR THE DEGREE OF MASTER OF ENGINEERING
DEPARTMENT OF CHEMICAL AND BIOMOLECULAR
ENGINEERING
NATIONAL UNIVERSITY OF SINGAPORE**

2004

ACKNOWLEDGEMENTS

I am deeply indebted to my supervisor, Associate Professor Nikolai. M. Kocherginsky for his invaluable supervision, continuous and constructive advice, careful reviews of the thesis through out my study. His strong and thorough grounding in physical chemistry, electrochemistry, membrane science and technology has benefited me greatly in the study and will be of great help in my future academic career.

I also wish to thank a number of people who have contributed either directly or indirectly to this study. Grateful acknowledgment is made to Dr. Yuri Kostetski and Mdm Khoh Leng Khim, Sandy for their kind help and continuous support. In addition, I would like to thank all my friends and labmates for making the study full of fun and happiness.

Most importantly, I am grateful to my wife Lu Ya for her love, support and understanding. Without her, the thesis would have never been written.

Finally, the financial support from National University of Singapore is very much appreciated.

TABLE OF CONTENTS

TITLE PAGE	
ACKNOWLEDGEMENTS	ii
TABLE OF CONTENTS	iii
SUMMARY	vii
NOMENCLATURE	ix
LIST OF FIGURES	xiii
LIST OF TABLES	xviii

CHAPTER 1 INTRODUCTION	1
1.1 Background	1
1.2 Research objectives and scope	8
 CHAPTER 2 LITERATURE REVIEW	 10
2.1 Humic acid	10
2.1.1 Properties of HA	10
2.1.2 Methods for HA removal	13
2.2 Theoretical background	16
2.2.1 Stability of colloidal systems	16
2.2.2 Double layer	19

2.2.3 Zeta potential	20
2.2.4 Electrokinetic effect	22
2.2.5 Ion exchange resin	24
2.2.6 Electrodialysis	26
2.2.7 Electrodeionization	29
 CHAPTER 3 METHODOLOGY	 32
3.1 Apparatus	32
3.2 Materials	33
3.3 Instruments and experimental procedures	38
 CHAPTER 4 DIFFERENT COMBINATIONS OF ION EXCHANGE	
MEMBRANE AND ION EXCHANGE RESIN	42
4.1 Introduction	42
4.2 Results and discussion	43
4.2.1 Resin in the beaker	44
4.2.2 Only membranes	46
4.2.3 MR3 resin and membranes	52
4.2.4 A550 resin and membranes	55
4.2.5 Marathon C resin and membranes	58
4.2.6 Summary and discussion for different combinations of membranes and resin	60
4.3 Conclusions	69

CHAPTER 5	EFFECT OF EXPERIMENTAL PARAMETERS ON HA	
REMOVAL IN SINGLE-PASS OPERATION MODE FOR A COMBINATION OF	AM+MR3+CM	72
5.1	Introduction	72
5.2	Results and discussion	73
5.2.1	pH change in HA and electrolyte solutions during the experiment	73
5.2.2	Current change of circuit during the experiment	74
5.2.3	Different parameters effect	74
5.2.3.1	Voltage effect	76
5.2.3.2	Electrolyte concentration effect	78
5.2.3.3	Flow rate effect	80
5.2.3.4	HA concentration effect	81
5.2.3.5	pH effect	83
5.2.3.6	Ionic strength effect	84
5.2.3.7	CuSO ₄ concentration effect	86
5.3	Conclusions	88

CHAPTER 6	EFFECT OF EXPERIMENTAL PARAMETERS ON HA	
REMOVAL IN A RECYCLING OPERATION MODE FOR A COMBINATION	OF AM+MR3+CM	90
6.1	Introduction	90
6.2	Results and discussion	90
6.2.1	HA particle size change during the experiment	90

6.2.2 pH change in HA and electrolyte solutions during the experiment	91
6.2.3 Current change in the circuit during the experiment	92
6.2.4 Different parameters effect	92
6.2.4.1 Voltage effect	94
6.2.4.2 Electrolyte concentration effect	97
6.2.4.3 Flow rate effect	98
6.2.4.4 HA concentration effect	99
6.2.4.5 pH effect	100
6.2.4.6 Ionic strength effect	101
6.2.4.7 Copper concentration effect	101
6.3 Conclusions	103
 CHAPTER 7 SUMMARY AND RECOMMENDATIONS	 104
REFERENCES	107
APPENDIX A	114

SUMMARY

This study describes the applicability of hybrid electrodialysis/ion exchange in removing humic acid (HA) from aqueous solutions. Experiments for different combinations of ion exchange membrane and ion exchange resin were carried out to investigate the mechanism of the process. It was found that the combination of AM+MR3+CM is the most efficient considering the effect of electrical field. In the absence of voltage, hybrid electrodialysis/ion exchange can remove HA particles due to electrostatic attraction between HA particles and the surface of membranes and resins. The Anion exchange resin and an anion exchange membrane can remove HA more efficiently than a cation exchange resin and a cation exchange membrane. In the presence of an applied voltage, a much stronger local electric field is induced due to the polarized resin. Initially the HA particles move under the applied electric field due to electrophoresis; But when the HA particles come close to the gap between resins, the stronger local electric field makes the HA particles deposit on the surface of resins. Secondly, the polarized HA particles form condensed sediments on the deposited HA particles on the surface of resin due to dipole-dipole interactions. Thus the electric field greatly enhances the HA deposition on the surface of resins. When the electric field is switched off, the electric forces and the dipole-dipole interactions disappear. HA particles are carried away when a fluid flows through the central chamber. The amount of released HA depends on the properties of resins, membranes and the feed solution.

Recycling operation mode and single-pass operation mode were used to study the effect of different parameters on HA removal, i.e. the voltage, the electrolyte concentration, the

flow rate of HA solution, the HA concentration, the pH of HA solution, the ionic strength of HA solution and the Cu^{2+} concentration in HA solution. Higher voltage leads to a higher HA removal. Lower salt concentration and lower HA concentration are desirable for HA removal. A suitable electrolyte concentration and flow rate are required in operation. In the recycling operation mode, alkaline pH helps to remove HA the most efficiently. In the single-pass operation mode, the neutral pH allows to remove HA the most efficiently. All the results have been physically explained. Also, a mathematical way was introduced to characterize the process.

NOMENCLATURE

Abbreviations

AM	Anion exchange membrane
CM	Cation exchange membrane
COD	Chemical oxygen demand
DBP	Disinfection by-product
DI	Deionized
DOC	Dissolved organic carbon
ED	Electrodialysis
EDI	Electrodeionization
FA	Fulvic acid
HA	Humic acid
HS	Humic substances
IHP	Inner Helmholtz plane
NF	Nano-filtration
NOM	Natural organic matter
OHP	Outer Helmholtz plane
RO	Reverse osmosis
PAX	Prepolymerized alum
SEM	Scanning electron microscopy
TOC	Total organic carbon
UF	Ultrafiltration

UPS Uniform particle size

UV Ultraviolet

Symbols

C Concentration

ΔC_t Change in concentration of HuA between times t and $t + \Delta t$

D Diffusion coefficient

e Electron charge

E Electric field

E Energy Consumption

F Faraday constant

i Current as function of time

I Electric current

i_{lim} Limiting current density

k Mass transport coefficient

J_D Flux of ions by diffusion

J_e Flux of ions by electrotransport

k_b Boltzmann constant

L Length of central chamber

N_A Avogadro's number

n Number of moles transported

q Charge

Q_f Flow rate

r	Distance from surface
R	Universal gas constant
T	Time
Δt	Sampling time
T	Temperature
U_p	Particle electrophoretic mobility
v_t	Volume of solution at time t
V	Potential difference across condensor
V_f	Volume of feed solution
V_0	Potential drop across membranes
V_p	Particle velocity
W	Electrical energy used/mg of HA removed
x	Distance from charged surface
z_i	Electrochemical valence
Z	Distance from the inlet of central chamber

Greek Symbols

δ	Distance of the Stern plane from the surface of particle
δ	Thickness of the boundary layer
ϵ	Dielectric constant of the medium
η	Removal efficiency
ζ	Zeta potential
ξ	Current utilization

λ	Filter coefficient
κ^{-1}	Diffused double layer thickness
τ	Total time for which voltage was applied
ϕ_{Don}	Donnan potential
ψ_0	Potential at the surface of the particle
ψ	Potential at a distance from the surface of the particle

LIST OF FIGURES

Fig. 1.1	Schematic diagram of the electrodialysis process	2
Fig. 1.2	Water desalination costs as a function of the feed solution concentration for 1. distillation, 2. ion exchange, 3. electrodialysis, and 4. reverse osmosis	3
Fig. 1.3	Electrodeionization process unit	6
Fig. 2.1	A hypothetical HA molecule	10
Fig. 2.2	The interaction energy between two colloidal particles as a function of their distance of separation, when the conditions favor stability of the colloid	18
Fig. 2.3	The interaction energy between two colloidal particles as a function of their distance of separation, when the conditions favor coagulation of the colloid	18
Fig. 2.4	A schematic representation of the distribution of charge near a charged particle based on the Stern model.	20
Fig. 2.5	A schematic representation of the variation of potential with distance from a charged particle based on the Stern model.	21
Fig. 2.6	Mass transport in the electrodialysis	27
Fig. 2.7	Diagram of the nickel front. This figure depicts the sections of the beds in the Ni^{2+} , H^+ and $\text{Ni}^{2+}/\text{H}^+$ forms. The bed is regenerated by the anolyte, while nickel is concentrated in the cathode compartment. The nickel solution is fed top-down.	30
Fig. 3.1	Schematic representation of the experimental set-up in a recycling operation mode	33

Fig. 3.2	Schematic representation of the experimental set-up in a single-pass operation mode	33
Fig. 3.3	Schematic representation of the IONICS CR-67 membrane	34
Fig. 3.4	Schematic representation of the IONICS AR-103 membrane	34
Fig. 4.1	HA concentration ratio as a function of time for the resin in the beaker	45
Fig. 4.2	HA concentration ratio as a function of time for only membrane without resin	48
Fig. 4.3	HA removal due to electrosorption as a function of time for only membranes without resin	51
Fig. 4.4a	SEM images showing the morphology of anion exchange membrane surface with HA deposition	52
Fig. 4.4b	Photo of anion exchange membrane before and after experiments and photo of a fresh cation exchange membrane	52
Fig. 4.5	HA concentration ratio as a function of time for combinations of MR3 resin and membranes	54
Fig. 4.6	HA removal due to electrosorption as a function of time for combination of MR3 resin and membranes	54
Fig. 4.7	HA concentration ratio as a function of time for a combination of A550 resin and membranes	56
Fig. 4.8	HA removal due to electrosorption as a function of time for a combination of A550 resin and membranes	57
Fig. 4.9	HA concentration ratio as a function of time for a combination of Marathon C resin and membranes	59

Fig. 4.10	HA removal due to electrosorption as a function of time for a combination of Marathon C resin and membranes	59
Fig. 4.11	Distribution of lines of an electric field's strength in the gap between two spherical resin gels in a less conducting solution	66
Fig. 4.12a	HA removal efficiency comparison for two system, one is hybrid electrodialysis/ion exchange, the other is electrodiaysis plus ion exchange (MR3 resin)	68
Fig. 4.12b	HA removal efficiency comparison for two system, one is hybrid electrodialysis/ion exchange, the other is electrodiaysis plus ion exchange (A550 resin)	68
Fig. 4.12c	HA removal efficiency comparison for two system, one is hybrid electrodialysis/ion exchange, the other is electrodiaysis plus ion exchange (Marathon C resin)	69
Fig. 5.1	pH of HA solution and pH of electrolyte solution as a function of time during experiment in single-pass operation mode	73
Fig. 5.2	Current of circuit as a function of time during experiment in a single-pass operation mode	74
Fig. 5.3	HA concentration ratio as a function of time for different voltage in a single-pass operation mode	77
Fig. 5.4	Filter coefficient as a function of voltage for different voltage in a single-pass operation mode	78
Fig. 5.5	HA concentration ratio as a function of time for different electrolyte concentration in a single-pass operation mode	79
Fig. 5.6	Filter coefficient as a function of electrolyte concentration in a single-pass operation mode	79

Fig. 5.7	HA concentration ratio as a function of time for different flow rates in a single-pass operation mode	80
Fig. 5.80	Filter coefficient as a function of flow rate in a single-pass operation mode	81
Fig. 5.9	HA concentration ratio as a function of time for different initial HA concentration in single-pass operation mode	82
Fig. 5.10	Filter coefficient as a function of HA concentration in a single-pass operation mode	82
Fig. 5.11	HA concentration ratio as a function of time for different pH of HA solution in single-pass operation mode	83
Fig. 5.12	Filter coefficient as a function of pH of HA solution in a single-pass operation mode	84
Fig. 5.13	HA concentration ratio as a function of time for different ionic strengths of HA solution in a single-pass operation mode	85
Fig. 5.14	Filter coefficient as a function of NaCl concentration in HA solution in a single-pass operation mode	85
Fig. 5.15	HA concentration ratio as a function of time for different copper concentrations in a single-pass operation mode	87
Fig. 5.16	Filter coefficient as a function of CuSO ₄ concentration in HA solution in a single-pass operation mode	88
Fig. 6.1	Effective particle diameter of HA at different time in a recycling operation mode. At 80 min, the voltage was switched off	91
Fig. 6.2	pH of HA solution and pH of Na ₂ SO ₄ solution as a function of time during experiment in a recycling operation mode	92

Fig. 6.3	HA concentration ratio as a function of time for different voltage in a recycling operation mode	95
Fig. 6.4	HA removal after 120min as a function of voltage applied in the recycling operation mode	95
Fig. 6.5	Total electrical energy consumed per mg of HA removed at different values of the applied voltage	96
Fig. 6.6	Variation of the current with the applied voltage across the module. The time interval between the 5 V step change was 2 min	97
Fig. 6.7	HA concentration ratio as a function of time for different electrolyte concentration in a recycling operation mode	97
Fig. 6.8	Current as a function of Na_2SO_4 concentration in the recycling operation mode with 40 V	98
Fig. 6.9	HA concentration ratio as a function of time for different flow rate in recycling operation mode	99
Fig. 6.10	HA concentration ratio as a function of time for different initial HA concentration in a recycling operation mode	100
Fig. 6.11	Total removed HA as a function of initial HA concentration in a recycling operation mode after 120 min	100
Fig. 6.12	HA concentration ratio as a function of time for different pH solution in a recycling operation mode	101
Fig. 6.13	HA concentration ratio as a function of time for different NaCl concentration in the HA suspension in recycling operation mode	102
Fig. 6.14	HA concentration ratio as a function of time for different CuSO_4 concentration in the HA suspension in recycling operation mode	102

LIST OF TABLES

Table 2-1	Composition of the resins	24
Table 3-1	Properties of ion exchange membranes	35
Table 3-2	Description of the resin	36
Table 3-3	Physical and chemical properties of the three resins	36
Table 3-4	Recommended operating conditions for the three resins	36
Table 4-1	Different combinations of ion exchange membrane and resin	44
Table 4-2	Summary for different combinations of membranes and resins	62
Table 4-3	HA removal efficiency comparison for the two systems (one is hybrid electrodialysis/ion exchange, the other is electrodialysis plus ion exchange process)	70
Table 5-1	Different experimental conditions for HA removal in a single-pass operation mode	75
Table 6-1	Different experimental conditions for HA removal in a recycling operation mode	93

Chapter 1

Introduction

1.1 Background

Electrodialysis is an electrochemical separation process, in which an electrically charged membrane and an electrical potential difference are used to separate ionic species from an aqueous solution and other uncharged components (Ho, Sirkar, 1992). It is widely used today in water desalination and table salt production. Other uses of electrodialysis, especially in the food, drug, and chemical process industries as well as in biotechnology and wastewater treatment, have recently gained a broader interest and it is stimulated by the development of new ion-exchange membranes with a better selectivity, a lower electrical resistance, and improved thermal, chemical, and mechanical properties (Belfort, 1984; Judd, Jefferson, 2003).

The principle of electrodialysis is illustrated in Figure 1.1, which shows a schematic diagram of a typical electrodialysis cell arrangement consisting of a series of anion and cation exchange membranes arranged in an alternating pattern between an anode and a cathode to form individual cells. A cell consists of a volume with two adjacent membranes. If an ionic solution is pumped through these cells and an electrical potential is established between the anode and cathode, the positively charged cations migrate towards the cathode and the negatively charged anions towards the anode. The cations pass easily through the negatively charged cation exchange membrane, but are retained

by the positively charged anion exchange membrane. Likewise, the negatively charged anions pass through the anion exchange membrane, but are retained by the cation exchange membrane. The overall result is an increase in the ion concentration in alternate compartments, while the other compartments simultaneously become depleted. The depleted solution is generally referred to as the dilute and the concentrated solution as the concentrate.

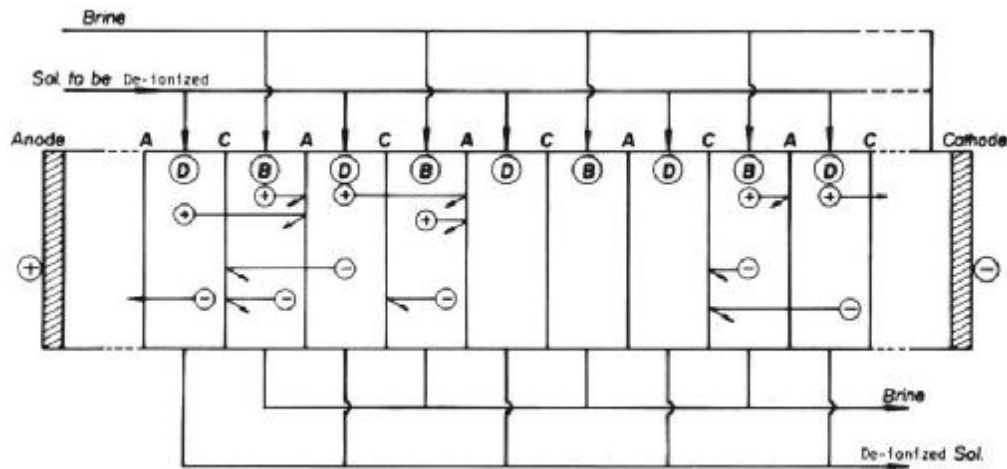


Fig.1.1 Schematic diagram of the electrodialysis process (Ho, Sirkar, 1992)

With the development of electronic, medical and pharmaceutical industries, ultrapure water is increasingly needed in order to obtain a high quality product. There are several processes utilized to desalinate water. Strathmann (1984) compared the costs of desalination by various processes as a function of the feed water salinity, as shown in Figure 1.2. The figure indicates that for very low feed solution salt concentrations, ion exchange is the most economical process. At about 500 ppm, electrodialysis becomes a more economical process. Ion exchange resin has an ion exchange capacity. After ion exchange, the resin should be regenerated with chemicals. Higher feed water salinity

increases the operational cost of an ion exchange resin at a faster rate than others. Furthermore, it generates second polluted wastewater, which is not suitable for sustainable development.

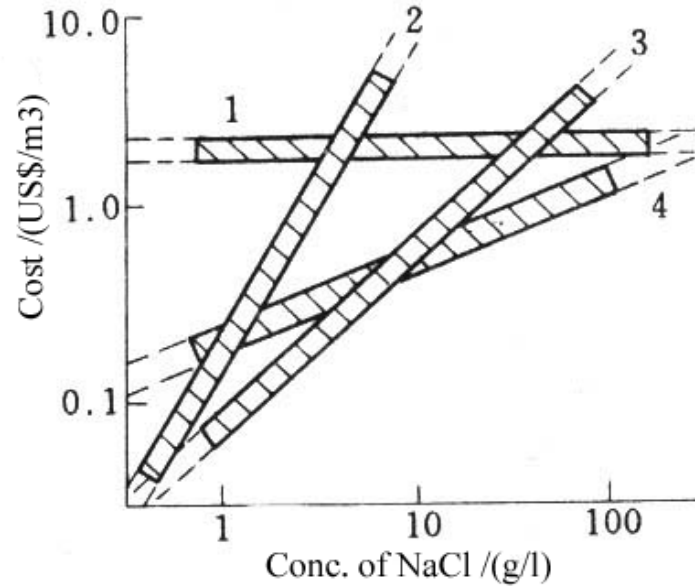


Fig.1.2 Water desalination costs as a function of the feed solution concentration for 1.distillation, 2.ion exchange, 3.electrodialysis, and 4.reverse osmosis (Strathmann, 1984).

The operating cost is proportional to the total energy consumption. Under the assumption that the concentration in the dilute is much lower than that in the feed and brine, the energy consumption can be expressed by Equation 1-1 (Ho, Sirkar, 1992).

$$E = \frac{InbV \log\left(\frac{c_f}{c_d}\right)}{x} \quad (1-1)$$

Here E is the practical energy consumption , I is electric current through the stack, n is number of moles transported, b is the constant, V is the total volume of the dilute

solution, C_f and C_d are the salt concentrations in the feed solution and dilute solution respectively, and ζ is current utilization.

Limiting current density can be described by Equation 1-2.

$$i_{\text{lim}} = \frac{c_d z_+ F k}{t_+ - t'_+} \quad (1-2)$$

Here i_{lim} is the limiting current density, c_d is the bulk solution concentration in the cell with the depleted solution, z_+ is the electrochemical valence of the ions in the solution (cations), F is the Faraday's constant, k is the mass transport coefficient, taking into account the influence of the hydrodynamics, flow channel geometry, spacer design, etc., t_+ and t'_+ are the ion transport numbers (cations) in the membrane and the solution, respectively.

According to Eq. 1-2, the limiting current density is proportional to the ion concentration in the dilute and the mass transfer coefficient. The more dilute of the dilute solution is, the lower the limiting current density will be. This can easily lead to concentration polarization and water splitting. And it increases the additional resistance of stack and decreases the current efficiency of ion transport from the dilute compartment to the concentrated compartment. Furthermore, due to the lower conductivity of the dilute solution, the resistance is higher and it decreases the current efficiency. From Eq.1-1, the operational cost increases with the concentration decrease of the feed solution.

In order to improve the performance of electrodialysis, the ion-conducting spacer instead of inert spacers between the ion-exchange membranes was introduced (Kedem, 1975; Kedem, Maoz, 1976; Weida, Dong, 1985; Korngold et al., 1998; Messalem, et al., 1998). Inert spacer is impenetrable for electric and diffusion flows, thus it screens a certain part of the ion exchange membrane surface. Conducting spacer reduces the electrical resistance due to its conductivity, and furthermore, it overcomes the additional resistance caused by water splitting and concentration polarization. Therefore, the power consumption greatly decreases and degree of solution demineralization increases (V.K.Shahi et al., 2001).

An ion exchange resin, like electrolyte solutions, contains mobile ions and is a good ionic conductor (Helfferich, 1995). It can be used to increase the conductivity of the dilute solution and decrease the resistance like a conducting spacer. Furthermore, ion exchange resins can exchange ions of the solution, which enhances mass transport of the ions through membranes. This phenomenon was first introduced at early stage of electrodialysis development by W.R.walters, et al. in 1955. Later a patent describing electrodeionization device and process was awarded to Kollsaman in 1957. The first pilot device for electrodeionization was developed by Permutit Company in the United Kingdom in the late 1950's for the Harwell Atomic Energy Authority, which was described in patent by Kressman, in 1959 and Tye in 1961. It was discussed on a theoretical level by Glueckauf in 1959. Electrodeionization device and systems were first fully commercialized in 1987 by a division of Millipore that is now part of U.S.Filter Corporation. From then on, the practice of electrodeionization has advanced worldwide in ultrapure water production.

The principle of electrodeionization (EDI) is illustrated in Figure 1.3.

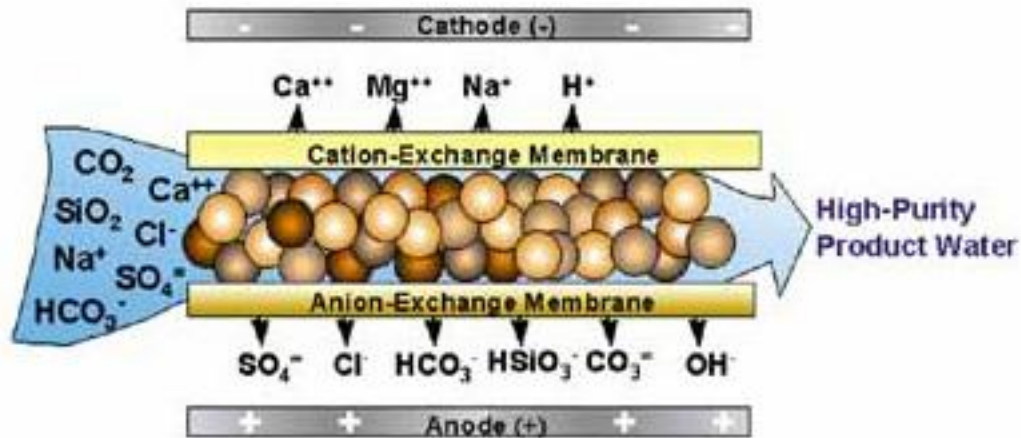


Fig.1.3 Electrodeionization Process Unit

Recent research of electrodeionization focuses on how to improve the performance of deionization. Different forms of ion exchange resins, such as cylindrical rods, spiral rods, braided net and net with grain were investigated by Shaposhnik et al. 2001. Different conducting spacers (Shahi et al., 2001) and ion exchange textile were described (Dejean et al., 1997). Other electroactive media combinations and specific configuration of electrodeionization have been published in patents (Berrocal, Chaveron, 1999, 2000; Dimascio et al., 2003; Sato, Shin, 2003).

Electrodionization(EDI) is also known as continuous deionization(CDI) or continuous electrodeionization(CEDI) or hybrid electrodialysis/ion exchange process. It has earned wide acceptance in various industries. Firstly, it is used to produce potable water and ultra-pure water (Salem et al., 1995; Goffin, J.C.Calay, 2000; Shaposhinik et al., 2002). It

is also used to extract of Zn from Na-containing solution (Grebenyuk et al., 1998), to purify water by removing radioactivity in a Counting Test Facility (Balata et al., 1996), or to remove polluting ions from solution. This method has many advantages comparing to other processes. It can be continuously operated without a special need to regenerate the resin. All the ion exchange resins can be electrochemically regenerated by means of H^+ and OH^- ions, which appear as the result of water splitting at the interfaces of resins and membranes during electrolysis.

However, continuous electrodeionization device must reach high standards of purity such that it does not foul the membrane and resin: it must be free of suspended matter because the beads of resin behave like a filter and there is no backwashing mechanism. Furthermore the stacks cannot be disassembled conveniently which is contrary to ED. The salinity must not be too high as in this procedure 10-20% of the applied current is used to transport ionized salts and the rest of the current serves to split the water. Too high salt concentration will consume higher energy than general desalination processes. In addition, calcium (Ca^{2+}), magnesium (Mg^{2+}) and hydro carbonate (HCO_3^-) ions content have to be as low as possible to prevent scaling because there is risk of precipitation within the anionic membrane. As a result, in a purifying water system, other processes such as reverse osmosis (RO) are often used as a pretreatment (Balata et al., 1996; Wang et al., 2000).

In a nuclear power plant, Goffin and Calay (2000) described the water quality requirement for EDI for reference. It must comply with the following specifications: Pressure: 20-50 psi; conductivity < 20 $\mu S/cm$; Hardness < 0.025 °F; TOC < 0.5 mg/l;

Temperature: 10-35 °C; pH 4-10, Free chlorine<0.1 ppm; CO₂<8 ppm and no suspended matter.

1.2 Research objectives and scope

EDI is used to remove the ions from solution to produce ultra pure water. However, usually the feed solution requires pretreatment in order to remove the fouling organics and suspended matter. In this research, the purpose is completely opposite. It investigates the applicability of this technology in separating and purifying organic particles from the aqueous solution. We suggest the term, hybrid electrodialysis/ion exchange instead of EDI in this thesis due to its different application area.

In this process, ion exchange resins can adsorb organic particles. However, they cannot penetrate through ion exchange membranes and stay in the central chamber. Thus, the central chamber acts like an ion exchange resin column to separate and purify organics. Secondly, as is described below under the electric field, the mass transport of the particles may be enhanced due to some kind of mechanism. Thirdly, under the electric field, the selectivity for organics may be enhanced and may be different from that for the general ion exchange column. Due to above three reasons, the hybrid electrodialysis/ ion exchange could be developed to separate and purify organics that may not be easily separated or purified in conventional method. Unfortunately, in all the references searched up to date, a few researchers are doing the similar research.

In this thesis, we describe humic acid (HA) removal from aqueous solutions by hybrid electrodialysis/ion exchange. This research was initiated by Aatmeeyata(2000). Chapter 2

presents a review of HA properties, separation methods and a theory background of the studied technology. Chapter 3 describes the methodology of the research, including the setup, materials, chemicals and the experimental procedure. Chapter 4 examines the different combinations of membrane and resin to find the best one for HA removal. Chapter 5 and Chapter 6 discuss the effect of different parameters on HA removal in a single-pass operation mode and in a recycling operation mode. The summary and recommendations are addressed in Chapter 7.

Chapter 2

Literature Review

2.1 Humic acid

2.1.1 Properties of HA

(1) Environmental effect

Humic acid is the main component of most humic substances (HS). It is generated when biological matter, especially plants decompose. A typical structure of HA is shown in Figure 2.1 (Livens, 1991). Such a structure has the ability to bind with both hydrophobic and hydrophilic materials. This function, in combination with their colloidal nature, makes HA effective in transporting both organic and inorganic contaminants in the environment.

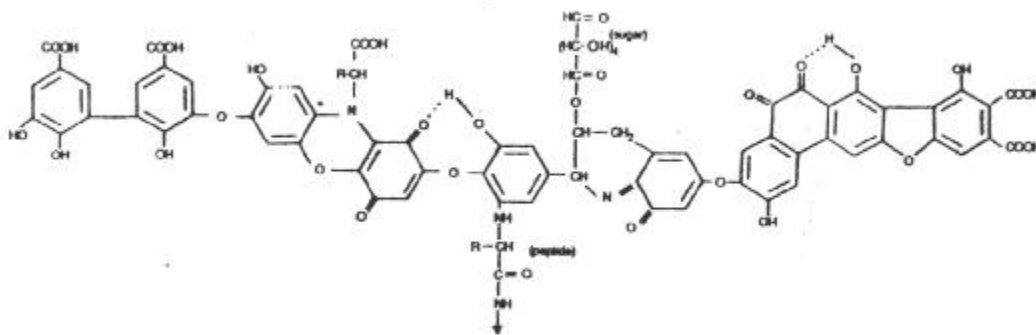


Fig. 2.1 A hypothetical HA molecule (Livens, 1991)

The chelating carboxylic and phenolic functional groups greatly enhance the concentration of heavy metals in surface waters. The concentration of these metals has been found to correlate with the DOC concentration in the form of humic colloidal materials (Nelson et al., 1985). Also, the transport of trace metals and radionuclides in the form of HA has been emphasized in applications such as metal bioavailability and the safety assessment of nuclear waste disposal facilities. Enrichment factors of trace heavy metals in humate sediments were found to be 10^4 to 1 over the supernatant waters. Thus, humic materials are extremely important in the mobilization and concentration of toxic metals and radionuclides in the aqueous environment. They can form soluble complexes that can migrate long distances or precipitate, carrying bound cations with them.

The presence of humic materials can also promote the solubilization of non-polar hydrophobic compounds. This decreases the sorption of materials, such as DDT, DBTC, etc., to soils or sediments (Amirbahman, 1994). The ability of HS to bind such substances affects not only their mobility, but also the rate of chemical degradation, photolysis, volatilization and biological uptake of these organic compounds.

Humic substances can affect water quality adversely in several ways. They not only lead to the aesthetically unappealing yellow-black color in water, but their ability to form complexes with heavy metals and pesticides leads to the bioaccumulation of these chemicals. The Blackfoot disease, a peripheral vascular disease observed in southwestern Taiwan, has been attributed to contaminated drinking water containing higher concentrations of HS in the local well water (Meng and Hung, 1997). More importantly, there is a greater health concern arising from the by-products of disinfecting humic

waters. The reaction of HS with disinfecting chemicals, mainly chlorine, produces trihalomethane, a carcinogenic compound, haloacetic acid, and other halogenated compounds linked to adverse health effects (Singer, 1999).

(2) Colloidal properties

The colloidal state represents a phase that is intermediate between true solutions and suspended particulates. The colloidal range is considered to extend from about 0.001 to 1 μm . Chemical and physical reactions are generally enhanced on colloidal particles. At the same time, the mobility through surface water or ground water is also enhanced. The range of molecular sizes for the majority of HA places them in the colloidal range when they are in aqueous solutions. HA is considered to consist of colloidal, long chain, or three-dimensional cross-linked macromolecules with electrical charges variously distributed on the particles. The presence of charged sites arising from ionized acidic groups results in mutual repulsion and causes considerable expansion of the molecule (Gaffney et al., 1996).

The most important factors controlling the molecular conformations of HA are their concentrations, the pH and the ionic strength of the system. At high sample concentrations, low pH and high electrolyte concentrations, HA exists as rigid, uncharged colloidal particles. At low sample concentrations, high pH and low electrolyte concentrations, HA exists as a flexible linear polyelectrolyte.

2.1.2 Methods for HA removal

(1) Conventional method----coagulation, flocculation and filtration

HA are large molecules that carry a negative charge. This gives them colloidal characteristics and makes them removable by coagulation and subsequent floc-separation. The positively charged coagulant species are adsorbed to sites on the negatively charged HA, leading to charge neutralization and the formation of insoluble complexes.

Eikebrokk (1996) studied the effect of three types of Al coagulants, viz., alum, pre-polymerized alum (PAX 14), and Ca-PAX (Ca:Al = 7-10). A stoichiometric relationship was found between the required coagulant dosage and the concentration of humics in the raw water. Of the three coagulants, PAX 14 and Ca-PAX were more effective than alum. In addition, Ca-PAX was found to be effective over a broader pH range.

O'Melia et al. (1999) studied the effectiveness of four different types of aluminum coagulants in the coagulation and sedimentation of waters containing turbidity and natural organic matter (NOM). It was found that the requirement of the coagulant was related to the total organic carbon concentration in the source water. Frequently, a stoichiometric relationship was found between the two.

Bolto et al. (1999) compared the removal of NOM by conventional and polymer-based processes in bench-scale treatment. His research focused on the performance as a function of the polymer structure and the nature of the NOM. An alum/polymer combination was found to be the most attractive option. The more hydrophobic fractions

of the NOM were more easily removed by the polymer. The performance of cationic polymers improved significantly on increasing their charge density and their molecular weight.

(2) Ion-Exchange

Humic substances can be removed by macro-porous anion exchangers due to the negative charge present on the humic molecules at normal pH values. Several studies have presented results of ion exchange, utilizing laboratory-scale experiments. Anderson and Maier (1979) found that a strong-base resin was able to remove most organic compounds from the Mississippi river water. Macko (1980) found that the resin also removed sulphate and several heavy metals complexed to the humic acid. Jorgensen (1979) performed experiments with a cellulose-based macroporous resin. The resin had a low capacity, but yield a high treatment efficiency due to the good kinetics of the adsorption process. Boening (1980) compared activated carbon with different types of resins for the removal of fulvic acids and commercial humic acids. They found activated carbon to be a less suitable adsorbent. The high molecular weight humic compounds were unable to penetrate through the micro-pores. Kolle (1979) performed experiments at the Hannover water plant on the resin, Lewatit MP 500A, and found that the proper regenerant was a 10% NaCl-1% NaOH solution. There were reports that the treatment efficiency of a plant decreased by 10% in 2 years. The reasons were fouling and a weight loss of the resin due to mechanical erosion during regeneration (Brattebo et al., 1987).

(3) Membrane

Humic acids are large molecules and they can be retained by the membrane which has a smaller pore size. Membrane filtration and reverse osmosis (RO) for drinking water treatment have been used for nearly thirty years, but its popularity for the treatment of surface waters has gained importance in the late 1980's.

Studies by Childress and Elimelech (1996) with RO and nanofiltration (NF) membranes showed that HS absorbs readily onto the membrane surface and markedly influences the surface charge. Kabsch-Korbutowicz and Winnicki (1996) found that ultrafiltration (UF) membranes of sulfonated poly-sulfone can be highly effective in the removal of HS from water. In addition, the membranes allowed an effective removal (of up to about 95%) of iron ions from solutions containing HS by retention of their metal organic complexes or co-precipitating metal hydroxides. Jucker and Clark (1994) characterized the interaction between humic and fulvic acids and UF membranes by direct adsorption measurements. According to them, low pH and, in some cases, high calcium concentrations increased the adsorption of HS on the membranes. Ruohomaki et al. (1998) investigated the removal of HS from different waters with UF and NF using salts and retention aids as pre-treatment methods. In both UF and NF of moorland waters, retention was good without any pre-treatment, but a small positive effect was obtained with AlCl_3 , NaCl , KCl and FeCl_3 . Retention aids, mostly powdered electrolytes, did not improve the retention, but the cationic ones led to slight improvements. In NF, higher pressures improved the retention. In every case, the pH was found to have a significant influence, because at low pH, the structure of HA is more compact and thus the fouling is reduced.

Thorten (1999) found that membranes are well suited to treat the typically soft surface waters in cold climates, which have high concentrations of NOM. However the fouling problem posed a challenge for practical applications.

Irreversible fouling curtails the economic effectiveness of membrane technology for water treatment and color removal. Specialized cleaning techniques are required to remove the absorbed foulants and increase the efficiency of UF (Jucker and Clark, 1994). Several fouling studies on humic acid solutions have been carried out with different pressures and vacuum filtration (Nystrom et al., 1996), and with membrane filtration (Nystrom et al., 1995). It was found that the effect of HS in pressure and vacuum filtration differs clearly from that in membrane filtration and is characterized with much higher fouling.

Odegaard et al. (1999) wrote about 63 membrane filtration plants currently in operation. The plants were based on spiral- wound modules and mainly contained UF and NF, using cellulose acetate membranes. The removal efficiency for color was near 85 ± 15 %, and for TOC, it was 60-70%. The cost was higher compared to plants based on conventional techniques, but their operational reliability was also higher.

2.2 Theoretical background

2.2.1 Stability of colloidal systems

The stability of colloidal systems is an important parameter in the area of colloid science. A thermodynamically stable colloidal system means that the system is in a state of

equilibrium, corresponding to the specified constraints on the system (e.g. Gibbs free energy at constant T and P) Most colloidal systems are metastable or unstable with respect to the separate bulk phases, with the exception of lyophilic sols, gels and xerogels of macromolecules.

A kinetically stable colloid, however, refers to particles which do not aggregate at a significant rate. Aggregation is the cohesion of two or more particles, forming an aggregate, in which individual particles retain their identity, but lose their kinetic independence. When a colloid is unstable, (i.e., the rate of aggregation is not negligible) the formation of aggregates is called coagulation or flocculation.

The rate of aggregations is generally determined by the frequency of collisions and the probability of cohesion during collisions. The attractive forces that make cohesion and aggregation possible are usually Van der Waals forces. These interactions are a combination of the dispersion interactions, which depends on r^{-6} , and the electron overlap repulsion, which varies as r^{-12} . Thus, Van der Waals interaction can be represented by $-Ar^{-6} + Br^{-12}$, where A and B are constants of the dispersed phase.

There are also repulsion forces and some colloidal systems are stable as a result. The electrostatic forces resulting when electrical double layers between two particles overlap will tend to counter the attraction from Van der Waals forces. When the two dispersed-phase species approach, they experience repulsive and attractive forces,, such as electrostatic repulsion and Van der Waals attraction. The Gibbs energy of interaction may be thought of as the difference between Gibbs energies of the system at a specified separation distance and at infinite separation. A colloidal system will be stable, if the

Gibbs free energy of interaction is close to zero. Figures 2.2 and Figure 2.3 show the potential energy as a function of distance of separation between the particles for a stable and an unstable dispersion, respectively.

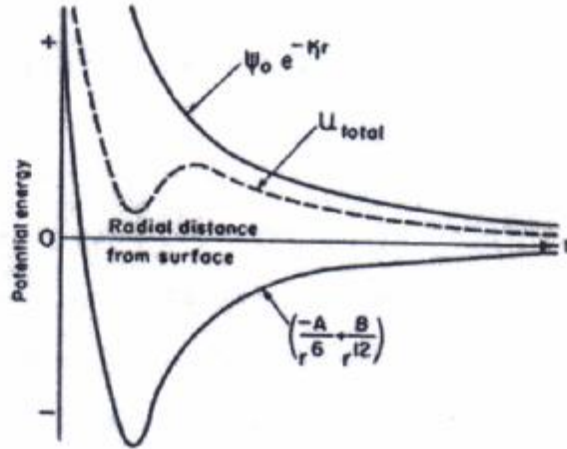


Fig. 2.2 The interaction energy between two colloidal particles as a function of their distance of separation, when the conditions favor stability of the colloid (Hiemenz, Rajagopalan, 1997)

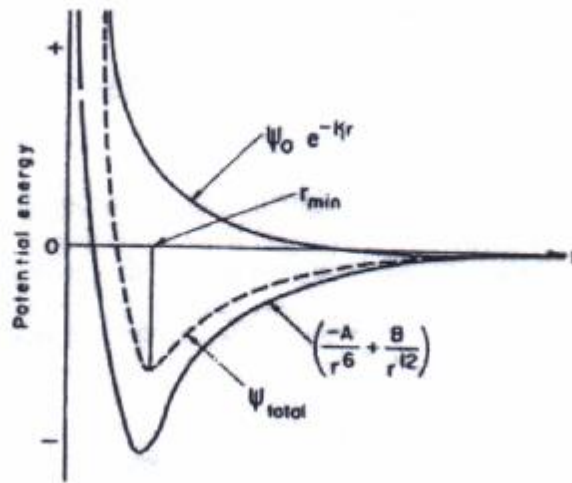


Fig. 2.3 The interaction energy between two colloidal particles as a function of their distance of separation, when the conditions favor coagulation of the colloid (Hiemenz, Rajagopalan, 1997)

A theory on the stability of colloidal dispersions to predict the stability versus aggregation of electrostatically charged particles in dispersion reconciles attractive and

repulsive forces and is known as the Deryaguin-Landau-Verwey-Overbeek (i.e. DLVO) theory. V_s is the total potential and it can be described as following.

$$V_s = V_c + V_a + V_r \quad (2-1)$$

Here, V_c is the core repulsive potential due to electrostatic repulsion, V_a is the Van der Waals attractive potential, and V_r is the double layer repulsive potential.

The DLVO theory is widely regarded as a cornerstone for understanding colloidal systems and forces on the molecular scale (Hiemenz and Rajagopalan, 1997).

2.2.2 Double layer

A particle immersed in a liquid can acquire charge either by adsorbing ions from the surrounding liquid or, at times, by the ionization or dissociation of surface groups. When a charged particle or an ion is present in an electrolyte, there will be variability in the ion density near the surface of the particles, leading to a potential difference.

Stern suggested that a particle has some ions attached to its surface, while others are distributed in a cloud-like fashion. The ion-centers are taken as not coming closer than a certain critical distance, δ , from the surface of the particle. The surface at this distance is called the Stern plane or the inner Helmholtz plane (i.e. IHP). This surface is drawn through the ions that are assumed to be adsorbed on the charged wall (Fig. 2-4). A surface running parallel to the IHP, through the surface of shear (as defined below), is called the outer Helmholtz plane (OHP). The diffuse part of the ionic cloud beyond the OHP is the diffuse double layer, also known as the Gouy-Chapman layer. For

concentrated solutions, most of the charge is squeezed onto the Helmholtz plane, while in dilute solutions, the charge is distributed mostly in the Gouy-Chapman layer.

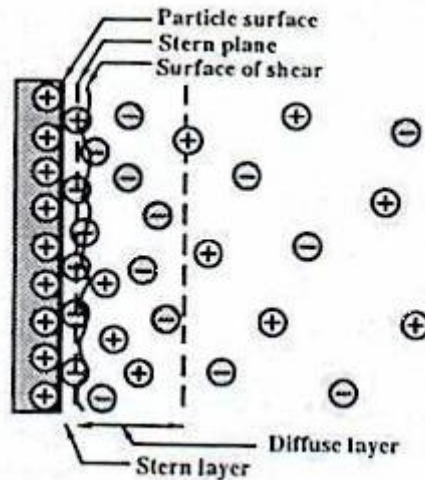


Fig. 2.4 A Schematic representation of the distribution of charge near a charged particle based on the Stern model (Bockeris and Reddy, 1970)

2.2.3 Zeta potential

The layer of liquid immediately adjacent to a particle moves with the same velocity as the surface, i.e., the relative velocity at the surface is zero (i.e., the no-slip condition). The surface at a distance at which relative motion sets in between the immobilized layer and the mobile fluid is termed the surface of shear. The surface of shear occurs well within the diffusion part of the double layer. The potential at the surface of shear is known as the zeta potential, ζ . This determines the effectiveness of the charge on the particle in repelling other particles (Heimenz and Rajagopalan, 1997).

The Stern model illustrates the potential variation across an interface as consisting of two regions, a linear region corresponding to the ions attached to the surface of the particle and an exponential region corresponding to the ions which, are under the combined

influence of the ordering electrical and the disordering thermal forces. Fig. 2-5 shows the variation in the potential with distance from a particle surface. The total thickness of the double layer is $\delta + \kappa^{-1}$, where κ^{-1} is the thickness of the diffuse part of the double layer. The electrical effect of the diffuse charge region can be simulated by placing the entire Gouy Chapman charge at a surface parallel to the particle at a distance, κ^{-1} .

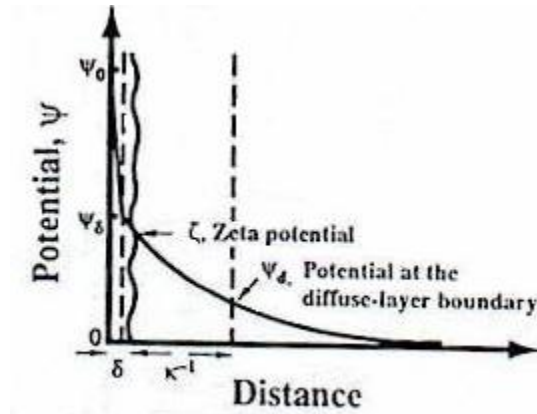


Fig. 2.5 A Schematic representation of the variation in the potential with distance from a charged particle based on the Stern model (Bockeris and Reddy, 1970)

Outside the Stern plane, the potential through the double layer continues to be described as in the Guoy-Chapman theory. The only modifications of the analysis of the diffuse double layer required by the introduction of the Stern plane was that x was measured from δ , rather than the particle surface and that ψ_0 was replaced by ψ_δ (Heimenz and Rajagopalan, 1997).

The stability of hydrophobic colloids depends on the zeta potential; When the absolute value of the zeta potential is above 50 mV, the dispersions are very stable due to mutual electrostatic repulsion and when the zeta potential is close to zero, the coagulation (i.e., the formation of larger assemblies of particles) is very fast and this causes a fast

sedimentation. Even when the surface charge density is very high, but the zeta potential is low, the colloids are unstable. Also the velocity of heterocoagulation (i.e., coagulation of different particles) depends on the zeta potentials of both kinds of particles. Therefore, the zeta potential is an important parameter characterizing colloidal dispersion.

2.2.4 Electrokinetic effects

The existence of charge on the particle and the surrounding double layer of opposite charge leads to electrokinetic effects (Hiemenz and Rajagopalan, 1997). The word electrokinetic implies the combined effects of motion and electrical phenomena. This may arise from the migration of a particle relative to the continuous phase that surrounds it. Alternatively, the solution phase can move relative to stationary walls. The following four phenomena are normally grouped under the term electrokinetic phenomena.

Electrophoresis: This refers to the movement of particles (and any material attached to the surface of the particles) relative to a stationary liquid under the influence of an applied electric field.

Electro-osmosis: The volume flow of aqueous electrolyte solution moves past a charged surface under the influence of an electric field. Thus, electro-osmosis is complementary to electrophoresis. The pressure needed to balance the electro-osmotic flow is known as the electro-osmotic pressure.

Streaming potential: This is a consequence of the electric field created when a liquid (i.e., an electrolyte) is forced to flow past a charged surface. This is the opposite of electro-osmosis.

Sedimentation potential: This is due to the electric field created by charged particle sedimentation in a liquid. This situation is opposite to electrophoresis.

Electrophoresis and electro-osmosis are the main phenomena of interest in this study. When an electric field is imposed on a dispersed colloidal system, the charged particles electrophoretically migrate in one direction. The velocity of the particles is determined by the strength of the electric field and the electrophoretic mobility of the particle, and is expressed as follows:

$$V_p = U_p \times E \quad (2-2)$$

Here V_p is particle velocity (cm/s), U_p is particle electrophoretic mobility (cm²/s-V) and E is electric field (V/cm).

The electrophoretic mobility is quantified by a number of factors and can be best described as a balance between the electro-osmotic forces on the particle and the viscous drag of the liquid phase. It can be stated as the Smolukhovski equation.

$$U_p = \frac{e\zeta}{4\pi\eta} \quad (2-3)$$

Here ϵ is the solution permittivity, ζ is the zeta potential and η is the viscosity of the solution.

2.2.5 Ion Exchange Resin

An ion exchange resin can be considered as a concentrated solution of anions and cations in its own phase, in which one of the ionic species is bound to an insoluble polymeric matrix, and the other is mobile and capable of exchanging with ions of its type in the external solution. The composition of the two main types of ion exchange resin can be summarized in Table 2-1.

Table 2-1 Composition of the resins

Type of ion exchange	Fixed charges	Counter-ions	Co-ions
Cation exchange resin	(-)	Cations (+)	Anions (-)
Anion exchange resin	(+)	Anions (-)	Cations (+)

An ion exchange process can be described as a reaction. Suppose that the ion exchange resin is initially in the A form and that the counter ion in the solution is B. A reaction occurs according to Eq. 2-4.



In equilibrium, both the ion exchange resin and the solution contain competing counter ions, A and B. The ion exchange reaction is reversible. So in real applications, it is not possible to exchange all the counter ions. The maximum amount of counter ions adsorbed by the resin per liter of wet resin is called the ion exchange capacity. Its level depends on

the extent of regeneration, the type of exchange reaction, the equipment used and the prevailing physical conditions.

For a counter ion in the solution to exchange another counter ion in the ion exchange resin, the following kinetic processes must take place:

- (1) Diffusion of ions from the bulk of the surrounding solution to a static layer or a film of solution around the resin particle;
- (2) Diffusion of ions through the film;
- (3) Diffusion of ions through the matrix of the resin to the exchange site;
- (4) The ion-exchange reaction itself (i.e., the chemical reaction step);
- (5) Diffusion of the released ions through the resin from the exchange site to the surface of the particle;
- (6) Diffusion of the released ions across the film;
- (7) Diffusion of the released ions through the bulk solution.

In most cases, the ion-exchange reaction itself is the fastest step, and the diffusion of ions through the bulk solution may be ignored, since the flow of solution through a resin bed results in rapid mixing. Generally, only two steps affect the kinetics of ion exchange:

- (1) Diffusion of ions across the film (i.e., film diffusion control);
- (2) Diffusion of ions through the matrix of the resin particle (particle diffusion control).

The nature of the rate-determining step can be predicted by use of the simple criterion (Eq. 2-5).

$$\frac{X \bar{D} d}{C D r_0} (5 + 2a_B^A) \ll 1 \quad \text{Particle diffusion control} \quad (2-5)$$

$$\frac{X \bar{D} d}{C D r_0} (5 + 2a_B^A) \gg 1 \quad \text{Film diffusion control}$$

Here X is the concentration of fixed ionic groups; C is the concentration of solution (in equivalents), \bar{D} is the interdiffusion coefficient in the ion exchange resin, D is the interdiffusion coefficient in the film, r_0 is the bead radius, δ is the film thickness, and $a_B^A = \bar{C}_A C_B / \bar{C}_B C_A$ is the separation factor (Helfferich, 1995).

Under an electric field, the total flux across the ion exchange resin is given by the Nernst-Planck equation below.

$$J_i = (J_i)_{diff} + (J_i)_{el} = -D_i (grad C_i + z_i C_i \frac{F}{RT} grad \phi) \quad (2-6)$$

Here J is the net flux, $(J)_{diff}$ is the flux due to diffusion, $(J)_{el}$ is the flux due to electric current, D is the diffusion coefficient in the solution, C is the concentration, z is the valence of ion, F is the Faraday constant, R is the gas constant, T is the absolute temperature, ϕ is the electric potential, and the subscript i is species i.

2.2.6 Electrodialysis

The principle of electrodialysis is described in Figure.1.1. Mass transport in the cell is carried out in three steps (Figure.2.6).

(1) Diffusion from the bulk stream through the boundary layer to the membrane-solution interface;

- (2) Diffusion inside the membrane;
- (3) Diffusion from the membrane-solution interface through the boundary layer on the other side of the membrane to the bulk stream.

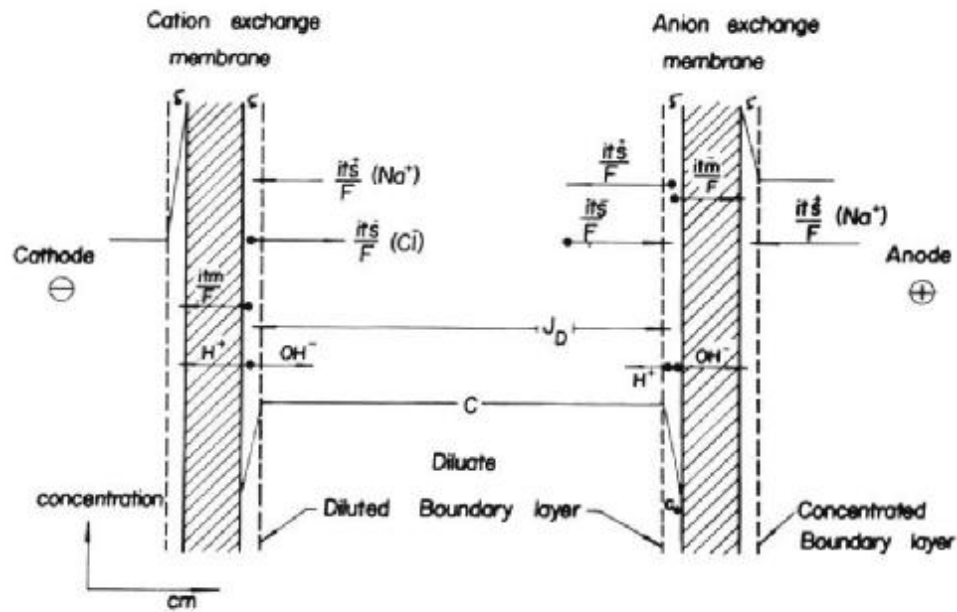


Fig. 2.6 Mass transport during electrodialysis (Belfort, 1984)

The first and third steps are given as the Fick's first law (Eq. 2-7).

$$J_D = \frac{D(C - C_0)}{\delta} \quad (2-7)$$

Here J_D is the flux of ions by diffusion, D is the diffusion coefficient, C is the concentration of the solution, C_0 is the concentration of the solution at the boundary layer, and δ is the thickness of the boundary layer.

The kinetics of the second step is given as the Nernst equation below (Belfort, 1984):

$$J_e = \frac{(\bar{t}_m - t_s)i}{F} \quad (2-8)$$

Here J_e is the flux of ions by electrotransport, i is the current density, F is the Faraday number, t_s is the transport number in solution, and \bar{t}_m is the transport number in the membrane.

If the second step is much slower than that in the boundary layer, the total rate of mass transport is controlled by the diffusion in the membrane (i.e., membrane diffusion control). If the opposite is true, then the diffusion in the boundary layer is rate determining (i.e., film diffusion control).

Polarization, water splitting, membrane fouling and membrane scaling are the common phenomena in the ED process.

In an ED process, the movement of ions in the solution and in the membrane are different. The difference arises because in the solution the movement of cations and anions are associated with roughly equal amounts of current, but in the highly selective ion exchange membrane, virtually all the current is carried by the counter ions, resulting in polarization. The movement of cations through the electrolyte solution is slower than that through the cation exchange membrane, thereby causing a cation deficiency near the membrane surface and hence a concentration polarization. Thus when the ion concentration reaches zero at the membrane surface, a limiting current density is reached. If the current is above the limiting current density, then it leads to water splitting, producing hydrogen and hydroxyl ion in the membrane-solution interface. Water splitting consumes energy, and reduces the current efficiency, which is not expected in the

operation. Furthermore, due to water splitting, the solution pH will be changed, which may lead to scaling (deposits such as hydroxides on the membrane) or degrade the membrane.

Large ions may be too large to penetrate the membrane and accumulate on the surface, thereby causing a dramatic increase in electrical resistance. Some organic ions may penetrate the membranes, but with lower electro mobility in the membranes, causing a dramatic increase in electrical resistance. These two phenomena are known as membrane fouling and poisoning.

2.2.7 Electrodeionization

Generally, electrodeionization process is complicated because two unit operations, i.e., ED and ion exchange, are incorporated. There are three paths available for ionic transport (Helfferich, 1995):

- (1) Solely through the ion exchange resin to the membrane;
- (2) Solely through the solution phase;
- (3) Alternating through the solution and resin phases.

These terms are additive. The basic mass transport model of the process is given by the Nernst-Planck equation (Eq. 2-6). Spoor et al. and Verbeek et al. have digitally simulated the electrodeionization process based on the Nernst-Planck equation. The concentration gradient and potential gradients in an electrodeionization process are formed along the central chamber. For a continuous deionization of a dilute nickel solution, Spoor et al.

proposed a diagram of the nickel concentration changes in the ion exchange bed (Figure.2.7) of a three-chamber EDI set-up.

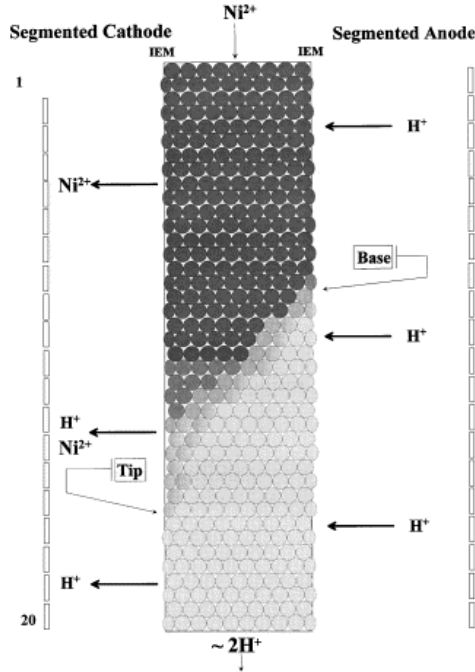


Fig.2.7. Diagram of the nickel front. This figure depicts the sections of the beds in the Ni^{2+} , H^+ and $\text{Ni}^{2+}/\text{H}^+$ forms. The bed is regenerated by the anolyte, while nickel is concentrated in the cathode compartment. The nickel solution is fed top-down.

From the above diagram, it can be absolved that there are two distinct operating regimes for the EDI process: enhanced transfer regime and electroregeneration regime. In the enhanced transfer regime, the rate-limiting step is most often film diffusion of the ions in the bulk solution to the ion exchange resin surface. The optimization of performance of this regime is possible due to an increase of the active surface area of the resin. The second operating regime is the electroregeneration regime. This regime is characterized by the continuous regeneration of resins by electrically induced water splitting reactions to their hydrogen and hydroxide forms. The optimization of this regime ensures sufficient water splitting in the chamber. So methods to enhance the water splitting are important

for the EDI process. Simons (1984) described a way to catalyze the electrochemical water splitting. The dissociation of water preferentially occurs at bipolar interfaces in the dilute chamber, i.e. resin/resin and resin/membrane interfaces. A mixed ion exchange resin is used and an anion exchange resin is arranged besides the cation ion exchange membrane and the cation exchange resin is arranged besides the anion ion exchange membrane. Performance enhanced using this approach is also shown in the experiment of Dejean, et al. (1997).

Spoor et al. also demonstrated that pH of the nickel solution, feed concentration, solution flow rate, bed width, cell voltage and temperature are important parameters for the EDI performance. The properties of the resins, such as ion exchange capacity, degree of cross-linking, and conductivity can affect the performance. On the other hand, the size and the valence of counter ions, the type of solvent and the co-ions in the system can also have varying effects on the performance of the EDI process.

Most of the research papers describes the effects of ion conducting spacer. It includes how it suppresses the polarization, reduces resistance and increases current density and current efficiency (Korngold, 1975; Kedem, 1975; Weida, Dong, 1985; Messalem, et al., 1998). Shaposhnik et al. numerically analyzed mass transfer due to the ion conducting spacer and visualized the concentration field by means of laser interferometry.

However, there is still no systematic theory available for the EDI process. Furthermore, there are no research publications on the effect of organic compound purification or separation by a hybrid ion exchange/electrodialysis process.

Chapter 3

Methodology

3.1 Apparatus

The schematic of the experimental set-up (provided by IONICS, USA) is shown in Figure 3.1 (For a recycling operation mode) and Figure 3.2 (For a single-pass operation mode). The main unit comprises of a module, separated into three chambers by a cation exchange membrane (CM) and an anion exchange membrane (AM). Both side chambers are electrolyte chambers with the electrolyte solution flowing through them. The volume of each electrolyte chamber is 4.4 ml. The chambers are connected in sequence, i.e., the outlet of the first is connected to the inlet of the second. Flat rectangular platinum electrodes with an area of 11 cm^2 are present at the walls of these two chambers. The distance between the electrodes is 3.5 cm. The central chamber has a volume of 21 ml. The solution under investigation flows through the chambers vertically (up-down or down-up). The distance from the inlet to outlet is about 6 cm.

Peristaltic pumps (MEDIMAT 5 electrodialysis system, IONICS) were used to pump the feed solution and the electrolyte solution.

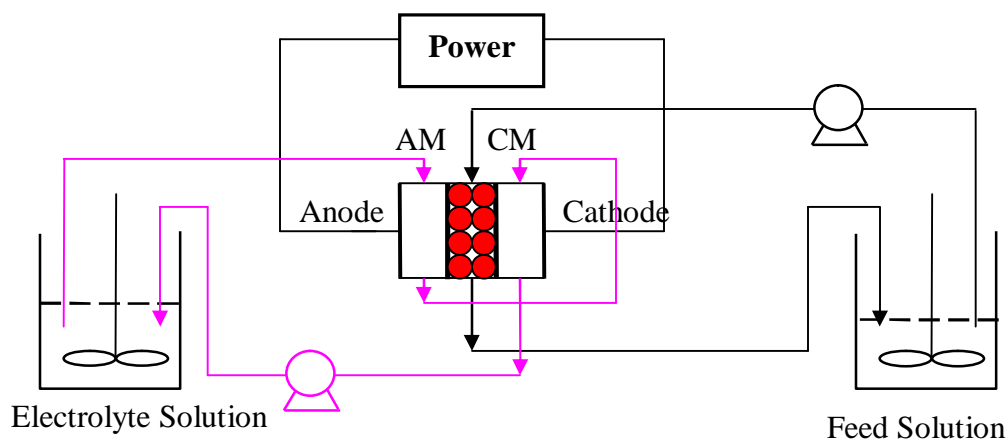


Fig.3.1 Schematic representation of the experimental set-up in the recycling operation mode

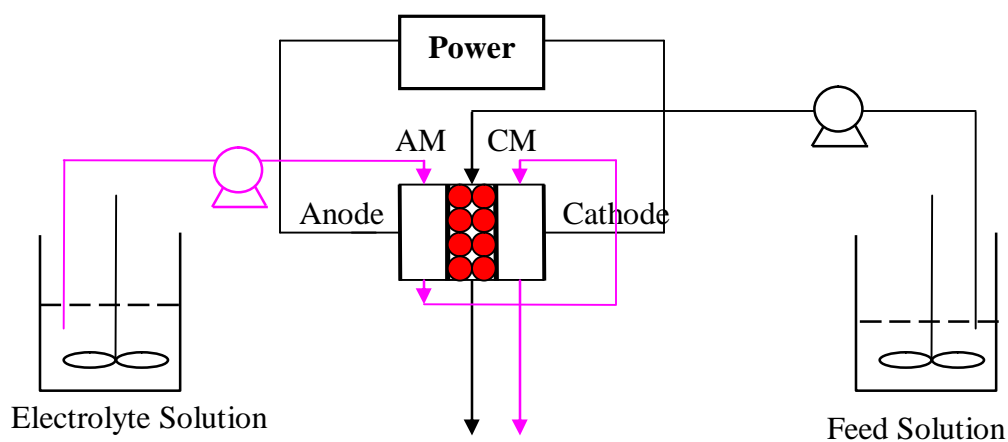


Fig.3.2 Schematic representation of the experimental set-up in the single-pass operation mode

3.2 Materials

(1) Membrane

In this study, an IONICS CR-67 cation exchange membrane and an IONICS AR-103 anion exchange membrane were used. The effective area in the module for the cation and anion exchange membranes was 11 cm² for each. The thickness of the IONICS CR-67

membrane is approximately 0.55mm. It is comprised of cross-linked sulfonated copolymers of vinyl compounds reinforced with an acrylic fabric (Figure 3.3). The specific weight of this membrane is 13.7mg/cm^2 and it has a burst strength of 7g/cm^2 (Bulletin No. CR 67.1, 1990). The membranes are resistant to 5-10% acid concentration and to bases with a pH of 11 (Bulletin No. CR 67.0, 1990). The thickness of the IONICS AR-103 membrane, on the other hand, is 0.5mm. The anion exchange membrane contains quaternary ammonium ions reinforced with a polypropylene fabric (Figure 3.4). The specific weight of this membrane is 15.9mg/cm^2 and its burst strength is 22kg/cm^2 (Bulletin No. AR 103, 1990). All the main properties of the membranes are shown in Table 3-1.

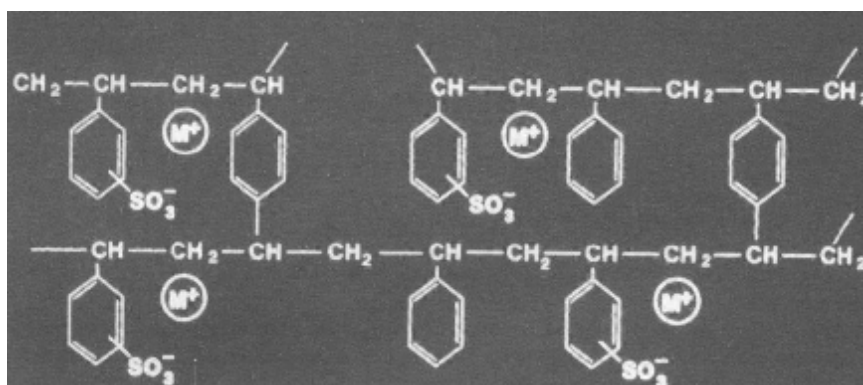


Fig. 3.3 A schematic representation of the IONICS CR-67 membrane.

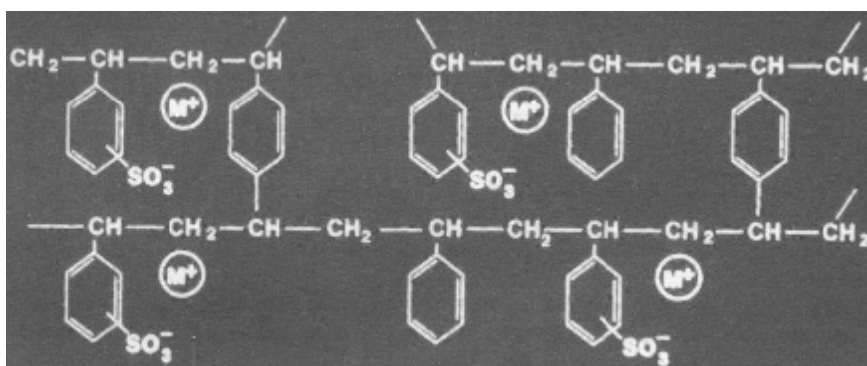


Fig.3.4 A schematic representation of the IONICS AR-103 membrane.

Table 3-1 Properties of the ion-exchange membranes employed

	IONICS CR-67 (cation exchange membrane)	IONICS AR-103 (anion exchange membrane)
Available area (cm ²)	11	11
Approximate thickness (mm)	0.55	0.50
Structure	Cross-linked sulphonated copolymers of vinyl compounds reinforced with an acrylic fabric	Quaternary ammonium ions reinforced with a polypropylene fabric
Specific weight (mg/cm ²)	13.7	15.9
Burst strength(kg/cm ²)	7	22
Resistance to acids/bases	5-10% acids, bases with pH a 11	5-10% acids, bases with a pH of 11

(2) Resins

Three types of resins were used in our study; cation exchange, DOWEX MARATHON C, anion exchange DOWEX MONOSPHERE 550A, and mixed DOWEX MARATHON MR3. The properties and the operating conditions for the resins are given in Tables 3-2, 3-3, 3-4 (Dow Chemical Company, Form No.177-01593-1296QRPCH 171-327-F-1296, 177-01789-1098QRPCH 171-488-F-1098, and 177-01668-496QRPCH 171-386-F-496).

The DOWEX MARATHON resins are uniform particle sized (UPS) resins designed specifically to have a longer operating run and lower operating costs in multi-bed demineralization. The resins have a narrow particle size distribution and small values of the average bead diameter (~ 550-600 μm), thus providing a higher surface area per unit volume of the resin as well as a shorter diffusion path in the beads. This means that DOWEX MARATHON resins can be rinsed and regenerated more quickly and

completely than conventional resins. This, in turn, leads to greater sustained operating capacities, longer runs, reduced regenerant chemical and rinse water requirements, and more productive and economic demineralization operation.

Table 3-2 Description of the resins

Product	Type	Matrix	Functional group
DOWEX MARATHON C	Strong acid cation resin	Styrene-DVB gel	Sulfonic acid
DOWEX MONO-SPHERE 550A	Type I strong base anion resin	Styrene-DVB gel	Quaternary amine
DOWEX MARATHON MR-3	1:1 by equivalent mixture of DOWEX MARATHON A (OH) anion and DOWEX MARATHON C (H) cation resins	Styrene-DVB gel	Sulfonic acid and quaternary amine

Table 3-3 Physical and chemical properties of the three resins

Physical and chemical properties	DOWEX MARATHON C	DOWEX MONOSPHERE 550A	DOWEX MARATHON MR-3	
Form of the resin	H ⁺ form	OH ⁻ form	OH ⁻ form	H ⁺ form
Total exchange capacity (eq/L)	1.8	1.1	1.0	1.8
Water content (%)	50-56	55-65	60-72	50-56
Mean particle size (μm)	600±50	590±50	610±50	600±50
Particle density (g/mL)	1.2	1.08	1.06	1.2

Table 3-4 Recommended operating conditions for the three resins

Recommended operating conditions	DOWEX MARATHON C	DOWEX MONOSPHERE 550A	DOWEX MARATHON MR-3
Maximum operating temperature (°C)	120	60	60
pH range	0-14	0-14	0-14
Total rinse requirement	2-5 bed volumes	2-5 bed volumes	/
Regenerant	1-8% H ₂ SO ₄	4-8% NaOH	/

DOWEX MONOSPHERE resins are also UPS resins and are commonly used in condensate polishers, ultrapure water systems, and other regenerable mixed beds. The size and the density relationships between these resins are optimized to provide maximum backwash separability, which minimizes the chance of cross-contamination during regeneration. Smaller average bead sizes and a very narrow particle size distribution lead to higher exposed particle surface areas across the resin bed, yielding faster kinetics.

(3) Chemicals

The copper sulphate penta-hydrate from Nacalai Tesque Inc., had a purity of about 99.5%, and was used as received. Sodium sulphate (Baker Analyzed) was also used without further purification. The sodium hydroxide (Mallinckrodt) had a purity of nearly 98.6%. 37% fuming sulphuric acid was purchased from Merck. De-ionized water was used for all experiments. The sodium chloride and hydrochloric acid was used without further purification.

The humic acid was supplied by Fluka Chemika (lot/product number 41968/53680, ash~20%, MW 600-1000 g/mol). It contains 48% carbon, 3.59% hydrogen and 0.94% nitrogen, and the remaining 45.35% predominantly oxygen, some sulphur and phosphorus. The elemental composition of humic materials, from the literature, ranges between 40-60% carbon, 4-5% hydrogen, 1-4% nitrogen, 30-50% oxygen, 1-2% sulphur and 0-0.3 % phosphorus (Gaffney et al., 1996).

3.3 Instruments and experimental procedures

A Biochrom Split-beam UV/VIS spectrophotometer (Libra S32) was used to measure the concentration of humic acid solution at a wavelength of 254 nm. In the experiments, a standard calibration curve at 254 nm was obtained by dissolving a known amount of HA at pH 11 to ensure total solubility.

The particle size distribution of HA solution was characterized by a laser light scattering system (Model: BI 200SM & 90 Plus Particle Size Analyzer, Brookhaven Instruments (ITS)). The instrument measures the hydrodynamic diameter, i.e., the particle diameter plus the double layer thickness.

All the resins were flushed using DI water for two days before being used in the experiments. Thus it reduced the probable effect on measurement of concentration due to organics that may be leached from the resins using UV/VIS spectrophotometer. Membranes were stored in DI water to keep the surface wet and to keep the function of membranes.

The HA solution was stirred for approximately two days and then filtered through the paper filters (Macherey-Nagel (MN) 617 type). The weight of the filter was measured pre- and post-filtration in order to find the amount of HA in solution. The stock solution was stored at 4°C to prevent microbial growth and to minimize the HA aggregation. The solution was diluted to desired concentrations and brought to room temperature prior to use. The addition of other ions was carried out just before the experiments to reach the experimental requirements.

When assembling the module, a side chamber with an inlet and an outlet was set on the lab desk, and a membrane was glued to the side chamber. Secondly, the central chamber with an inlet and an outlet was glued to the membrane, thus the central chamber can be filled with the resins. After that, another membrane was glued to the central chamber and lastly the side chamber was connected to the membrane. After experiments, the module was disassembled and the glue was removed from the surface. All the chambers needed to be washed.

(1) Morphology of membrane

The morphology of anion exchange membrane before and after experiments were got by Scanning Electron Microscopy (SEM) (Model: MP-5600LV). According to the manual of SEM, the samples should be dried first and then coated with Pt for scanning.

(2) Particle size distribution of HA

200 ml of a 12-15ppm HA solution was recirculated through the central chamber and 200 ml of 0.005M Na_2SO_4 solution was recycled through the electrolyte chamber. The experiment was done at 40 V in the system of AM+MR3+CM. 10 ml of HA sample were collected from the solution passing through the central chamber at different intervals. At 80 min, voltage was cut off. Later, a sample was collected for analysis. The particle size distribution of all the HA samples was measured.

(3) Kinetics of HA adsorption on the resin in the beaker

14g of each resin were placed in three separate beakers and 500ml of a HA solution (about 25ppm) was placed into each beaker. The solution was stirred all the time at a slow rate. 10ml samples of the solutions were collected at regular intervals and the concentration of HA was measured.

(4) Recycling operation mode

The HA solution and the electrolyte solution were put in the beakers with the solution well mixed. All the solutions were recirculated through the chambers (Figure 3.1). The circuit current, pH of the HA and electrolyte solution and HA concentration in the feed can be measured continuously.

In the recycling operation mode, in order to clarify the role of different components (i.e., the membrane, the ion exchange resin and the voltage), different combinations of membrane and resins were used. Effect of different parameters were studied in the recycling operation mode (i.e., the voltage, the electrolyte concentration, the flowrate, the HA concentration, the pH, the ionic strength and the copper).

(5) Single-pass operation mode

HA solution and electrolyte solution were pumped from the tanks (Figure 3.2). The feed solution flew through the central chamber. Electrolyte solution flew through the first side chamber, then through the second side chamber and finally out of the second side chamber.

The effect of different parameters was studied in the single-pass operation mode (i.e., the voltage, the electrolyte concentration, the flowrate, the HA concentration, the pH, the ionic strength and the copper). The HA solution out of the central chamber can be analyzed continuously to obtain the HA concentration and pH. The pH of the electrolyte solution out of the side chamber was also measured. The circuit current was measured by Amperemeter.

Chapter 4

Different Combinations of Ion Exchange Membrane and Ion Exchange Resin

4.1 Introduction

Humic acid (HA) particles are negatively charged at normal pH and can be removed by an anion exchange resin due to ion exchange mechanism. Generally, ion exchange resin columns were used to remove HA (Anderson, Maier, 1979; Kolle, 1979; Macko, 1980; Boening, 1980; Brattebo, et al., 1987; Odegaard et al., 1999) in the absence of an electric field. Several researchers paid attention to the particles (polystyrene latex particles) removal by ion exchange fiber in the application of electric field (Judd; Solt, 1989; Fletcher, et al., 1994). It was found that electric field can enhance the particles removal.

Ion exchange membrane can adsorb charged particles from aqueous solution and recently a new bio-separation method has been developed based on adsorptive membrane due to its adsorption properties and faster binding (Suen, Etzel, 1994; Lin, Suen, 2002). On the other hand, in the electrodialysis (ED) process, the adsorption of charged particles by an ion exchange membrane causes membrane fouling under the electric field. It has been an important issue, especially in the organic anion fouling. Fouling due to negatively charged organics occurs in many streams of ED applications, some of the foulants being sodium dodecylbenzene sulfonate (Lindstrand, 2000), sulfonated lignin (Watkins and

Pfromm, 1999), sodium humate (Korngold, et al., 1970), grape must (Audinos, 1989), and milk whey (Lonergan, et al., 1982) as well as the Kraft pulp (Rapp and Pfromm, 1998).

Both the ion exchange membrane and the ion exchange resin may behave differently in HA removal in the absence of an electric field and in the presence of an electric field. Aatmeeyata (2000) has studied three combinations of ion exchange membrane and resin, i.e. the combination of anion exchange membrane and cation exchange membrane only (AM+CM), the combination of AM, MR3 resin and CM (AM+MR3+CM), and the combination of AM, A550 resin and AM (AM+A550+AM). Experiments were carried out for the different combinations in the absence of applied voltage and in the presence of applied voltage in the recycling operation mode. It was found that the HA removal in the presence of applied voltage was much higher than that without voltage. However, the enhancement for different combinations was quite different. In order to investigate the mechanism and kinetics of the process and to evolve an optimal combination, all possible combinations of ion exchange membrane and resin were used to do experiments.

4.2 Results and discussion

The experimental procedure is described in Chapter 3. The arrangement of different combinations and experimental conditions are shown in Table 4.1. All the resins used were fresh and they were washed only with DI water. For all the experiments with AM+CM, AM was in the anode side and CM was in the cathode side. Thus the current direction was from anode to AM, to CM and to cathode. This is a normal current direction mode in the experiments. For the other combinations that had the same membrane (i.e., AM+AM and CM+CM), the current direction is of no importance.

Table 4.1 Different combinations of ion exchange membrane and resin

Combinations		Experimental conditions	
		Without Voltage	With Voltage (40V)
Resin in the beaker		500ml 25ppmHA solution, 14 g resin	/
Only membranes	AM+CM	200ml 0.005M Na ₂ SO ₄ , pH 6.0-7.0; 200ml 17-18ppm HA solution, pH 6.0-7.0, no salt; flow rate of electrolyte solution is 3.7ml/min; flow rate of HA is 4.8ml/min; 14 g resin; recycling operation mode	
	AM+AM		
	CM+CM		
MR3 resin and membranes	AM+MR3+CM		
	AM+MR3+AM		
	CM+MR3+CM		
A550 resin and membranes	AM+A550+CM		
	AM+A550+AM		
	CM+A550+CM		
Marathon C resin and membranes	AM+MarathonC+CM		
	AM+MarathonC+AM		
	CM+MarathonC+CM		

4.2.1 Resin in the beaker

As suggested by Aatmeeyata (2000), 14 g of resin was used to perform experiments in the hybrid electrodialysis/ion-exchange process. In order to make the experimental results comparable, 14g of resin was used in this experiment as well. Three different resins (washed with a large amount of DI water before the experiments) were placed in three separate beakers filled with 500ml of 25ppm HA solution (pH 6.5). The solution was

stirred continuously at a slow rate. 10ml samples of the solutions were collected at regular intervals and the concentration of HA was measured using a UV spectrophotometer. The ratio of C_t of C_0 as a function of time is plotted in Figure 4.1 (C_t is HA concentration at time t, and C_0 is the initial HA concentration, here it was 25ppm).

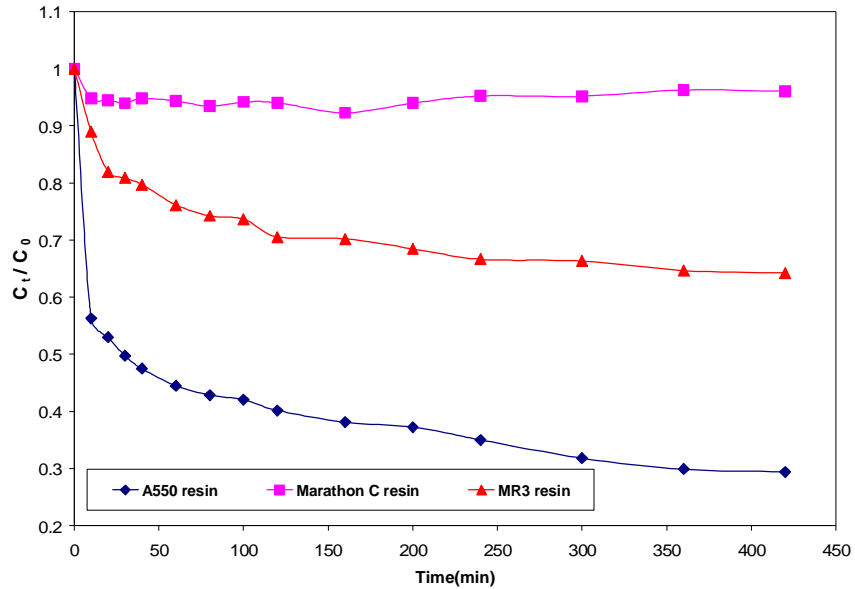


Fig. 4.1 HA concentration ratio as a function of time for the resin in the beaker (experimental conditions refer to Table 4.1)

The final HA concentration ratio is 0.29, 0.64 and 0.96 for the A500 resin, MR3 the resin and the Marathon C resin, respectively. The total removal of HA for the anion exchange A550 resin (71%) is about twice of that for the MR3 resin (36%), which is in accordance with the amount of the effective counter-ions in each resin. There is a small removal of HA for the cation exchange resin Marathon C (about 4%, it may be due to the surface adsorption), which is in accordance with fact that there are no effective counterions for anions in the Marathon C resin. It seems that the main mechanism is “ion exchange”.

In general, two possible mechanisms could be responsible for the removal of organic acids by an ion exchange resin. One mechanism that is responsible for the attachment of the carboxyl groups of an organic acid to the resin ionogenic groups involving the replacement of counterions on the resin is described as “ion exchange”. The other mechanism that is responsible for the attachment of the nonionic portion of an organic acid to the internal surface of the resin without interacting with any ionogenic groups is termed “surface adsorption” (Sengupta, 1995).

There is another feature in HA removal by an ion exchange resin (A550 resin and MR3 resin) that at initial times of about 10 minutes. it removes HA quickly and later very slowly. This feature was also reported for humic acid removal by activated carbon (Fetting, 1999).

4.2.2 Only membranes

Three combinations of membranes, i.e. AM+CM, AM+AM and CM+CM, were used to perform the experiments. The process is similar to ED. The HA solution and electrolyte solutions were recycled through the central chamber, and electrolyte chamber respectively. HA concentration in the feed solution tank was continuously measured by an UV spectrometer. After every experiment, a sample of the electrolyte was collected to see whether HA particles were transferred from the central chamber to the electrolyte chamber.

The dimensionless HA concentration, C_t/C_0 , as a function of time is plotted for three combinations in Figure 4.2. C_t is HA concentration in the feed solution tank; C_0 is the initial feed HA concentration before experiments.

For the experiments without applied voltage, HA concentration decreased slowly. For both AM+CM and CM+CM, it decreased from 1 to 0.99, less than 1% total HA removal in 120 min. For AM+AM, it decreased from 1 to 0.93, about 7.0% total HA removal in 120 min. It seems that AM can adsorb to HA particles from the solution. After experiments, HA particles can be seen attached on the surface of AM (it became brownish yellow, refer to Fig. 4.4). This shows that the adsorption occurred due to interactions of the ion exchange membrane and the bulk HA (i.e. mono adsorption layer) as well as of the HA adsorbed on the ion exchange membranes and the bulk HA (multiple adsorption layer after the saturation of sorption sites). It was reported by Kim et al. (2002) that Freundlich-type isotherm was more suitable than the Langmuir-type isotherm for the adsorption equilibrium of natural organic matter. However no HA particles were observed attached on the surface of CM. It is known that AM membrane with tertiary or quaternary amine groups is positively charged over a wide range of pH (Strahmann, 1992; Krol, et al., 1999), and HA particles are negatively charged. Thus there is an electrostatic attraction force between AM and HA particles and the particles accumulate near the membrane surfaces. There is no adsorption of HA particles for CM due to electrostatic repulsion between its negatively charged functional groups and negatively charged HA particles. Similar phenomenon was also reported by Grossman et al. (1972, 1973), Lindstrand, et al. (2000), Kim, et al. (2002) when studying membrane fouling using different organic matter such as octanoic, propanoic and decanoic acid. However, a

small fraction of HA is not dissociated, there may be hydrophobic interactions between HA molecules and membranes and thus leads to a small amount of HA particles adsorbed. The physical and electrochemical properties of the solute: charge, hydrophobicity, molecular size and solubility, the physical parameters of the membrane, i.e. surface charge and hydrophobicity are crucial for solute deposition on the surface of membranes (Lindstrand, et al. 2000; Lee et al., 2002).

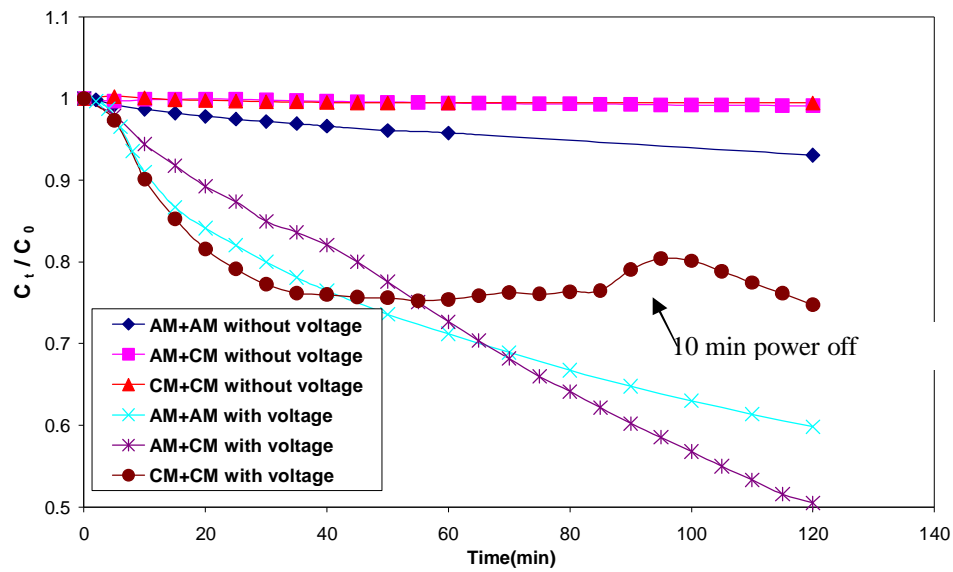


Fig. 4.2 HA concentration ratio as a function of time for membrane only without the resin (experimental conditions refer to Table 4.1)

On the other hand, for the experiments with applied voltage, HA concentration decreased in a very different fashion. For AM+CM, it decreased from 1 to 0.50, about 50% total HA removal in 120 min. This shape of the curve is the same as experimental results obtained by Aatmeeyata (2000). For CM+CM, it decreased quickly at the beginning of the experiment (about 20 min). Then it decreased slowly and finally after 40 min, it remained almost constant (Except the concentration change after 85 min, this change will be explained later). The HA concentration changed from 1 to 0.75, about 25% of total

HA removal. For AM+AM, HA concentration changed from 1 to 0.60, an about 40% of total HA removal. It is demonstrated that the voltage can enhance the HA removal efficiently for AM+CM (from 1% to 50%, while for CM+CM, it is from less than 1% to 25% and for AM+AM, from 7% to 40%).

For AM+AM and AM+CM, the negatively charged HA particles moved toward the anion exchange membranes under the electric field and then deposited on the membrane surfaces due to coagulation effect and electrokinetic forces. After the saturation of membrane sorption sites, HA particles deposited on the adsorbed HA layer surfaces (i.e., multiple layer adsorption). For CM+CM, negatively charged HA particles moved toward cation exchange membranes under the electric field and then deposited on the membrane surfaces, because the electrokinetic force is larger than the electrorepulsion force. After the saturation of membrane sorption sites, HA particles deposited on the adsorbed HA layer surfaces (multiple layer adsorption) due to coagulation. However, the adsorbed HA layer on AM and CM is different when the voltage was switched off after 120 min and the solution was still flowing for about 10 min. It was found that for CM+CM, almost all the adsorbed HA particles were released (i.e., desorbed). There is an equilibrium of adsorption and desorption, which was observed in the experiment. When the power was off in 85 min, HA particles were released. But after the power was on again, the HA particles attached the membrane surface again and reached the balanced HA concentration. For AM+AM, about 4.59% of the adsorbed HA was released after switching off the power. For AM+CM, about 0.52% of the adsorbed HA was released after the power was switched off. For AM+CM, the surface color of AM was brownish yellow and for AM+AM, both AM surfaces were brownish yellow with one AM deeper.

Interestingly, for CM+CM, almost no color change was observed on the surface of CM. The adsorption for CM+CM is totally reversible, for AM+AM and AM+CM, it is a combination of reversible adsorption and irreversible adsorption. The equilibrium for CM+CM was observed after 40 min due to its high desorption rate (i.e., reversible process). It is reasonable to imagine that there is an equilibrium between adsorption and desorption for AM+AM and AM+CM only if the experiments is sufficiently long enough.

We can assume that the total HA removal η_T equals to the addition of η_{static} due to static adsorption and η_{ele} due to electrosorption.

$$h_T = \frac{V_f (C_0 - C_t)}{V_f C_0} = \frac{C_0 - C_t}{C_0} \quad \text{With Voltage} \quad (4-1)$$

$$h_T = h_{static} + h_{ele} \quad (4-2)$$

Here V_f is the volume of the feed HA solution.

It is also assumed that the HA removal in the absence of voltage η_{static} is due to static adsorption and is the same as that in the presence of voltage. HA removal due to electrosorption η_{ele} as a function of time for membranes only is plotted in Figure 4.3. For CM+CM, initially it increased and later the process reached a steady state. For AM+AM, it also initially increased and the rate of removal decreased with time, but the process did not reach a steady state. For AM+CM, it increased all the time during the experiment. It shows that the combination of AM+CM can remove HA efficiently.

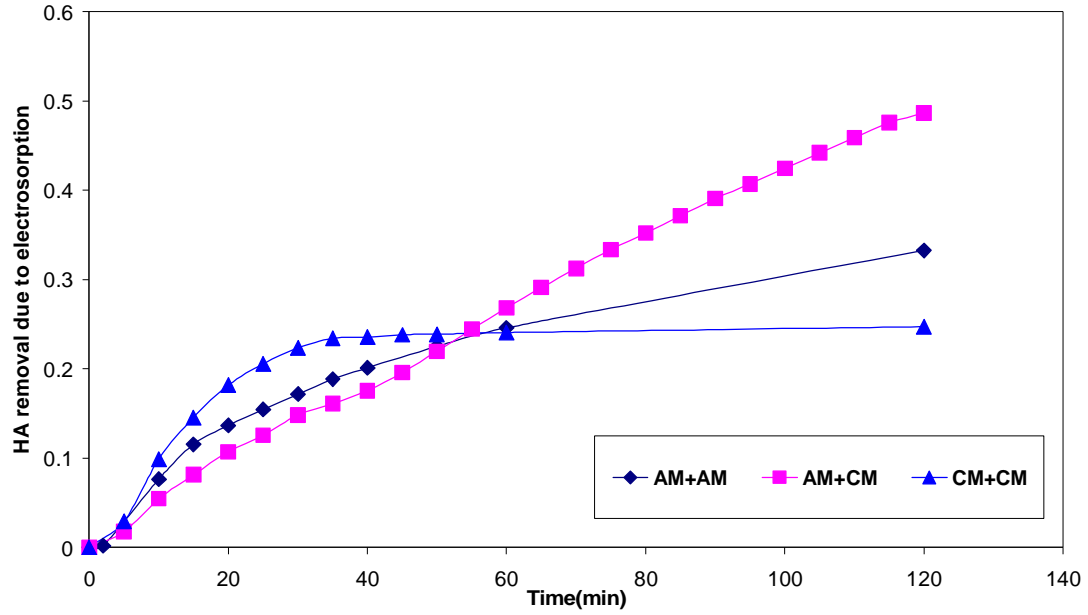


Fig. 4.3 HA removal due to electrosorption as a function of time for membranes only without resin (experimental conditions refer to Table 4.1)

In all the experiments, no HA particles were found in the electrolyte solution. It means that HA particle size is large (the size is about 1000nm, referring to Section 6.2) and it cannot diffuse through the membrane to the electrolyte chamber.

Figure 4.4a shows the SEM images of morphology of the anion exchange membrane surface with HA deposition. Figure 4.4b shows the photo of anion exchange membrane before and after the experiments. Both methods show that HA was attached onto the surface of the anion exchange membrane and formed the deposit.

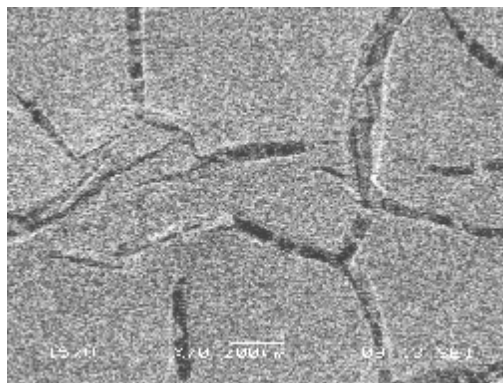
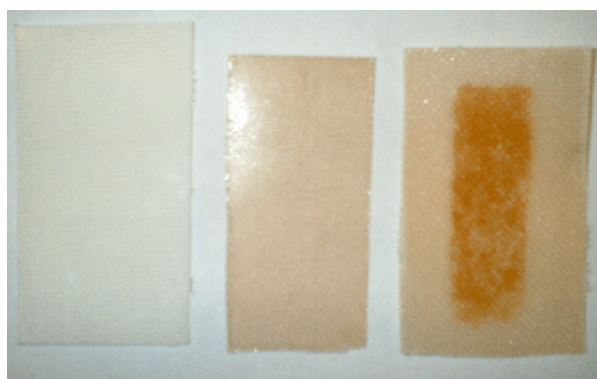


Fig. 4.4a SEM images showing the morphology of an anion exchange membrane surface with HA deposition



Fresh CM Fresh AM AM with HA

Fig. 4.4b Photo of an anion exchange membrane before and after experiments and a photo of a fresh cation exchange membrane

4.2.3 MR3 resin and membranes

In the thesis of Aatmeeyata (2000), the combination of AM+MR3+CM was used to do experiments. In this chapter, three combinations of membranes and MR3 resin, i.e. AM+MR3+CM, AM+MR3+AM and CM+MR3+CM were used in a recycling operation mode. The experimental procedure was described in Chapter 3.

The dimensionless HA concentration, C_t/C_0 as a function of time is plotted in Figure 4.5. In the absence of applied voltage, the HA concentration decreased slowly for all combinations. For CM+MR3+CM, the HA concentration changed from 1 to 0.85. For AM+MR3+CM, the HA concentration decreased from 1 to 0.83. For AM+MR3+AM, the HA concentration decreased from 1 to 0.81. After the experiments, no HA particles can be seen attached on the CM surface, while AM surface became brownish yellow. If we supposed that HA removal due to MR3 resin is almost the same (about 15%, CM does not adsorb HA particles), HA removal due to one piece of AM is about 2% (from 15% to 17% to 19%). The adsorption mechanism on the AM is analyzed in Section 4.2.2 and the adsorption mechanism on the resin is analyzed in Section 4.2.1.

In the presence of applied voltage, the HA concentration decreased faster than that without applied voltage. For AM+MR3+CM, it decreased from 1 to 0.31. The HA removal and curve shape is similar to that obtained by Aatmeeyata (2000). The combination of AM+MR3+AM was less efficient and HA concentration decreased from 1 to 0.38. For CM+MR3+CM, it decreased much less than for the above two, from 1 to 0.63. In the presence of voltage, two factors lead to HA removal, i.e. static adsorption (membrane and resin) and electrosorption (due to electric field). HA removal due to electrosorption was calculated according to Equation 4-1 and Equation 4-2, and plotted in Figure 4.6. It is obvious that the voltage can enhance HA removal for AM+MR3+CM.

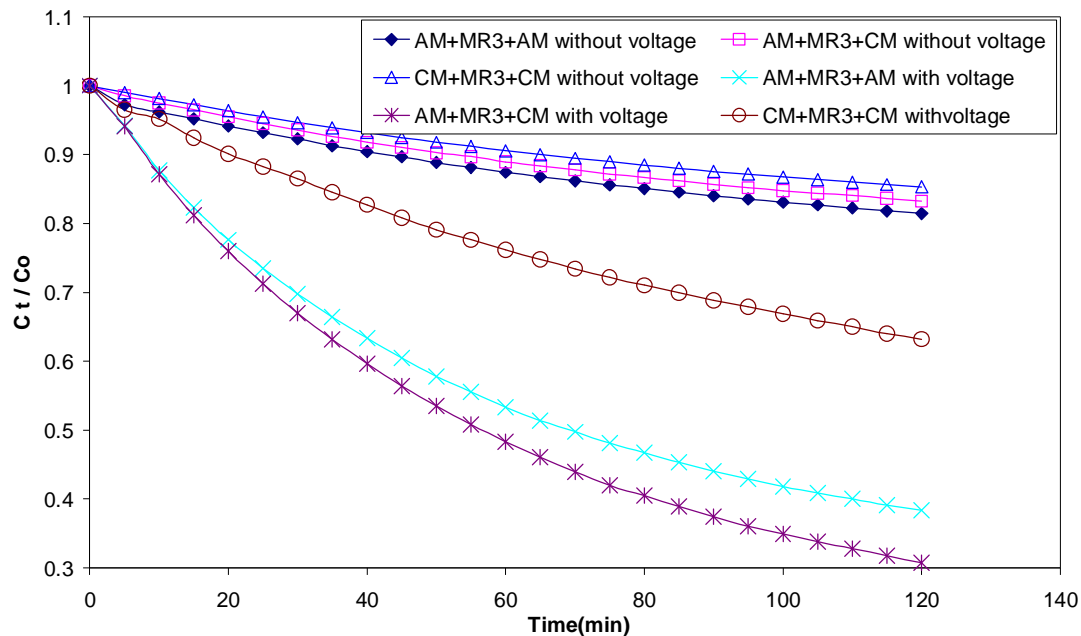


Fig. 4.5 HA concentration ratio as a function of time for combinations of MR3 resin and membranes (experimental conditions refer to Table 4.1)

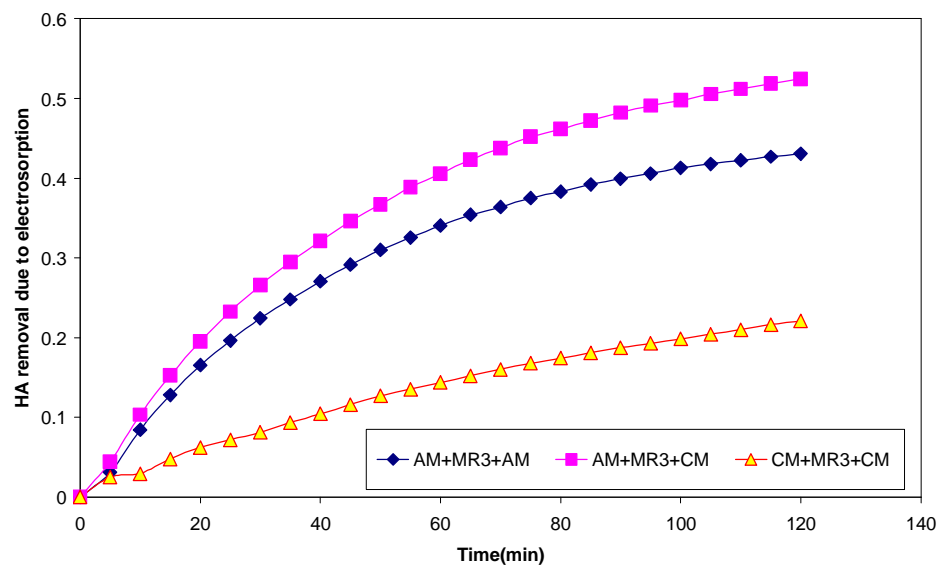


Fig. 4.6 HA removal due to electrosorption as a function of time for combinations of MR3 resin and membranes

After 120 min, the power was switched off and the experiment ran for another 10 min. For CM+MR3+CM, about 18% of removed HA was released to the solution. A small

amount of HA particles was attached on the CM on the anode side and no HA particles were attached on the CM on the cathode side. For AM+MR3+CM, about 7.0% of removed HA was released to the solution. The AM surface was brownish yellow while no HA particles were attached on the CM surface. For AM+MR3+AM, about 14% of removed HA was released to the solution. Both AM surfaces were brownish yellow and the anode side AM surface was darker than the other side. It seems that the attractive force of HA particles for a combination of AM+MR3+CM is stronger than the other two.

In the absence of voltage, a combination of AM+MR3+AM is the most efficient one for HA removal, however, in the presence of voltage, a combination of AM+MR3+CM is the most efficient one.

4.2.4 A550 resin and membranes

Three combinations, i.e. AM+A550+CM, AM+A550+AM and CM+A550+CM were used to perform the experiments. The experimental procedure was the same as the above.

The dimensionless HA concentration, i.e. C_t/C_0 as a function of time is plotted in Figure 4.7. For CM+A550+CM, the HA concentration changed from 1 to 0.43. For AM+A550+CM, HA concentration decreased from 1 to 0.42. For AM+A550+AM, HA concentration decreased from 1 to 0.40. Adsorption yielded a color change on the membrane surface. After experiments, no HA particles can be seen attached on the CM surface, while the AM surface became brownish yellow. HA removal due to A550 resin can be assumed to be the same for the above three combinations (about 57%), while the HA removal due to one piece of AM is about 1% (from 57% to 58% to 60%).

In the presence of applied voltage, HA concentration decreased faster than that without applied voltage. For AM+A550+CM, it decreased from 1 to 0.21. For AM+A550+AM, the HA concentration decreased from 1 to 0.22. For CM+A550+CM, it decreased a little slower than the above two. It changed from 1 to 0.24, about 76% HA removal. Similarly according to Equation 4-1 and Equation 4-2, HA removal due to electrosorption could be calculated and plotted in Figure 4.8. It is clear that the voltage can enhance HA removal efficiently for combination of AM+A550+CM.

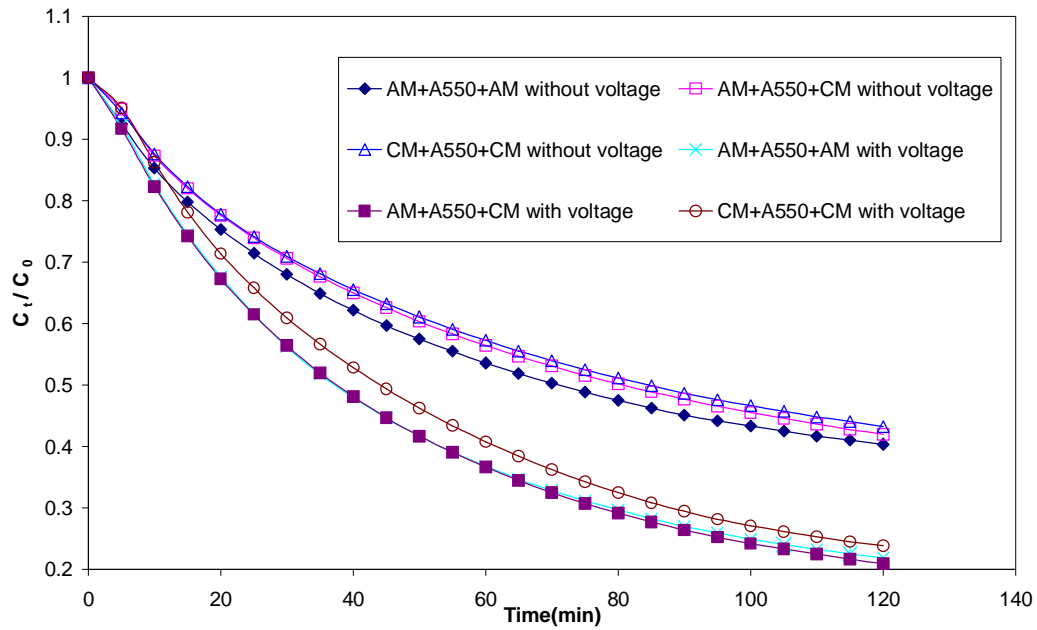


Fig. 4.7 HA concentration ratio as a function of time for a combination of A550 resin and membranes (experimental conditions refer to Table 4.1)

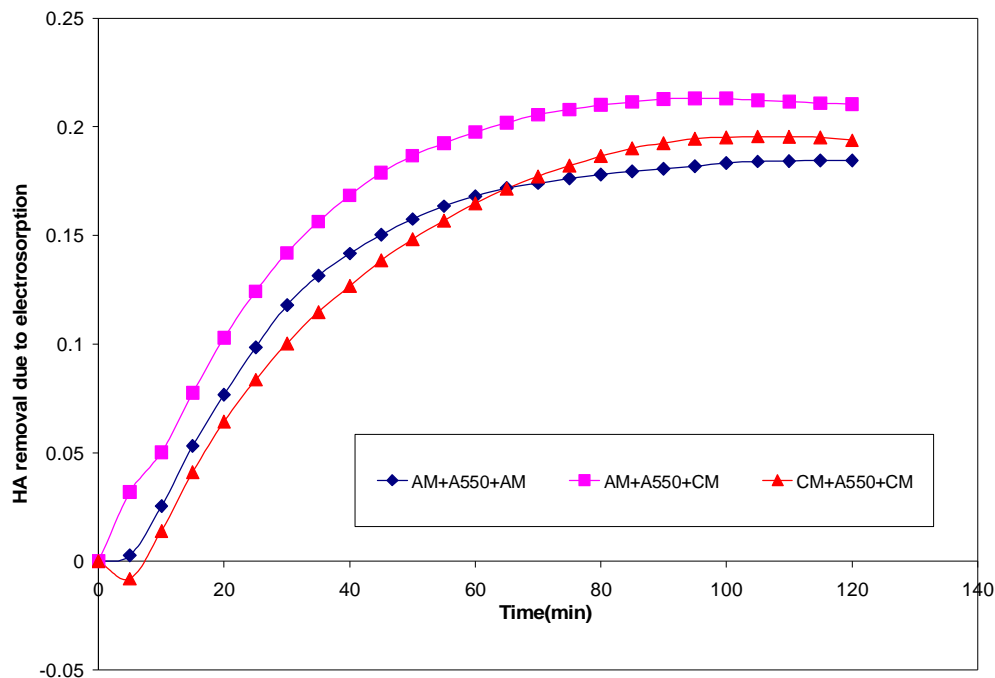


Fig. 4.8 HA removal due to electrosorption as a function of time for a combination of A550 resin and membranes (experimental conditions refer to Table 4.1)

After 120 min, the power was switched off and experiment ran for another 10 min. For CM+A550+CM, about 6.2% of removed HA particles was released to the solution. A small amount of HA particles was attached on the CM surface in the anode side and no HA particles were attached on the CM surface in the cathode side. For AM+A550+CM, about 2.4% of removed HA was released to the solution. The AM surface was brownish yellow while no HA particles attached on the CM surface. For AM+A550+AM, about 4.9% of removed HA was released to the solution. AM surface was brownish yellow and the color of the AM surface in the anode side was darker than the other.

The combination of AM+A550+AM is the most efficient way to remove HA from aqueous solution when the voltage is not applied. When the voltage is applied, it can enhance HA removal for a combination of AM+A550+CM the most.

4.2.5 Marathon C resin and membranes

Three combinations, i.e. AM+Marathon C+CM, AM+Marathon C+AM and CM+Marathon C+CM were used to do experiments. The experimental procedure was the same as described above.

The dimensionless HA concentration, i.e. C_t/C_0 as a function of time is plotted in Figure 4.9. In the absence of applied voltage, The HA concentration decreased very slowly for all three combinations. For CM+Marathon C+CM, the HA concentration changed from 1 to 0.96. For AM+Marathon C+CM, the HA concentration decreased from 1 to 0.95. For combination AM+Marathon C+AM, the HA concentration decreased from 1 to 0.94.

In the presence of applied voltage, the HA concentration decreased faster than that without voltage for all combinations. For AM+Marathon C+CM, it decreased from 1 to 0.40. For AM+Marathon C+AM, the HA concentration decreased from 1 to 0.55. For CM+Marathon C+CM, it decreased much slower than the above two. It changed from 1 to 0.83. Similarly the HA removal due to electrosorption was calculated according to Equation 4-1 and Equation 4-2 and plotted in Figure 4.10. It shows that the electric field can enhance the AM+Marathon C+CM the most evidently.

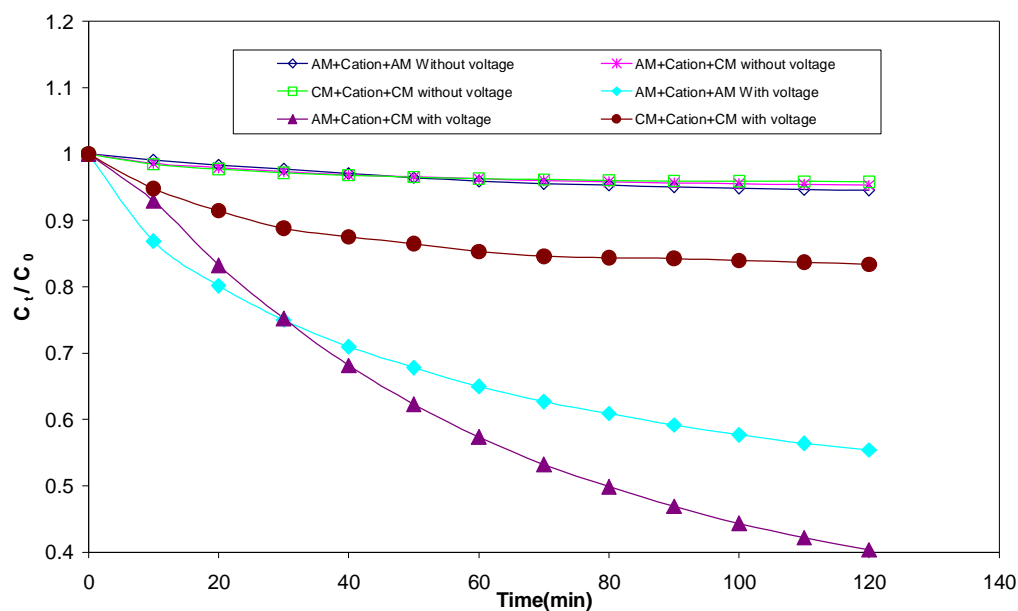


Fig. 4.9 HA concentration ratio as a function of time for a combination of Marathon C resin and membranes (experimental conditions refer to Table 4.1)

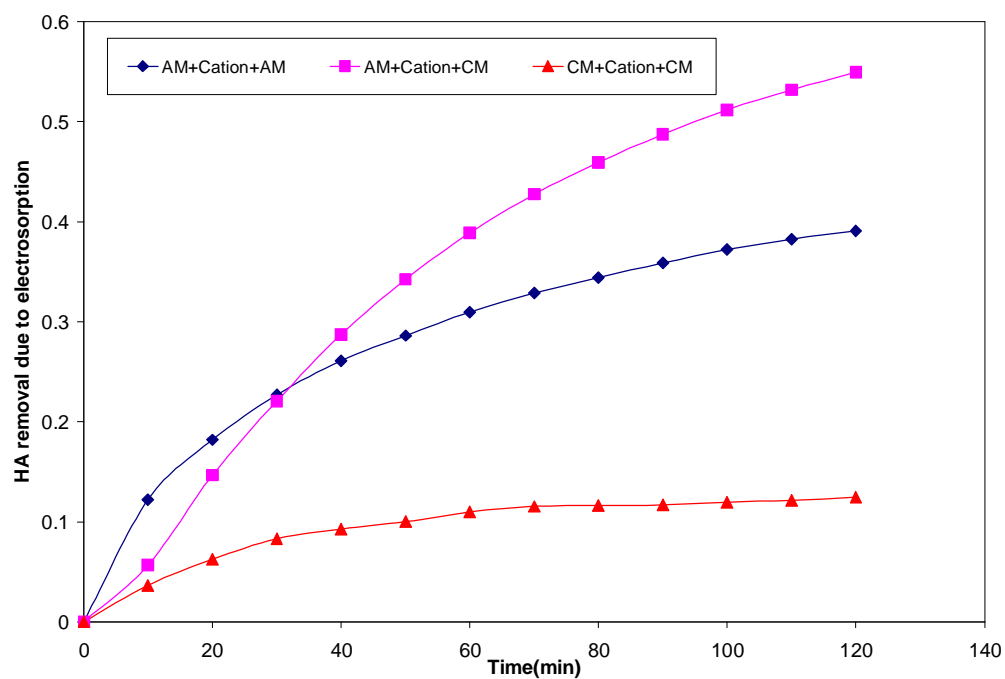


Fig. 4.10 HA removal due to electrosorption as a function of time for a combination of Marathon C resin and membranes (experimental conditions refer to Table 4.1)

After 120 min, the power was switched off and the solution was still flowing for another 10 min. For CM+Marathon C+CM, about 27.2% of removed HA particles were released to the solution. Similarly a small amount of HA particles attached on the CM surface in the Anode side and no HA particles were attached on the CM surface in the cathode side. For AM+Marathon C+CM, about 14.8% of removed HA was released to the solution. The AM surface was brownish yellow, while no HA particles were attached on the CM surface. For AM+Marathon C+AM, about 22.4% of removed HA was released to the solution. AM surface was brownish yellow and the color of AM surface in the anode side was darker than the other.

4.2.6 Summary and discussion for different combinations of membranes and resin

The total HA removal for different combinations after 120 min is calculated according to Eq.4-1 and Eq.4-2 (Table 4.2). The enhancement factor is calculated according to the following equation.

$$Enhancement \quad Factor = \frac{(h_T)_{with \quad voltage}}{(h_T)_{without \quad voltage}} \quad (4-3)$$

HA removal for different resins in the beaker is a little higher than that in the hybrid electrodialysis/ion exchange. Anion exchange resin is favorable for HA removal due to the electrostatic forces between resins and HA particles. Furthermore, Fig.4.1 shows that HA removal occurred mainly during the first 10 min for the resin in the beaker, but for the resin in the central chamber of hybrid electrodialysis/ion exchange, the concentration decreased slowly all the time. The resin and the HA solution in the beaker were stirred sufficiently and the HA removal rate may be controlled by the adsorption onto the resin

surface. Thus the HA concentration decreased quickly and the process finally reached an equilibrium. However, for the resin in the central chamber without voltage, the flow of the HA solution was not so fast. The HA removal rate may be controlled by the diffusion of ions through the film outside the resin particle and thus the removal of HA is slow. When the voltage was applied, it enhanced the diffusion of ions through the film and increased the HA removal obviously.

In the absence of voltage, the combination of AM+AM is the most favorable for HA removal with different resins (then AM+CM and CM+CM) due to adsorption of HA particles on the AM. However in the presence of voltage, the most favorable one is AM+CM (then AM+AM and CM+CM) and this is consistent with the situation without the resin. The results can be observed in Fig.4-6, Fig.4-8 and Fig. 4-10. When considering the enhancement of electric voltage on the HA removal, the MR3 resin is the most efficient in the presence of voltage for different membrane combinations (except AM+MarathonC+CM, refer to the fifth column in Table 4.2). After the power was switched off, HA was partially released from the central chamber to the solution. This means that the process was a combination of reversible and irreversible adsorption.

Table 4.2 Summary for different combinations of membranes and resins

Combination		Total HA removal ($\eta_{T \times 100}$)		HA removal due to electro-sorption ($\eta_{ele \times 100}$)	Removal enhancement factor	Release after power off (%)
		Without Voltage	With Voltage (40V)			
		I	II	II - I	II / I	
Only resin in the beaker	MR3	36	/	/	/	/
	A550	71				
	Marathon C	4.0				
Only membranes	AM+CM	<1.0	50	49	50	0.5
	AM+AM	7.0	40	33	5.8	4.6
	CM+CM	<1.0	25	24	25	100
MR3 resin and membranes	AM+MR3+CM	17	70	53	4.1	6.8
	AM+MR3+AM	19	62	43	3.3	13.9
	CM+MR3+CM	15	37	22	2.5	18.3
A550 resin and membranes	AM+A550+CM	58	79	21	1.4	2.4
	AM+A550+AM	60	78	18	1.3	4.9
	CM+A550+CM	57	76	19	1.3	6.2
Marathon C resin and membranes	AM+MarathonC+CM	5.0	60	55	12	14.8
	AM+MarathonC+AM	6.0	45	39	7.5	22.4
	CM+MarathonC+CM	4.0	17	13	4.3	27.2

In the absence of the electric field, HA particles may be retained by resins when the solution is passing around the resins. The capture takes place if particles come close to resin gels(due to pressure) to allow short-range attractive Van der Waals forces,

electrostatic attraction forces between the HA particles surface and resin surface to induce attachment (Matijevic et al., 1995; Johnson et al., 1996). In the presence of electric field, electric field adds other external forces to increase the probability of particles approaching sufficiently close to resin surfaces and consequently being captured (Judd, Solt, 1989). In the process, there are two stages (it is same as the two-step deposition process: transport and adhesion). The first stage consists of electrophoretic transport of HA particles from the flow to the surface of resins. Next, the HA particles are fixed there and the flow cannot remove them. For a suspended particle passing near the resins in the solution, there is a force balance.

For all the systems, the negatively charged HA particles move to the membrane surfaces and deposit on it. For AM in the Anode side, the electrophoretic force is favorable for deposition and more HA particles deposit in this case in comparison to that in the cathode side. For CM in the anode side, the electrophoretic force is able to overcome the electrostatic repulsion between CM and HA particles, thus HA particles deposit on the CM surfaces.

Similarly, HA particles move toward the surfaces of the resins under the above forces and the particles deposit on the resin surfaces. For example, A550, due to its positive charge, is desirable for deposition. However for Marathon C, the electrophoretic force should overcome the electrostatic repulsive force between HA particles and the negatively charged resin in order to deposit HA on the resin surfaces. For MR3, a mixture of anion and cation exchange resins, both situations occurred.

The collector's properties (the membrane and the resin) are important in attracting colloid particles in the presence of electric field. Zhang et al., (2000), Judd and Solt (1989), Barker et al., (1991) demonstrated that the surface charge and conductivity of collectors may affect the removal efficiency of colloid particles. The use of a conductive medium is desirable for particles collection. If the collector is nonconducting, the electric field lines will be diverted around the collector (granules or fibers). If the collector is a better conductor than the fluid, the electric field lines will be diverted toward the collector (granules or fibers). Since the particles are attracted along the electric field lines, it is desirable to have the lines diverted into (rather than around) the granule or fibers. The oppositely charged collector is desirable for particles attraction and the surface charge reduction has different effect for different collector medium. It is consistent with this study. AM and anion exchange resin are favorable for HA deposition.

After the power was switched off, part of the attached HA particles may be released to the bulk solution due to the disappearance of electrophoretic and other forces related to the electric field. For Marathon C, more HA particles were released due to electrostatic repulsive forces. HA was released more for the combinations containing Marathon C and CM (Table 4-2). The phenomenon that part of deposited colloid particles may be released after switching off the power was reported by many researchers (Verbich, et al., 1991; Barker, et al., 1991; Grebenyuk, et al., 1998). Verbich and Grebenyuk reported another mechanism of release after the power was turned off. When an electric field is turned on, the particles acquire an induced dipole moment, and dipole-dipole forces between them provide for cohesive interactions between particles, forming a multilayered sediment. With the electric fields that are not too high, the electrodeposition is of a reversible

nature, so that when the current is turned off and, accordingly, the induced dipole moments disappear, the cohesive forces between particles in the sediment disappear. Therefore, the sediment falls apart under the influence of viscous stresses of the liquid flow, and particles of the sediment are carried away.

When the conducting resin is in the electric field, it is polarized and there are numerous local interactions between the induced fields created by polarized granules (Barker et al., 1991). The distribution of lines of electric field strength in the gap between two spherical resin gels in a less conducting solution is shown in Figure 4.11. Lines in the gap begin at the surface of one granule and end at the surface of another. When the charged HA particles flow through the gap between granules, the particles will be retained on the surface of the resin due to the much higher electric strength in the gap between granules. The local electric field due to the polarized granule plays an important role in the deposition of HA particles. Thus it is easy to understand why the effect of electrical field was stronger for the mixture of different resins. Anion and cation exchange resin can form higher local electric field than only cation exchange resin or only anion exchange resin can. On the other hand, the combination of AM+CM is the best for HA removal. The mixture of resin is similar to the combination of many anion exchange and cation exchange membranes. The structure is similar to a bipolar membrane and may lead to high HA removal due to easier water dissociation and higher energy efficiency.

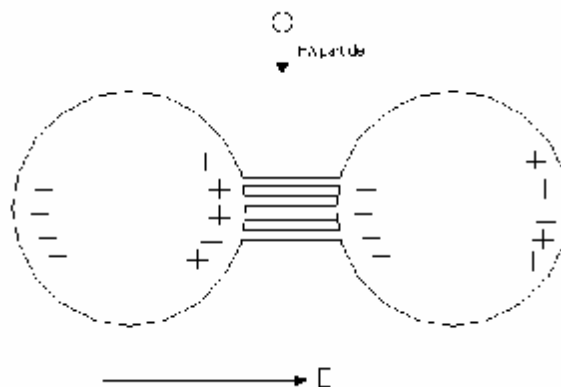


Fig. 4.11 Distribution of lines of an electric field strength in the gap between two spherical resin gels in a less conducting solution

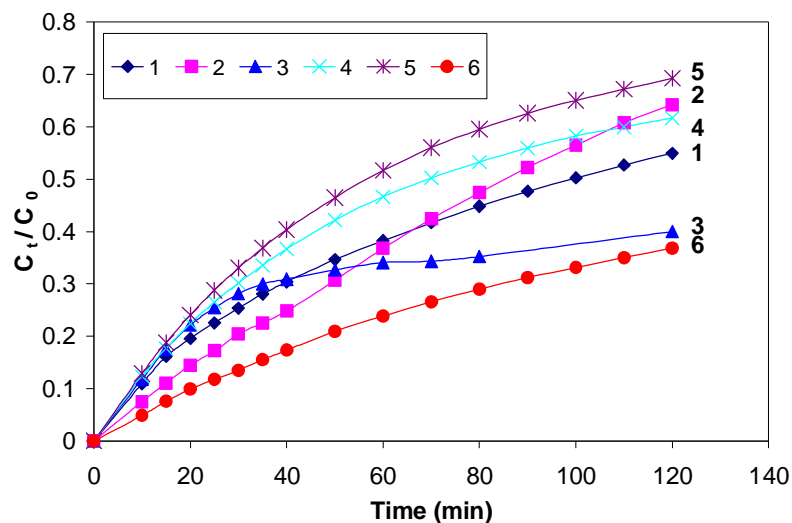
In order to describe the pros and cons of the hybrid electrodialysis/ ion exchange process in one unit in comparison to the system of electrodialysis and ion exchange connected in sequence, we need to compare HA removal efficiency of hybrid electrodialysis/ ion exchange process with that due to an electrodialysis process plus an ion exchange process (two separate processes together). Earlier experimental results of HA removal efficiency were obtained due to electrodialysis. HA removal due to only ion exchange in the system can be estimated in the following way:

One can assume that cation exchange membrane does not adsorb HA in the hybrid electrodialysis / ion exchange process without voltage, thus the HA removal rates due to ion exchange in the central chamber without voltage are equal to the experimental results for combinations of resin and CM+CM without voltage.

We obtained the HA removal efficiency of the hybrid electrodialysis/ion exchange from experiments (lines 4, 5, 6). We can calculate the HA removal efficiency due to electrodialysis plus ion exchange in sequence based on above two statements (lines 1, 2, 3). The comparisons are shown in Figure 4.12a, b, c. For the MR3 resin (Fig. 4.12a) and

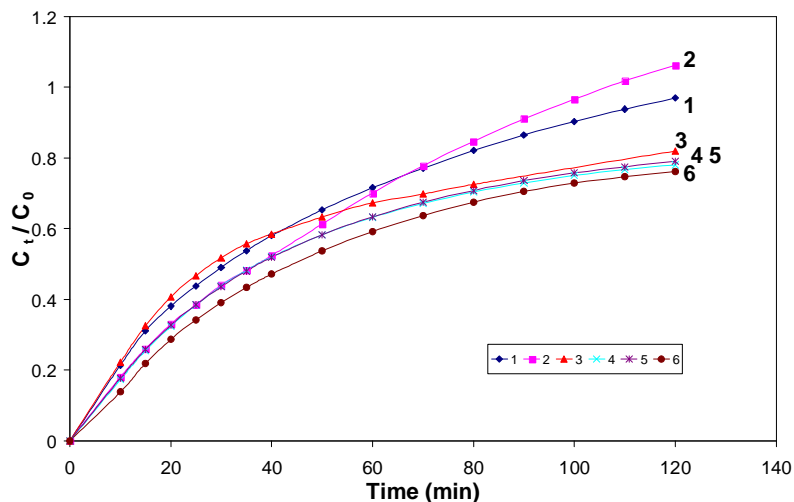
the Marathon C resin (Fig. 4.12 c), when combinations AM+AM and AM+CM (the normal ED membrane combination) were used, the experimental hybrid electro dialysis/ion exchange was better than the addition of electro dialysis and ion exchange (line 4 is higher than line 1, and line 5 is higher than 2). When CM+CM was used, the simple addition of electro dialysis and ion exchange was better than the hybrid electro dialysis/ion exchange (line 3 is higher than line 6). For the A550 resin (Figure 4.12b), the addition of electro dialysis and ion exchange was always better than the hybrid electro dialysis/ion exchange (lines 1, 2, 3 are higher than lines 4, 5, 6 respectively). Evidently, the effect of voltage is not that important or strong when the system (A550 resin) itself is effective in HA removal even without voltage. But to MR3 and Marathon C resin, the effect of voltage is more evident probably due to the induced dipole-dipole interaction. It is interesting that when the CM+CM was used, the simple addition of electro dialysis and ion exchange was always better than the hybrid electro dialysis/ion exchange no matter what resin was used.

A similar situation is observed when one considers the HA removal efficiency after 120min. The comparison is shown in Table 4.3. It is clear that for the A550 resin, it is better to have two processes in sequence to remove more HA particles. For example, HA removal rate for AM+AM plus A550 is about 97%, it is better than the hybrid system (78% removal efficiency). For the other two resins, it is better to have the two processes in one unit to have a hybrid electro dialysis/ion exchange process, leading to a higher HA removal efficiency. This would also save the space and probably decrease the capital investment in industry applications.



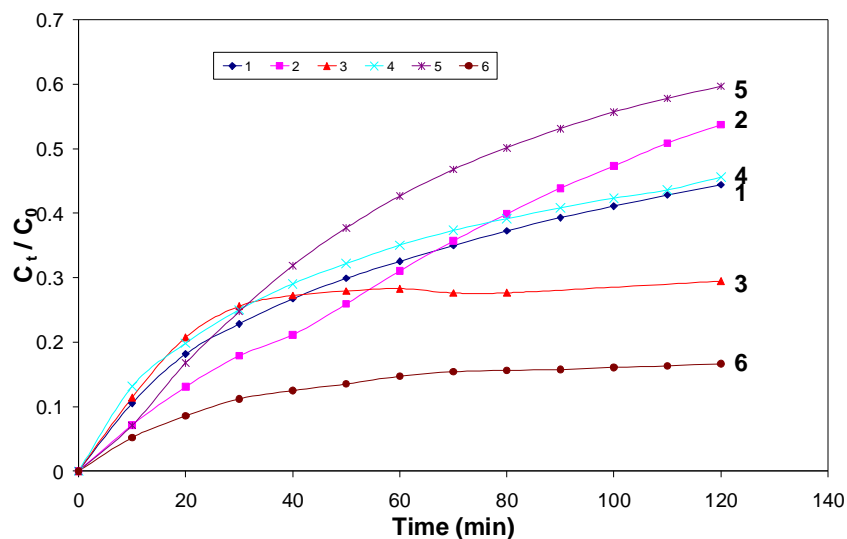
1:electrodialysis (AM+AM) plus MR3 resin; 2:electrodialysis (AM+CM) plus MR3 resin
 3:electrodialysis (CM+CM) plus MR3 resin; 4: hybrid system AM+MR3+AM
 5:hybrid system AM+MR3+CM; 6: hybrid system CM+MR3+CM

Fig.4.12a HA removal efficiency comparison for two systems, one is hybrid electrodiaysis/ion exchange, the other is electrodiaysis plus ion exchange (MR3 resin)



1:electrodialysis(AM+AM) plus A550 resin; 2:electrodialysis(AM+CM) plus A550 resin
 3:electrodialysis(CM+CM) plus A550 resin; 4: hybrid system AM+A550+AM
 5:hybrid system AM+A550+CM; 6: hybrid system CM+A550+CM

Fig.4.12b HA removal efficiency comparison for two systems, one is hybrid electrodiaysis/ion exchange, the other is electrodiaysis plus ion exchange (A550 resin)



1:electrodialysis (AM+AM) plus Marathon C resin; 2:electrodialysis (AM+CM) plus Marathon C resin; 3:electrodialysis (CM+CM) plus Marathon C resin; 4: hybrid system AM+Marathon C +AM; 5:hybrid system AM+Marathon C+CM; 6: hybrid system CM+Marathon C+CM

Fig.4.12c HA removal efficiency comparison for two systems, one is hybrid electrodialysis/ion exchange, the other is electrodiaysis plus ion exchange (Marathon C resin)

4.3 Conclusions

In the absence of applied voltage, the hybrid electrodialysis/ion exchange process can remove HA particles due to electrostatic attraction forces between HA particles and surfaces of membranes and resins. Anion exchange resin and anion exchange membrane can remove HA more efficiently than cation exchange resin and cation exchange membrane. Thus, the combination of AM+A550+AM is the most favorable for HA removal.

Electric field can enhance HA removal for the hybrid process. However the enhancement factor is different for different combinations. The combination of AM+ MR3+CM is the best one for HA removal, because the MR3 resin and the combination of AM+CM can

form the strongest local electric field and can easily dissociate water, which may enhance HA removal.

Table 4-3 HA removal efficiency comparison for the two systems (one is hybrid electrodialysis/ion exchange, the other is electrodialysis plus ion exchange process)

Combination of membranes and resins	Removal efficiency (%)			
	Electrodialysis(ED) plus ion exchange(IX)			Hybrid electrodialysis/ion exchange
	ED	IX	ED+IX	
AM+MR3+CM	50	15	65	70
AM+MR3+AM	40	15	55	62
CM+MR3+CM	25	15	40	37
AM+A550+CM	50	57	127	79
AM+A550+AM	40	57	97	78
CM+A550+CM	25	57	82	76
AM+Marathon C+CM	50	4.0	54	60
AM+Marathon C+AM	40	4.0	45	45
CM+Marathon C+CM	25	4.0	29	17

In the presence of applied voltage, a much stronger local electric field is induced due to the polarized resin and the HA particles are polarized. Initially, HA particles move under the electric field. When the HA particles come close to the gap between resins, the stronger local electric field makes the HA particles deposit on the surface of resin. Secondly the polarized HA particles can have dipole-dipole interactions and form condensed sediment on the surface of the resin. The electric field clearly enhances the

HA deposition on the surface of the ion exchange resin. In the process, there is a state that depends on the physical and electrochemical properties of solution, resins and membranes. When the electric field is switched off, the electric force and the dipole-dipole interaction disappear and thus the force balance breaks down. HA particles are released and carried away when a fluid flows through the central chamber. The amount of released HA depends on the properties of resins, membranes and solution.

Chapter 5

Effect of Experimental Parameters on HA Removal in Single-pass Operation Mode for a Combination of AM+MR3+CM

5.1 Introduction

In the hybrid electrodialysis/ion exchange process, many factors could affect the HA removal efficiency. It is discussed in Chapter 4 that AM+MR3+CM is the best combination in enhancing HA removal under the 40 V electric field. Many operational parameters, such as voltage, flow rate and electrolyte concentration may affect the HA removal efficiency. The physical and chemical properties of HA solution, i.e. pH, ionic strength, concentration, heavy metal ions may affect HA removal in adsorption, microfiltration, electrodialysis process(Yuan et al., 1999; Keil et al., 2000; Arnason, et al., 2000; Bai et al., 2001; Kim et al., 2002; Lee et al. 2002; Ka tsumata et al., 2003; Zhang et al., 2003). Thus these properties may affect HA removal in hybrid electrodialysis/ion-exchange process.

In order to investigate the effects of different parameters, a series of experiments were conducted in the single-pass operation mode and in the recycling operation mode. This Chapter describes the results in the single-pass operation mode. Firstly, pH change of HA solution/electrolyte solution and current change in a single-pass operation mode are described. Secondly, the effects of different parameters on HA removal efficiency are

discussed. The next Chapter shows the experimental results in the recycling operation mode.

5.2 Results and discussion

5.2.1 pH Change in HA and electrolyte solutions during the experiment

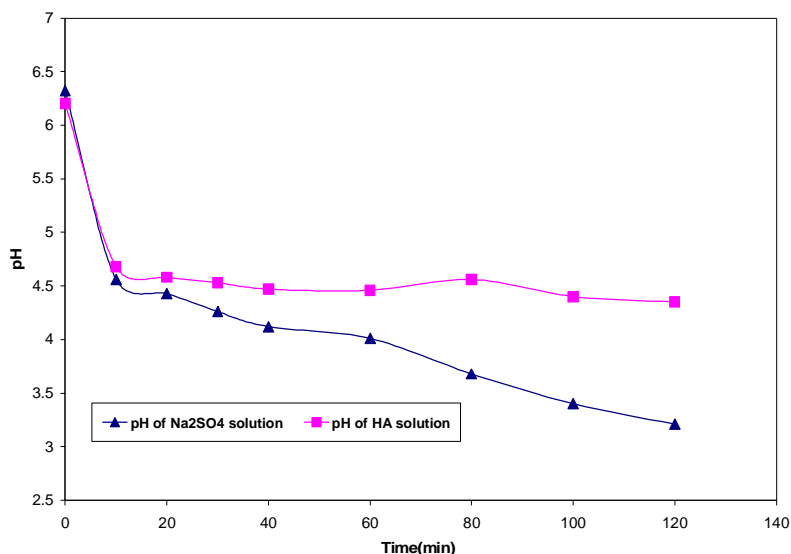


Fig.5.1 pH of HA solution and pH of electrolyte solution as a function of time during the experiment in single-pass operation mode (12.6 ppm HA solution without salt, pH of HA solution and electrolyte solution about 6.0-6.9, 4.8ml/min for HA solution, 3.7ml/min for electrolyte, 40V voltage applied)

In a single-pass operation mode, pH of HA solution and pH of Na₂SO₄ solution changed during experiment (Figure 5.1). Both pH of HA solution and electrolyte solution decreased quickly from 6.5 to 4.5 in about 10 min. Later pH of HA solution was practically constant while pH of electrolyte solution further decreased from 4.5 to 3. When the A⁻ was retained in the central chamber, H⁺ was formed due to HA particles dissociation and pH of HA solution after the central chamber decreased. Probably it

reached a steady state and pH was practically constant. On the other hand, probably due to electrolysis in the electrode, pH of electrolyte solution further decreased.

5.2.2 Current change of circuit during the experiment

The current of the circuit was measured by an Ampermeter. A typical change is shown in Figure 5.2. Although during the process, the surface of the resin and membrane changed, the current decreased only slightly, i.e. from 95.0mA to 94.2mA in 120min. This means that the electrical resistance of the circuit was practically constant and equaled to 420 Ω (40V/95.0mA).

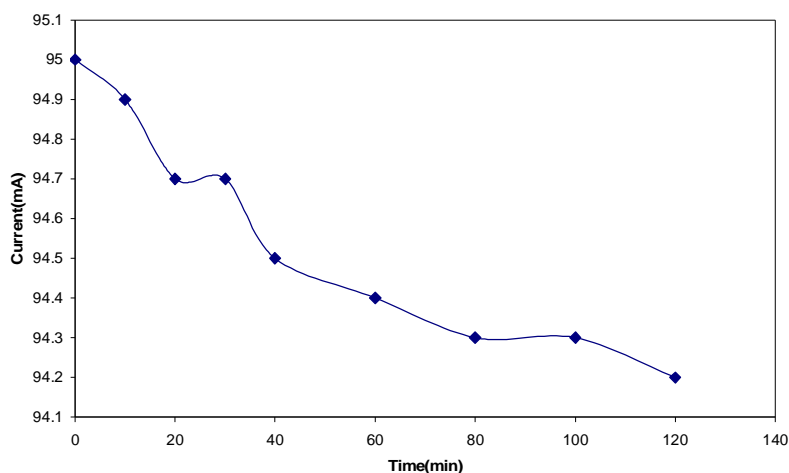


Fig.5.2 Current of circuit as a function of time during experiment in single-pass operation mode (12.6 ppm HA solution without salt, pH of HA solution and electrolyte solution about 6.0-6.9, 4.8ml/min for HA solution, 3.7ml/min for electrolyte, 40V voltage applied)

5.2.3 Different parameters effect

Different parameters effects in a single-pass operation mode were also studied. The particulars of the experiments are shown in Table 5.1. All the resins (14g) used were

fresh and washed with DI water. The combination of AM+MR3+CM and the normal current direction mode were applied.

Table 5.1 Different experimental conditions for HA removal in a single-pass operation mode

Different Parameters	Experimental Conditions	
	Change	Other
Voltage	10V, 20V, 30V, 40V and 50V	12.6 ppm HA solution without salt, 0.005M Na ₂ SO ₄ , pH of HA solution and electrolyte solution about 6.0-6.9, 4.8ml/min for HA solution, 3.7ml/min for electrolyte
Electrolyte concentration	0.005M, 0.01M and 0.025M Na ₂ SO ₄	12.6 ppm HA solution without salt, pH of HA solution and electrolyte solution about 6.0-6.9, 4.8ml/min for HA solution, 3.7ml/min for electrolyte, 40V voltage applied
Flowrate	2.4ml/min, 7.8ml/min and 7.2ml/min of HA solution	10.0ppm HA solution without salt, 0.005M Na ₂ SO ₄ , pH of HA solution and electrolyte solution 6.0-6.9, flowrate of electrolyte solution is 3.7ml/min, 40V voltage applied
HA concentration	10.5ppm, 17.0ppm and 24.3ppm	pH of HA solution (without salt) and electrolyte solution about 6.0-6.9, 0.005M Na ₂ SO ₄ , 4.8ml/min for HA solution, 3.7ml/min for electrolyte, 40V voltage applied
pH	pH2.21, pH6.42 and pH12.01	24 ppm HA solution without salt, 0.005M Na ₂ SO ₄ , pH of electrolyte solution about 6.8, 4.2ml/min for HA solution, 4.0ml/min for electrolyte, 40V voltage applied
Ionic Strength	0M, 0.02M and 0.1M NaCl	24 ppm HA solution, 0.005M Na ₂ SO ₄ , pH of HA solution and electrolyte solution about 6.0-6.9, 4.2ml/min for HA solution, 4.0ml/min for electrolyte, 40V voltage applied
Cu	0mM, 0.0104mM, 0.515mM and 2.507mM Cu ₂ SO ₄	12.6 ppm HA solution, 0.005M Na ₂ SO ₄ , pH of HA solution and electrolyte solution about 6.0-6.9, 4.8ml/min for HA solution, 3.7ml/min for electrolyte, 40V voltage applied

We assume that HA removal in the hybrid electrodialysis/ion exchange is similar to deep-bed filtration when it reaches steady state. In this case, a similar equation to the equation developed by Herzig, et al and Tien could be used to interpret the experimental data:

$$\ln\left(\frac{C}{C_o}\right) = -\lambda Z \quad (5-1)$$

Here C is HA concentration at the distance Z from the inlet of central chamber, C_o is feed concentration at the inlet of central chamber, and λ is the filter coefficient.

Considering the HA concentration at the outlet of central chamber when the length of central chamber is L, one obtains:

$$\ln\left(\frac{C_t}{C_o}\right) = -\lambda L \quad (5-2)$$

Generally, λ is a function of the state of filter media as well as the operating variables, such as voltage, flowrate and solution properties.

5.2.3.1 Voltage effect

Five different voltages (10V, 20V, 30V, 40V and 50V) were used to study the voltage effect on HA removal in the single-pass operation mode. The results (C_t/C_o) are shown in Figure 5.3 (C_t is HA concentration at the outlet of central chamber, C_o is the feed HA concentration.). The concentration C_t changed with time and then reached steady state. It

shows a transient process and it means that filter coefficient is a function of time. Time to reach the steady state was shorter (reason is still not clear) and the final steady state effluent concentration was higher for the lower applied voltage. Higher voltage led to higher HA removal; however when voltage was higher than 40 V, the removal efficiency did not increase so much as it was between 10 and 40V. It means that when the voltage is higher than the voltage related to the limiting current which was demonstrated in Aatmeeyata's thesis, the energy is wasted in the form of heat due to higher current generated by water dissociation and concentration polarization.

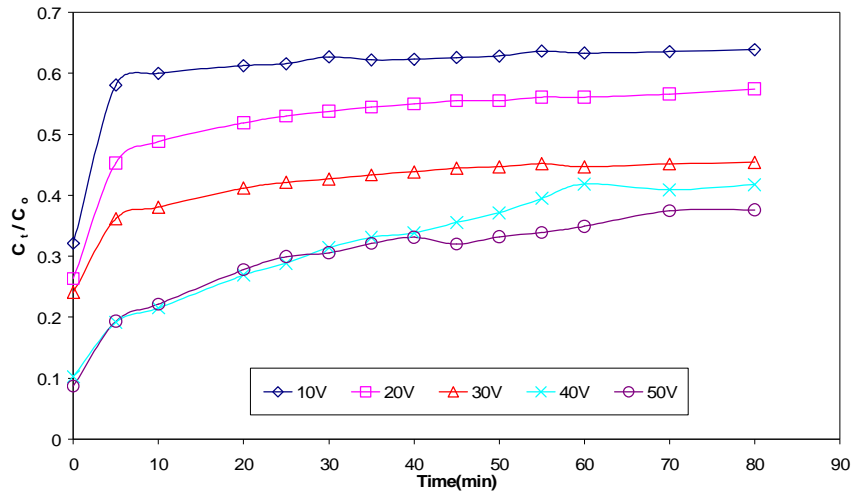


Fig. 5.3 HA concentration ratio as a function of time for different voltages in a single-pass operation mode (experimental condition refer to Table 5.1)

λ (cm^{-1}) at 80 min could be calculated by Eq. 5-2 when L is 6 cm for different voltage. λ as a function of voltage is plotted in Figure 5.4. It shows that λ increased with the applied voltage.

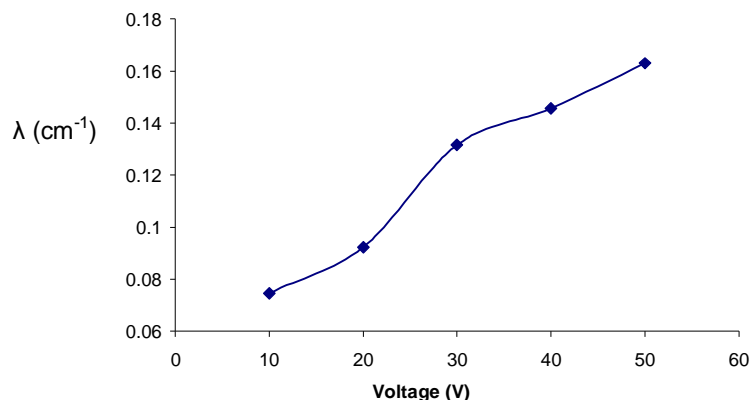


Fig. 5.4 Filter coefficient as a function of voltage in a single-pass operation mode(experimental conditions refer to Table 5.1)

5.2.3.2 Electrolyte concentration effect

Three different concentrations of Na_2SO_4 solution (0.005M, 0.01M and 0.025M) were used in the side chamber to find out the electrolyte concentration effects on HA removal in the single-pass operation mode. HA concentration ratio as a function of time is plotted for different electrolyte concentrations (Figure 5.5). Again the data shows a transient behavior. Furthermore, an increase in the electrolyte concentration led to higher HA removal and when the electrolyte concentration was high (0.01M and above), the resistance was controlled by other steps; the increase in electrolyte concentration did not affect the current anymore and thus did not affect HA removal.

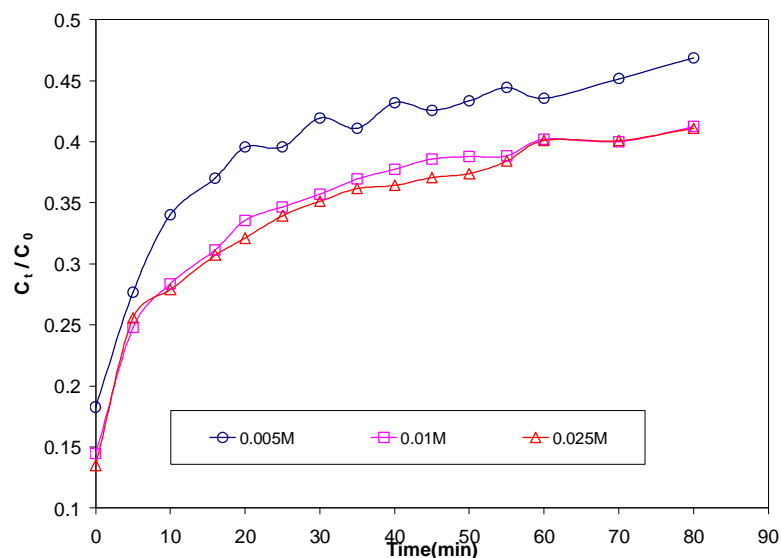


Fig. 5.5 HA concentrations ratio as a function of time for different electrolyte concentration in single-pass operation mode(experimental conditions refer to table 5.1)

λ as a function of electrolyte concentration (calculated by Eq. 5-3 at 80 min) is plotted in Figure 5.6. It is clear that λ increased with the electrolyte concentration and kept constant at higher concentrations.

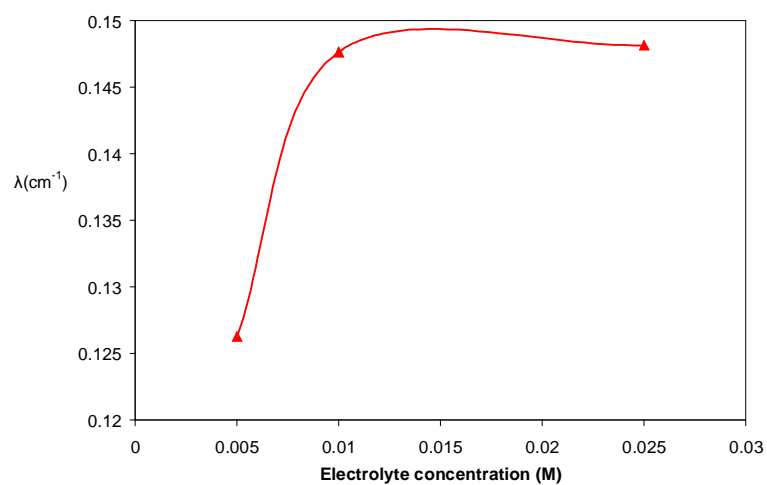


Fig.5.6 Filter coefficient as a function of electrolyte concentration in a single-pass operation mode

5.2.3.3 Flow rate effect

Three different flow rates of the HA solution (2.4ml/min, 4.8ml/min and 7.2ml/min) were used to do experiments in order to find out the flow rate effects on HA removal in the single-pass operation mode. The HA concentration ratio as a function of time in the single-pass operation mode is shown in Figure 5.7. Similarly, all the kinetics had a transient behavior. HA removal decreased with an increase in the flow rate from 2.4 to 4.8ml/min, but when the flow rate was higher than 4.8ml/min, HA removal stayed almost the same.

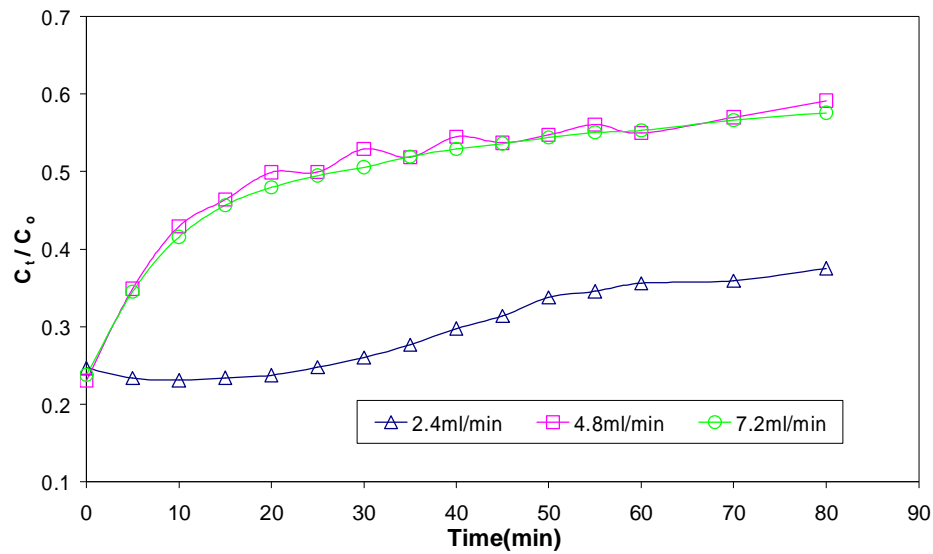


Fig 5.7 HA concentration ratio as a function of time for different flow rates in a single-pass operation mode(experimental conditions refer to Table 5.1)

λ as a function of flow rate at 80 min, is plotted in Figure 5.8. Similarly, λ decreased with an increase in the flow rate and remained constant at higher flow rates. A higher flow rate means higher velocity of HA particles passing through and a shorter time to pass through the central chamber. On the other hand, it can be interpreted from the perspective of force

balance of the HA particles and possibility of deposition. Firstly, higher flow rate makes the HA particles easier to reach the surface of resin than the lower flow rate, which means the possibility of HA attaching on the surface of resin and membrane increases. Secondly, higher flow rate means a higher drag force, which leads to the difficulties for the HA particles to deposit onto the surface of resins and membrane. When the flow rate increases, the negative effect is dominant, thus higher flow rate leads to a lower HA removal. However, later there is a balance of the two effects and the removal rate keeps practically constant.

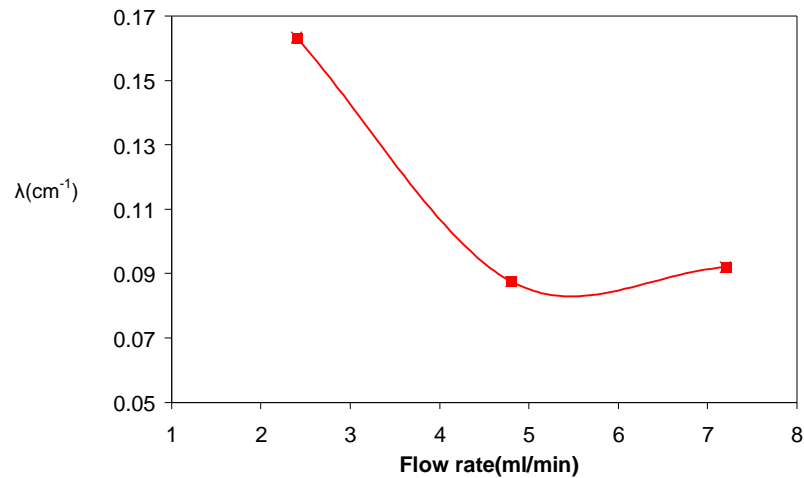


Fig.5.8 Filter coefficient as a function of flow rate in a single-pass operation mode(experimental conditions refer to Table 5.1)

5.2.3.4 HA concentration effect

Three different HA concentrations (10.5ppm, 17.0ppm and 24.3ppm) were used in these experiments. The results are shown in Figure 5.9. Firstly, a transient process was observed. Secondly, at initial phase, higher concentration led to higher relative HA removal, but at the steady state, lower concentration led to slightly higher HA removal.

For higher concentrations, there may have aggregation and particles are larger, which is easier for the resin to retain in the chamber at the initial phase.

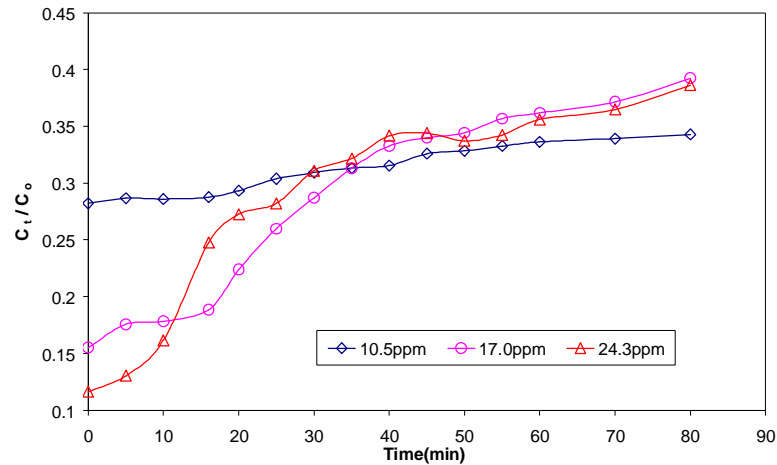


Fig.5.9 HA concentration ratio as a function of time for different initial HA concentration in a single-pass operation mode (experimental conditions refer to Table 5.1)

At 80 min, λ as a function of HA concentration is plotted in Figure 5.10. λ decreased with an increase in the HA concentration and remained almost constant at higher HA concentrations.

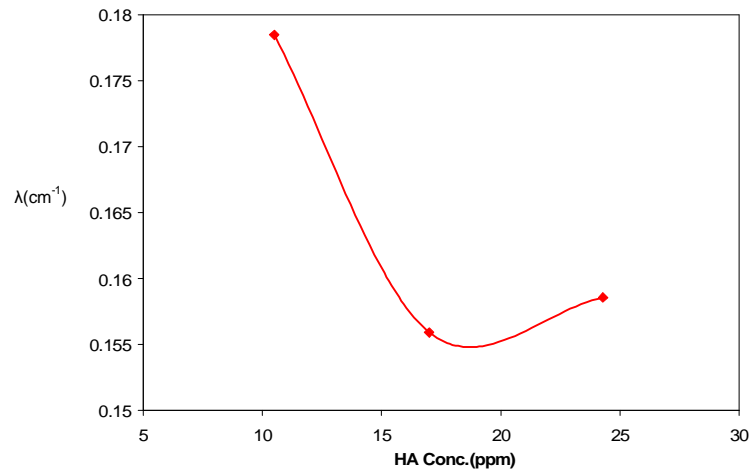


Fig.5.10 Filter coefficient as a function of HA concentration in a single-pass operation mode (experimental conditions refer to Table 5.1)

5.2.3.5 pH effect

Three different HA solutions with pH 2.21, pH6.42 and pH 12.01 were used. HCl and NaOH were used to adjust the pH of the HA solution. The HA concentration ratio (C_t/C_0) as a function of time is shown in Figure 5.11. A transient process was observed as well. For pH 2.21, the effluent concentration increased from 0.1 to 0.85 during the time from 5min to 100min. For pH 6.42, the effluent concentration increased from 0.26 to 0.58 and for pH 12.01, the effluent concentration increased from 0.30 to 0.67. It seems that the final effluent concentration is the lowest for pH 6.42. The reason is still needs more investigation.

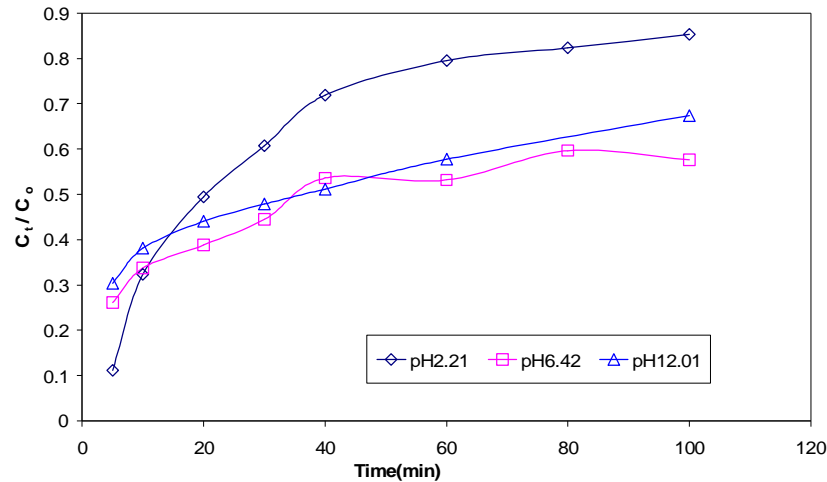


Fig.5.11 HA concentration ratio as a function of time for different pH values of HA solution in a single-pass operation mode (experimental conditions refer to Table 5.1)

At 20min, 40min, 60 min and 80 min, λ as a function of pH of HA solution is plotted in Figure 5.12. Firstly, λ decreased with time going for the same pH. Secondly, λ increased first and then decreased with the increase of pH of HA solution. So it is clear that pH near neutral is desirable for HA removal. However the difference between 6.42 and 12.01 is not evident.

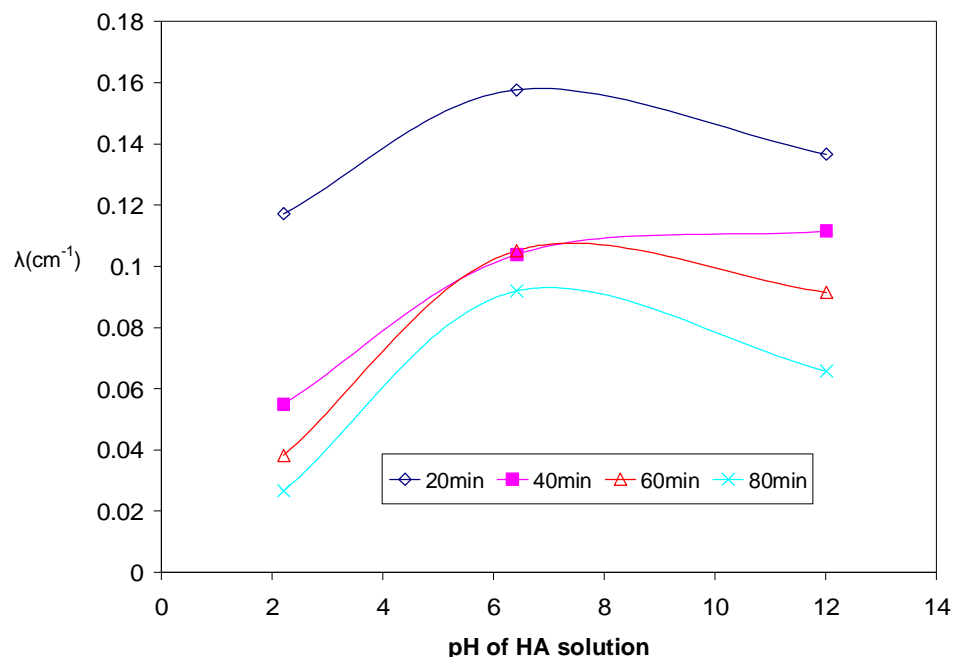


Fig.5.12 Filter coefficient as a function of pH of HA solution in a single-pass operation mode(experimental conditions refer to Table 5.1)

5.2.3.6 Ionic strength effect

Three 24 ppm HA solutions containing different concentrations of NaCl (0M, 0.02M and 0.1M) were used in these experiments. Results are shown in Figure 5.13. Again, a transient process was observed. In the initial phase, a higher salt is desirable for HA removal. In the end, a HA solution without salt is desirable for HA removal. But the difference was not evident.

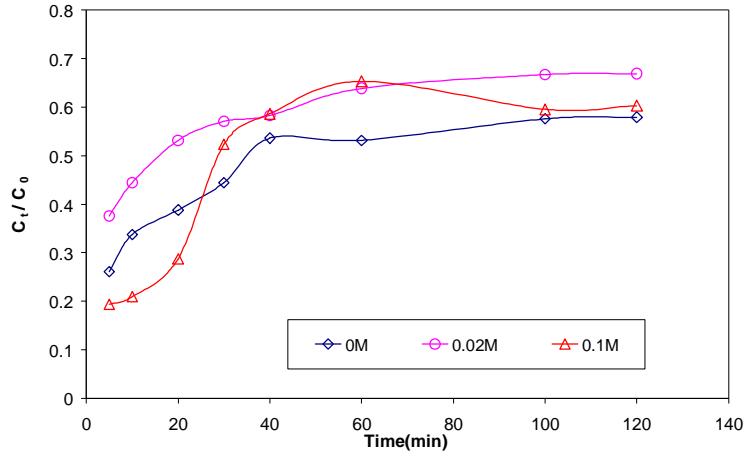


Fig.5.13 HA concentration ratio as a function of time for different ionic strengths of the HA solution in a single-pass operation mode (experimental conditions refer to Table 5.1)

λ as a function of NaCl concentration in the HA solution is plotted in Figure 5.14. λ without NaCl and with higher concentration were the largest during the experiment, but the difference was near 10-20%..

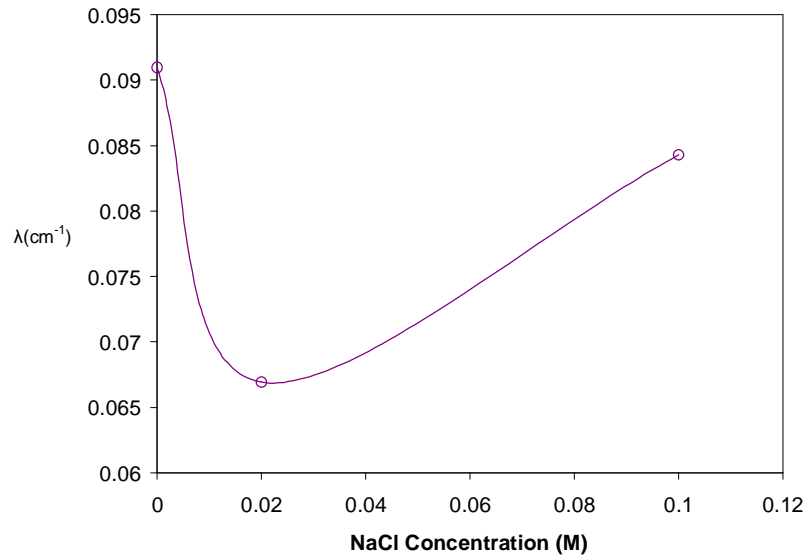


Fig.5.14 Filter coefficient as a function of NaCl concentration in HA solution in a single-pass operation mode(experimental conditions refer to Table 5.1)

5.2.3.7 CuSO₄ concentration effect

Four HA solutions containing different CuSO₄ concentrations (0mM, 0.1mM, 0.5mM and 2.5mM) were used to do experiments in order to investigate the Cu effects on HA removal. The result is shown in Figure 5.15. For 0mM, the effluent HA concentration increased from 0.19 to 0.41. For 0.1mM, the effluent HA concentration increased from 0.20 to 0.42. For 0.5mM, the effluent HA concentration increased from 0.30 to 0.43. However for 2.5mM, the effluent HA concentration increased from 0.15 to 0.22 in about 20 min and then reached steady state. When the Cu concentration is sufficiently high, the HA removal increases and is even higher than that without the addition of Cu.

When the copper concentration is not so high, the behavior of copper is just like other salts, such as NaCl. For lower copper concentration, initial HA removal decreases with the addition of copper. At higher copper concentration, HA particles become positively charged due to compound. Thus it may lead to a higher HA removal.

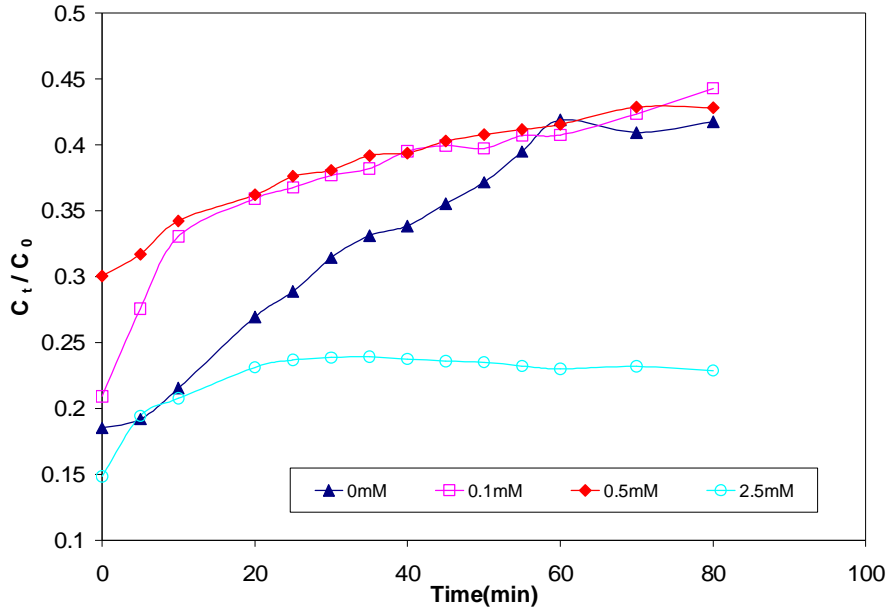


Fig.5.15 HA concentration ratio as a function of time for different copper concentration in a single-pass operation mode(experimental conditions refer to Table 5.1)

Another phenomenon was observed during the experiments. When 2.5mM CuSO₄ was used, at the inlet of the central chamber, the mixture of anion and cation ion exchange resins became blue with time. It means that copper ions were concentrated at the surface of the resin and inside the structure of resin. There maybe two reasons for this phenomenon. One is the HA particles attached on the surface of resin and membrane interacts with Cu²⁺ and acts as a large resistance to copper ion migration. The other is the flux of copper through the membrane is less than the adsorption of copper complex and ion exchange of copper ion. similar to the common EDI set-up, the copper stays in the inlet of resin and can not be recovered by the water dissociation.

At 80 min, λ as a function of CuSO₄ concentration in HA solution is plotted in Figure 5.16. λ decreased initially and then increased with the addition of CuSO₄. It seems that a

lower CuSO_4 concentration or a higher concentration in HA solution are desirable for HA removal.

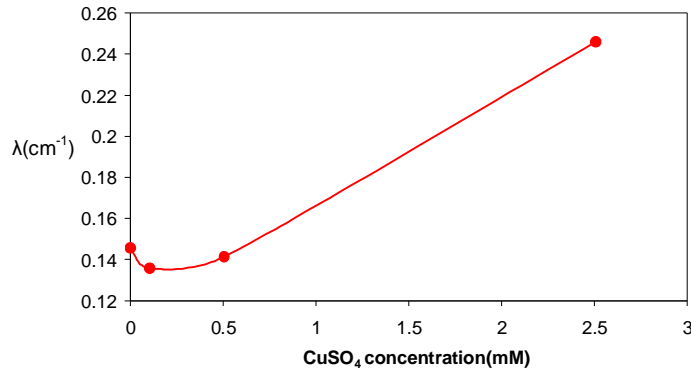


Fig.5.16 Filter coefficient as a function of CuSO_4 concentration in HA solution in a single-pass operation mode(experimental conditions refer to Table 5.1)

5.3 Conclusions

Effect of different parameters on HA removal was studied in the single-pass operation mode for the system AM+MR3+CM. During all these experiments, both the pH of HA solution and electrolyte solution decreased and the electrical current of the circuit was practically constant. An increase of voltage from 10 to 40 V leads to higher HA removal. Higher electrolyte concentration, lower flow rate and lower HA concentration could lead to higher HA removal rate. Because the ions in the central chamber will diffuse through the membrane, the effect of pH and salt concentration are special. It was found that neutral pH and lower salt concentrations are favorable for HA removal by a hybrid electrodialysis/ion-exchange process.

All the experiments show a transient behavior and the process can be explained by an equation similar to the dead-end filtration equation when it reaches a steady state. During

the transient behavior, the filter coefficient is not a constant and it decreases with time. The filter coefficient is also a function of different operational parameters and solution properties. Because there are not sufficient experiments for one parameter, the function can not be developed in this thesis.

Chapter 6

Effect of Experimental Parameters on HA Removal in Recycling operation mode for Combination of AM+MR3+CM

6.1 Introduction

In Chapter 5, effect of different parameters on HA removal in the single-pass operation mode were demonstrated. This chapter shows effect of different parameters on HA removal in the recycling operation mode.

Firstly, HA particle size changes, pH change of HA solution and electrolyte solution and electrical current changes are demonstrated. Secondly, effect of different parameters on HA removal are discussed (Former students experiments results are included. However the data are reanalyzed by the author.). Finally a conclusion is drawn.

6.2 Results and Discussion

6.2.1 HA particle size change during experiment

The effective diameter of HA particles at different time is shown in Fig.6.1. During the experiment, it decreased slowly, but after the voltage was turned off, the diameter of released HA particles increased quickly. The reason was that large HA particles could be easily moved to surface of the resin and membrane under the electric field and deposited there, forming larger aggregates. Similar results were observed by Arnarson et al.

(2000), Lee et al. (2002), Katsumata et al. (2003) in adsorption and electrodialysis process. However, after the voltage was cut, the electric force and the dipole-dipole interactions between particles disappeared. HA particles of deposited sediment came out with large size (larger than 5000 nm) under the drag force of the fluid.

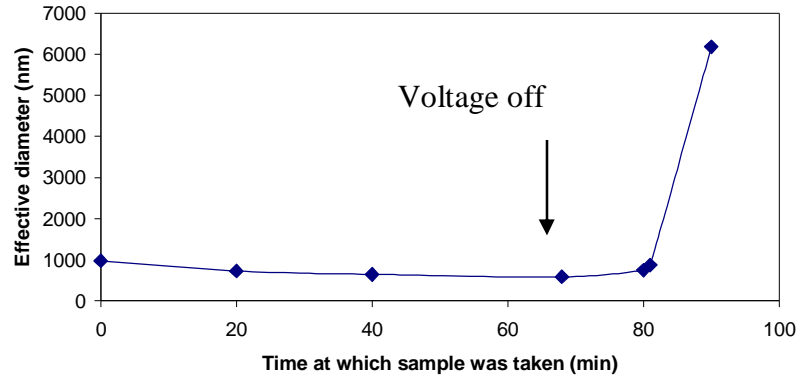


Fig.6.1 Effective particle diameter of HA at different time in a recycling operation mode
At 80min, the voltage was switched off

6.2.2 pH change in HA and electrolyte solutions during experiment

In a recycling operation mode, pH change of HA solution and pH change of Na_2SO_4 solutions are shown in Figure 6.2. Both pH of HA solution and electrolyte solution decreased quickly from 5.5 to 4 in about 20 min. The A^- is retained by the resin and H^+ stays in the HA solution, leading to pH decrease. At the same time, H^+ diffuse through the membrane to the side chamber, leading to pH decrease of electrolyte solution.

6.2.3 Current change in the circuit during the experiment

The electrical current of the circuit kept almost same between $89.0 \pm 0.1 \text{ mA}$ for a typical experiment in a recycling operation mode. It meant that the electrical resistance of the circuit did not change. The resistance was about 450Ω ($40 \text{ V} / 89 \text{ mA} = 450 \Omega$).

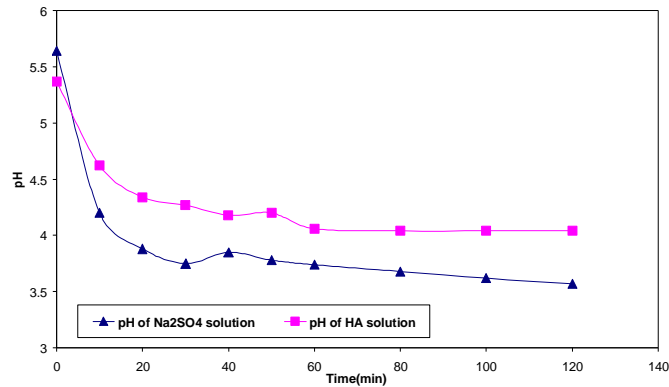


Fig.6.2 pH of HA solution and pH of Na_2SO_4 solution as a function of time during the experiment in a recycling operation mode

6.2.4 Different parameters effect

The particulars of the experiments are shown in Table 6.1. The resin (14g) used was fresh and washed with DI water. The combination of AM+MR3+CM and the normal current direction mode (The anode was in the side of AM) were applied.

In Chapter 5, Eq.5-3 is used to describe the process in a single-pass operation mode. λ is function of time (transient behavior) for the same experiment conditions. In a recycling operation mode, mass balance for feed tank could be formulated when the system reaches steady state.

$$-V_f \frac{dC}{dt} = Q_f [C - C \cdot \exp(-I \cdot l)] = Q_f \cdot C [1 - \exp(-I \cdot l)] \quad (6-1)$$

where V_f is the volume of feed solution, Q_f is flow rate of feed solution.

λ is not a constant (not steady state), thus it is difficult to get a equation to describe the concentration change in the recycling operation mode mathematically. However, when λ is large, HA concentration changes more.

Table 6.1 Different experimental conditions for HA removal in the recycling operation mode

Different Parameter	Experimental Conditions	
	Change	Others
Voltage	0V, 20V, 40V, 50V and 60V	320ml 14-16ppm HA solution without salt, 320ml 0.005M Na ₂ SO ₄ , 96ml/min flowrate for HA solution and electrolyte solution
Electrolyte concentration	0.005M and 0.025M Na ₂ SO ₄	200ml 17-18ppm HA solution without salt, 200ml Na ₂ SO ₄ , 4.8ml/min for HA solution, 3.7ml/min for electrolyte, 40V voltage applied
Flowrate	96ml/min and 192ml/min of HA solution	320ml 14-16ppm HA solution without salt, 320ml 0.005M Na ₂ SO ₄ , flowrate of electrolyte solution is 96ml/min, 40V voltage applied
HA concentration	7.3ppm, 14.3ppm, 26ppm and 29.2ppm	320ml HA solution without salt, 320ml 0.005M Na ₂ SO ₄ , 96ml/min for both HA solution and electrolyte solution, 40V voltage applied
pH	pH3.68, pH6.23 and pH10.90	200ml 23-24 ppm HA solution without salt, 200ml 0.005M Na ₂ SO ₄ , 4.8ml/min for HA solution, 3.7ml/min for electrolyte, 40V voltage applied
Ionic Strength	0M, 0.01M and 0.05M NaCl	200ml 16 ppm HA solution, 200ml 0.005M Na ₂ SO ₄ , 96ml/min for both HA solution and electrolyte solution, 40V voltage applied
Cu	0mM, 0.1mM and 0.5mM Cu ₂ SO ₄	200ml 16-18 ppm HA solution, 200ml 0.005M Na ₂ SO ₄ , 4.8ml/min for HA solution, 3.7ml/min for electrolyte, 40V voltage applied

6.2.4.1 Voltage effect (Aatmeeyata, 2000)

Five different voltage experiments were done to study the effect of voltage in the recycling operation mode. The concentration ratio of C_t/C_o as a function of time is plotted in Figure 6.3.

From Chapter 5, it is known that higher voltage has higher filter coefficient λ . From Eq. 6-1, higher filter coefficient λ leads to higher HA removal. The final HA removal (120min) as a function of applied voltage is shown in Figure 6.4. It shows the linear relationship between HA removal and voltage and it is in agreement with the results in the single-pass operation mode. The slope is about 1.2(%) / V. Similar linear relationship between removal and voltage in other electrofiltration systems was also reported by researchers when investigating the relationship in deep-end filtration (Judd and Solt, 1989; Barker et al., 1991; Zhang et al., 2000) and cross-flow membrane filtration (Verbich and Grebenyuk, 1991). It is justifiable because HA removal depends on the electrophoretic velocity of HA particles and the velocity is directly proportional to electric strength.

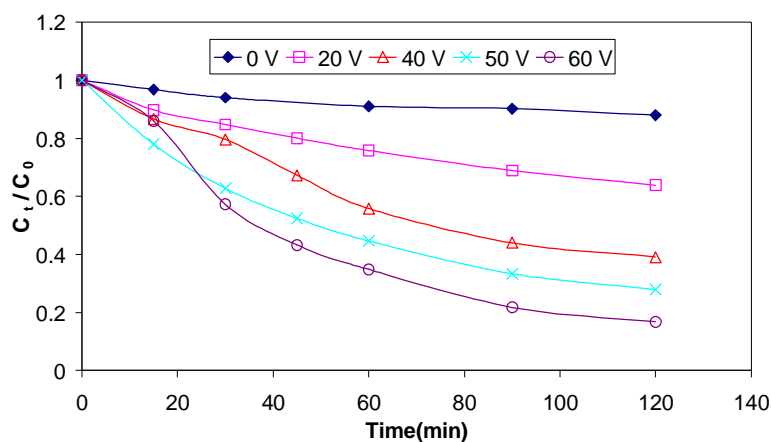


Fig.6.3 HA concentration ratio as a function of time for different voltage in a recycling operation mode (experimental conditions refer to Table 6.1)

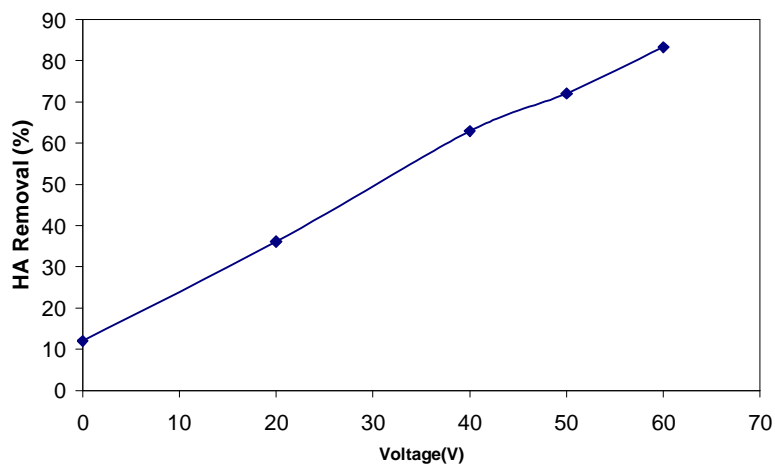


Fig.6.4 HA removal after 120 min as a function of voltage applied in the recycling operation mode (experimental conditions refer to Table 6.1)

However, the electrical energy consumed per mg of HA removed was different. It can be calculated using the following equation:

$$W = \frac{V \int_0^{\tau} i(t) dt}{\sum_0^{\tau} v_t \times \Delta C_t} \quad (6-2)$$

where W is electrical energy consumed per mg of HA removed (J/mg), V is voltage applied in the whole cell (V), $i(t)$ is the current at time t (A), v_t is the volume of solution in feed solution tank at time t (l), ΔC_t is the change of the concentration of HA in the feed solution tank between times t and $t + \Delta t$ (mg/l), τ is the total time for which the voltage was applied (min).

The total electrical energy consumed per mg of HA removed is presented in Fig. 6.5.

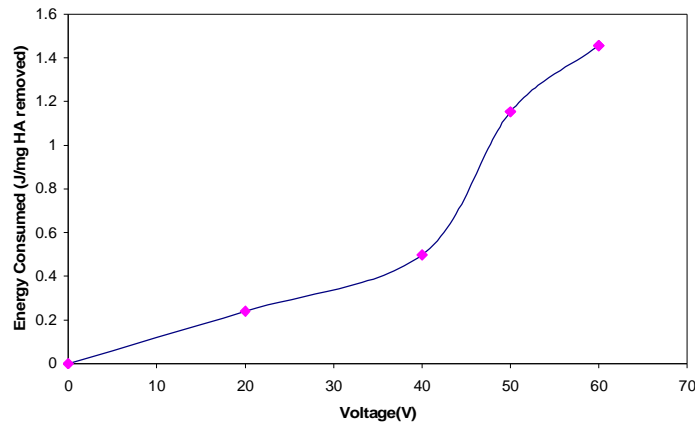


Fig.6.5 Total electrical energy consumed per mg of HA removed at different values of the applied voltage

It was observed that W increased as the applied voltage increased. But when the voltage was higher than 40 V, the increase rate was much faster. When the applied voltage was below 40 V, the electrical power was mainly consumed for removing HA. However, at higher voltage, electricity is wasted in the dissociation of water and electrolysis to produce hydrogen and oxygen gas in the electrode chambers. This can be confirmed by the current-voltage characteristics of the setup (see Fig.6.6). When the voltage is higher than 40V, the resistance decreases and the current increases very quickly due to additional electrochemical processes.

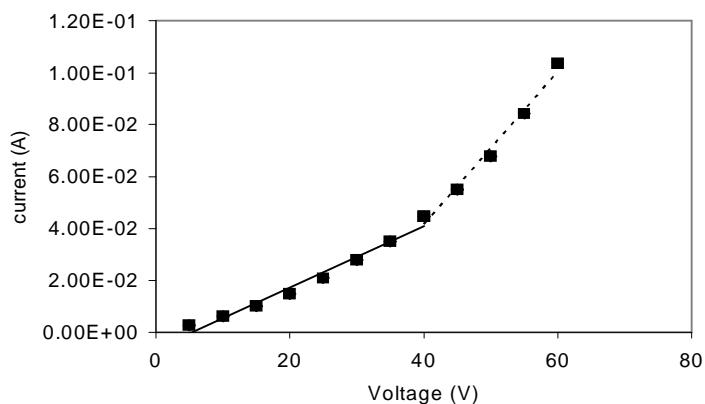


Fig. 6.6 Variation of the current with the applied voltage across the module. The time interval between the 5 V step change was 2 min.

6.2.4.2 Electrolyte concentration effect

Two experiments with different electrolyte concentrations (in the side chamber) were performed. The concentration ratio as a function of time is shown in Figure 6.7. It seems that there is no obvious effect on HA removal. The result is consistent with Figure 6.8. Higher Na_2SO_4 concentration has no clear effect on circuit current. Thus the electric potential between two membranes is almost same and HA removal is also the same.

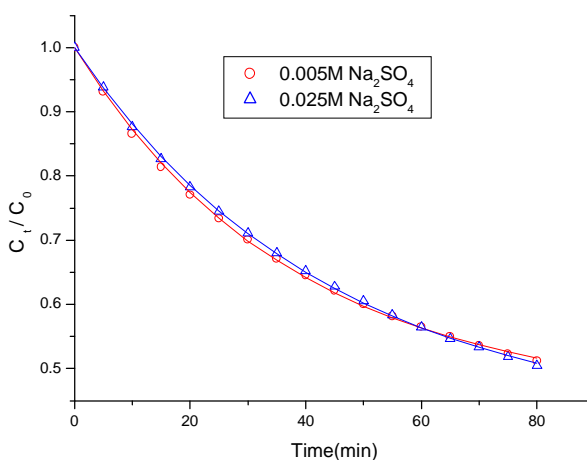


Fig. 6.7 HA concentration ratio as a function of time for different electrolyte concentration in the recycling operation mode (experimental conditions refer to Table 6.1)

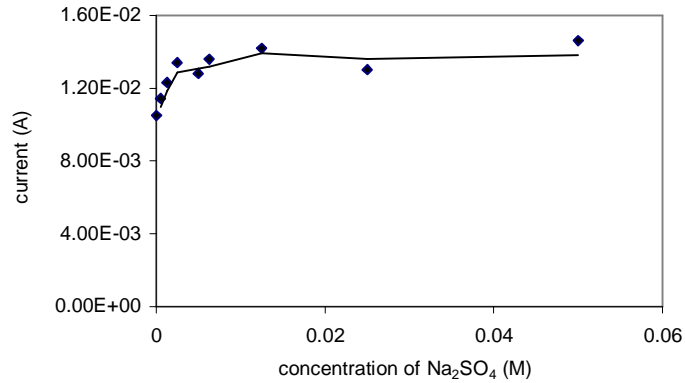


Fig.6.8 Current as a function of Na₂SO₄ concentration in the recycling operation mode with 40V (Aatmeeyata, 2000)

6.2.4.3 Flow rate effect (Aatmeeyata, 2000)

Two experiments were performed to study the effect of flow rate. HA solution was pumped at two different flow rates, 96 ml/min and 192ml/min, through the central chamber. The concentration ratio of HA for different flow rates is shown in Fig. 6.9. Higher flow rate enhanced the particles diffusion by reducing the thickness and resistance of external diffusion layer outside of resin surface. Thus at the beginning of the experiments, it led to higher HA removal for higher flow rate due to a decrease in resistance. However, higher flow rate played a negative role in determining the final HA concentration. Higher flow rate had higher drag force to desorb the deposited HA particles on the resin and membrane surfaces. Therefore flowrate had negative and positive effect on HA removal. Here the flow rate is higher and there is almost no difference for the above two flow rate. This result is in agreement with those in single-pass operation mode.

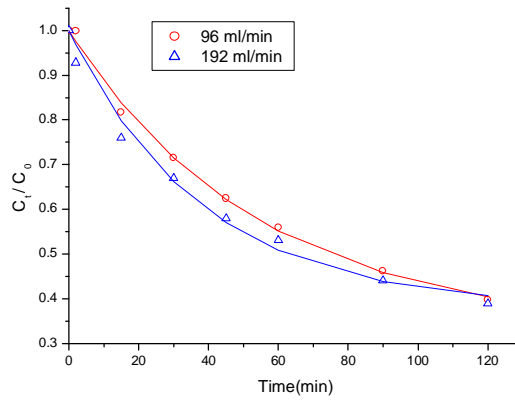


Fig.6.9 HA concentration ratio as a function of time for different flow rate in a recycling operation mode (experimental conditions refer to Table 6.1)

6.2.4.4 HA concentration effect (Aatmeeyata, 2000)

In order to find out the HA concentration effect on HA removal, experiments with initial concentrations of HA of 7.3, 14.3, 26 and 29.2 ppm were performed. The HA concentration ratio as a function of time is shown in Figure 6.10. It is clear that higher HA concentration leads to lower relative HA removal. This is in agreement with the result in single-pass operation mode. However, Fig.6.11 indicates that the total HA removed increased with increase of initial HA concentration.

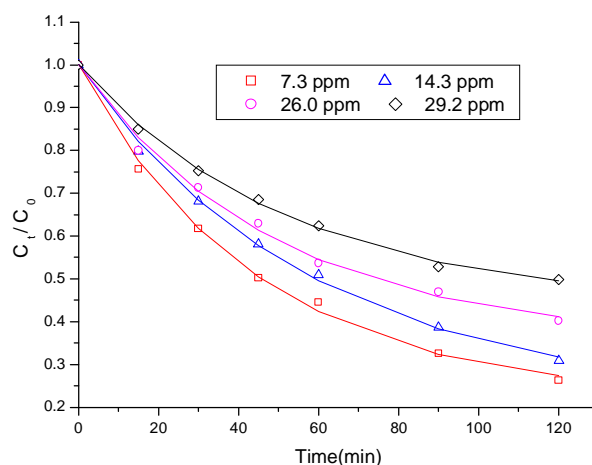


Fig.6.10 HA concentration ratio as a function of time for different initial HA concentration in a recycling operation mode (experimental conditions refer to table 6.1)

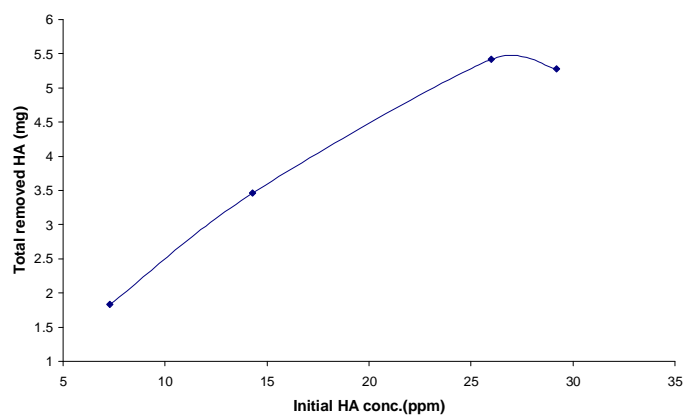


Fig.6.11 Total removed HA as a function of initial HA concentration in recycling operation mode after 120 min

6.2.4.5 pH effect

Three experiments with different pH (3.68, 6.23 and 10.90) were carried out. Sulfuric acid (H_2SO_4) and sodium hydroxide (NaOH) were used to adjust the pH of HA solution. The results are shown in Fig. 6.12. The results indicate that higher pH leads to higher HA removal in the recycling operation mode. Higher pH leads to much more negatively

charged HA particles due to ionizable function groups such as carboxylic and phenolic (Kim et al., 2002) and then leads to higher HA removal efficiency.

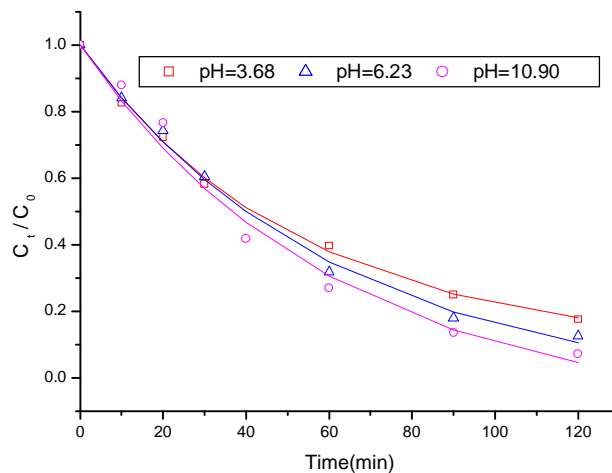


Fig. 6.12 HA concentration ratio as a function of time for different pH solution in recycling operation mode (experimental conditions refer to Table 6.1)

6.2.4.6 Ionic strength effect (Aatmeeyata, 2000)

Three experiments with different NaCl concentrations (0.0, 0.01 or 0.05 M) were performed. The result shown in Figure 6.13 demonstrates that higher NaCl concentration results in a lower HA removal after 80min which is in agreement with the results in single-pass operation mode. However the difference is not very evident.

6.2.4.7 Copper concentration effect

$\text{CuSO}_4 \cdot 5\text{H}_2\text{O}$ was added to HA solution to study the effect of Cu ion on HA removal. Figure 6.14 shows HA concentration ratio as a function of time for different Cu concentrations (0mM, 0.1mM and 0.5mM). It shows that the addition of copper ion could

decrease HA removal just like addition of NaCl. The result is in agreement with that in single-pass operation mode when the copper concentration is not very high.

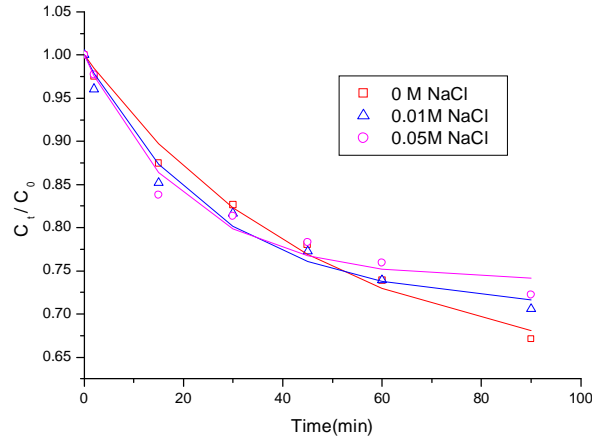


Fig. 6.13 HA concentration ratio as a function of time for different NaCl concentration in the HA suspension in a recycling operation mode (experimental conditions refer to Table 6.1)

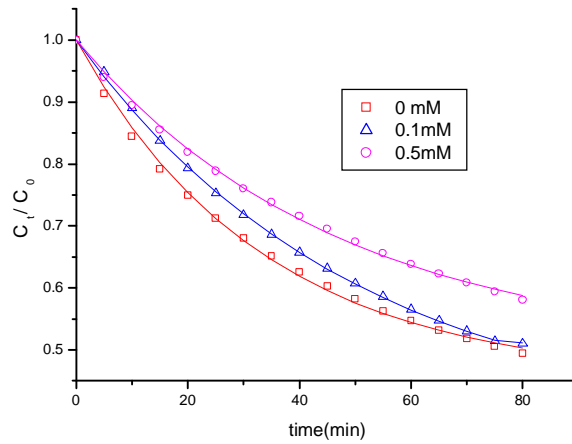


Fig. 6.14 HA concentration ratio as a function of time for different CuSO_4 concentration in a recycling operation mode (experimental conditions refer to Table 6.1)

6.3 Conclusions

Effect of different parameters on HA removal in the recycling operation mode for combination of AM+MR3+CM were studied. During the experiments, the pH of HA and electrolyte solutions both decreased. Higher voltage, lower HA concentration, higher pH, lower NaCl concentration and lower Cu^{2+} concentration in HA solution could lead to higher HA removal rate. Electrolyte solution concentration is not an important parameter when it reaches high concentration. Flow rate has double effect, one is positive and the other is negative on HA removal. All the experimental results have been physically explained. The process had a transient behavior and it did not reach steady state in our experiments. Furthermore, for every parameter, only a few set of experiments were carried. So there was not sufficient data to obtain a theoretical equation to analyze the kinetics.

Chapter 7

Summary and Recommendations

Hybrid electrodialysis/ion exchange is widely used in industry to produce ultrapure water. In our research, we aim to describe the applicability of this technology in separating and purifying biomaterials from aqueous solutions. In this thesis, humic acid removal from aqueous solutions is discussed.

Experiments for different combinations of ion exchange membrane and ion exchange resin were carried out to investigate the mechanism of HA removal. In the absence of voltage, hybrid electrodialysis/ion exchange can remove HA particles due to electrostatic attractive forces between HA particles and the surface of membranes and resins. Anion exchange resin and anion exchange membrane can remove HA more efficiently than cation exchange resin and cation exchange membrane. Thus the combination of AM+A550+AM is the most efficient one in removing HA. Its HA removal reaches about 60%. However, in the presence of applied voltage, it was found that the combination of AM+MR3+CM is the most efficient one considering the electric field effect (electrosorption). The HA removal due to electrosorption is about 52%. Initially the HA particles move faster under the applied electric field due to electrophoresis. When the HA particles come close to the gap between resin, the stronger local electric field induced due to the polarized resin makes the HA particles deposit on the resin surface. Secondly, the polarized HA particles due to dipole-dipole forces interact and form condensed sediment on the deposited HA particles on the resin surface. Thus the electric field greatly

enhances the HA deposition on the resin surface. When the electric field is switched off, the electric force and the dipole-dipole interaction disappear and thus the force balance of the HA particles breaks down. HA particles are carried away when a fluid flows through the central chamber. The amount of HA released depends on the properties of resins, membranes and the feed solution.

Different parameters effect on HA removal were studied in the single-pass operation mode, i.e. applied voltage, electrolyte concentration, flow rate of HA solution, HA concentration, pH of HA solution, ionic strength of HA solution and Cu^{2+} concentration in HA solution. For all experiments, the effluent HA concentration changed with time, which meant a transient behavior. HA removal was voltage dependent. Higher voltage led to higher HA removal. Lower flow rate of HA solution was desirable for HA removal. However, when flow rate was higher, the HA removal was almost same. HA removal increased with the increase of electrolyte concentration. When it was much high, the HA removal kept constant. Lower HA concentration, lower salt concentration resulted in higher HA removal. Neutral pH was favorable for HA removal in single-pass operation mode.

Recycling operation mode was also evaluated to study the effect of different parameters on HA removal. Similarly higher voltage, lower salt and HA concentrations led to higher HA removal. A suitable electrolyte concentration and flow rate are desirable in operation. Alkaline condition could remove HA much more efficiently, which was different from that in single-pass operation mode.

Aatmeeyata and others also did experiments on system regeneration, tannic removal, bioreactor waste removal. It was found that the technology could efficiently remove the particles from the aqueous solution and the system could be regenerated by switching off the power and acid washing. Thus we believe that this technology can be applied in future for other biomaterials such as proteins, enzyme, blood, coffee etc..

In future work, different materials may be used to do experiments. On the other hand, in order to optimize the technology, different membranes and resins should be applied. Furthermore, this technology can be developed to separate different biomaterial from their mixture.

References

- Aatmeeyata, An experimental study of electrofiltration of humic acid, Master Thesis, National University of Singapore, Singapore, 2000
- Amirbahman, A, Transportation of humic matter-coated colloids in packed beds, Ph.D. Thesis, University of California, Irvine, CA. 1994
- A.K.Sengupta, Ion Exchange Technology, Technomic Publishing Company, Inc., Lancaster, 1995
- A.I.Zouboulis, W.Jun, I.A.Katsoyiannis, Colloids and Surfaces A, 231(2003)181
- Bolto, G. A. Braun, D. Dixon, R. Eldridge, F. Frimmel, S. Hesse, S. King and M. Toifl, Wat. Sci. Tech., 40(1999)71
- Brattebo, H. Odegaard and O. Halle, Wat. Res., 21(1987)1045
- Bulletin No. AR 103, Ionics, Incorporated January 1997
- Bulletin No. CR 67.0, Ionics, Incorporated July 1990
- Bulletin No. CR 67.1, Ionics, Incorporated July 1990
- Childress, and M. Elimelech., J. Membr. Sci., 119(1996)253
- C.Goffin, J.C.Calay, Desalination, 132(2000) 249
- C.Tien, Granular Filtration of Aerosols and Hydrosols, Butterworth, Stoneham, 1989
- C. T. Anderson, and W. J. Maier, J. Amer. Water Works Assoc., 71(1979)283
- D.A. Lonergan, O.Fennemma, C.H.Amundson, J.Food Sci., 47(1982)1429
- D.H.Kim, S.H.moon, J.Cho, Desalination, 151(2002)11

- D.H.Kim, J.Cho, S.H Moon, Desalination, 151(2002)43
- Eikebrokk. Removal of Humic Substances by Coagulation. In Chemical Water and Wastewater Treatment, IV, ed by H. H. Hahn, E. Hoffman and H. Odegaard, Berlin/Heidelberg: Springer Verlag. 1996
- E.Dejean, E.Laktionov, J.Sandeaux, R.Sandaus, G.Pourcelly, C.Gavach, Desalination, 114(1997) 165
- E.J.Watkins, P.H.Pfromm, J. Membr. Sci., 162(1999)213
- E.Korngold, Desalination, 16(1975) 225
- E.Korngold,L.Aronov, O.Kedem, J.Membr.Sci., 138(1998)165
- E.Korngold, E.Korsoy, R.Rahav, M.F.Taboch, Desalination, 8(1970)195
- E. Matijevic, N.P.Ryde, J.Adhesion, 51(1995)1
- Fetting, J.Water Sci. Technol., 40(1999)25
- Fluka Chemika-Biochemika, # 53680, 725, 1993-1994
- F.Dimascia, A.Jha, G.C.Ganzi, F.Wilkins, United States Patent 6,514,398, Feb.4, 2003
- F.Helfferich, "Ion Exchange", Dover, New York, 1995
- Gaffney, N. A. Marley and S. B. Clark., ACS Symposium Series, No. 651, ed by J. S. Gaffney, N. A. Marley and S. B. Clark, Washington, DC: American Chemical Society. 1996
- G.Belfort, "Synthetic Membrane Processes", Academic Press, 1st edn., 1984
- G.Grossman, A.A.Sonin, Desalination, 10(1972)157
- G.Grossman, A.A.Sonin, Desalination, 12(1973)107

Hiemenz and R. Rajagopalan. Principles of Colloids and Surface Chemistry, 3rd edn., New York: Marcel Dekker. 1997

H.J.Lee, D.H.Kim, J.Cho, S.H.Moon, Desalination, 151(2002)43

H.J.Lee, J.H.Choi, J.Cho, S.H Moon, J.Membr.Sci., 203(2002)115

H.Katsumata, S.Kaneco, R.Matsumo, K.Itoh, K.Masuyama, T.Suzuki, K.Funasaka, K.Ohta, Chemosphere, 52(2003)909

H.M.Verbeek, L.Furst, H.Neumeister, Comput. Chem. Eng., 22(1998) S913

H.Rapp, P.H.Pfromm, J. Membr. Sci., 146(1998)249

H.Strathmann, J.Sep. Process Technol., 5(1984) 1

H.Strahmann, in: W.S.Winston Ho, K.K.Sirkar (Eds.), Membrane Handbook, Van Norstrand Reinhold, New York, 1992, 100

Jorgensen, Wat. Res., 13(1979)1239

Jucker and M. M. Clark, J. Membr. Sci., 97(1994)37

J.J. Krol, M.Wessling, H.Strathmann, J.Membr.Sci., 162(1999)145

J.P.Herzig, D.M.Leclerc, P. LeGoff, Ind. Eng. Chem. 62(1970)8

J.Wang, S.Wang, M.Jin, Proceedings of the Conference on Membranes in Drinking and Industrial Water Production, 2(2000) 665

J.Weida, L.Dong, Desalination, 54(1985) 197

Kabsch-Korbutowicz and T. Winnicki., Desalination, 105(1996)41

Kolle, Humic Acid Removal with Macroreticular Ion Exchange Resins at Hannover., NATO Congress, 1979, Reston VA, USA

K.Salem, J.Sandeaux, J.Molenat, R.Sandeaux, Desalination, 101(1995) 123

L.H.H.Lionel, An experimental study of eletrofiltration of humic acid and bioreactor waste, Bachelor Thesis, National University of Singapore, Singapore, 2001

Livens, Env. Poll., 70(1991)183

Macko, The removal of organic waters from surface water supplies by anion exchange resins, Ph.D Thesis, University of Minnesota, Minneapolis, MN, USA, 1980

Meng, and T. C. Hung, Toxicol. Env. Chem., 64(1997)61

M.Balata, L.Cadonati, M.Laubenstein, G.Heusser, M.G.Giammarchi,R.Scardaoni, V.Torri, G.Cecchet, A.D.Bari, A.Perotti, Nucl. Instr. and Math. in Phys. Res. A 370(1996) 605

M.J.Collins, A.N.Bishop,P.Farrimond, Geochim.Cosmochim. Acta. 59(1995)2387

Nelson, W. R. Penrose, J. O. Karttunen and P. Mehlhaff., Env. Sci. Tech, 19(1985)127

N.S.S. Susan, Removal of humic acid from aqueous solution containing copper ions by eletrofiltration, Bachelor Thesis, National University of Singapore, Singapore, 2000

Nystrom, K. Ruohomaki and L. Kaipia., Desalination, 106(1996)79

O'Melia, W. C. Becker and K. K. Au, Wat. Sci. Tech., 40(1999)47

Odegaard,. B. Eikebrokk and R. Starhaug. Wat. Sci. Tech., 40(1999)37-46

O.Kedem, Desalination, 16(1975) 105

O.Kedem, Y.Maoz, Desalination, 19(1976) 465

P.B.Spoor, L.Koene, L.J.J Janssen, J. App. Electrochem., 32(2002)369

P.B.Spoor, L.Grabovska, L.Konene, W.R.T. Veen,L.J.J Janssen, Chem. Eng. J., 89(2002)193

P.B.Spoor, L.Konene, W.R.T. Veen,L.J.J Janssen, Chem. Eng. J., 85(2002)127

P.B.Spoor, L.Konene, W.R.T. Veen, L.J.J Janssen, J. App. Electrochem., 32(2002)1

P.B.Spoor, W.R.T. Veen, L.J.J Janssen, J. App. Electrochem., 31(2001)523

P.B.Spoor, W.R.T. Veen, L.J.J Janssen, J. App. Electrochem., 31(2001)1071

P. H. Boening, J. Amer. Water Works Assoc., 72(1980)54

P.Fletcher, T.Stephenson, S.Judd, Chem. Engng. Sci., 14(1994)2371

P.R.Johnson, N.Sun, M.Elimelech, Environ. Sci. Technol. 30(1996)3284

Ruohomaki, P. Vaisanen, S. Metsamuuronen, M. Kulavaara and M. Nystrom.,
Desalination, 118(1998)273

R.Audinos, J. Membr. Sci., 41(1989)115

R.Bai, X.Zhang, J.Colloid Interface Sci., 243(2001)52

R.Berrocal, Mchaveron, United States Patent 6,003,700 March 7,2000

R.Berrocal, Mchaveron, United States Patent 5,980,961 Nov.9,1999

R.E.Barker, R.R.Brunso, S.D.Clinton, J.S.Watson, Separations Technol., 1(1991)166

R.Messalem, Y.Mirsky, N.Daltrophe, G.Sveliev, O.Kedem, J.Membr.Sci., 138(1998)178

R.Simons, Electrochim.Acta, 2(1984) 151

Sato, Shin, United States Patent 6,565,726 May 20,2003

Singer, P., Wat. Sci. Tech., 40(1999)25

S.Judd, B.Jefferson, Membranes for Industrial Wastewater Recovery and Reuse,
(Elsevier, 2003)

S.J.Judd; G.S.Solt, Colloids Surf., 39(1989)189

S.J.Judd; G.S.Solt, Chem. Eng. Sci., 46(1991)419

S.V.Verbich, O.V.Grebenyuk, *Khimiya i Tekhnologiya Vody*, 12(1991)1059

S.Y.Lin, S.Y.Suen, *J.Membr.Sci.*, 204(2002)37;

S.Y.Suen, M.R.Etzel, *J.Chromatogr.A* 686(1994)179;

S.Zhang, R.B.H.Tan, K.G.Neoh, C.Tien, *J.Colloid Interface Sci.*, 228(2000)393

Thorten, T., *Wat. Sci. Tech.*, 40(1999)105

T.S.Arnarson, R.G.Keil, *Mar.Chem.*, 71(2000)309

V.A.Shaposhnik,N.N Zubets, B.E. Mill, I.P. Strigina, *Desalination*, 133(2001)211

V.A.Shaposhnik,N.N Zubets, I.P. Strigina, B.E. Mill, *Desalination*, 145(2002)329

V.A.Shaposhnik,N.N Zubets, I.P. Strigina, B.E. Mill, *Desalination*, 145(2002)329

V.D. Grebenyuk, L.Kh.Zhiginas, *Khimiya i Tekhnologiya Vody*, 2(1998)152

V.D. Grebenyuk, R.D.Chebotareva, N.A.Linkov, V.M.Linkov, *Desalination*, 115(1998) 255

V.K.Shahi, S.K.Thampy,R.Rangarajan, *Desalination*, 133(2001)245

V.Lindstrand, A.Jonsson, G.Sundstrom,*Desalinaiton*, 130(2000)73

V.Lindstrand, G.Sundstrom, A.Jonsson, *Desalinaiton*, 128(2000)91

W.R.Walters, D.W.Weiser,I.J.Marek, *Ind.Eng.Chem.*, 47(1955)61

W.Stumm, J.J.Morgan, *Aquatic Chemistry*. Wiley, New York, 1996, 1022pp

W.S.W. Ho, K.K.Sirkar, “*Membrane Handbook*”, Chapman & Hall, New York, London,1992

W.T.Hua, *Eletrofiltration of humic acid and tannic acid*, Bachelor Thesis, National University of Singapore, Singapore, 2002

W.Yuan, A.L.Zydney, Desalination, 122(1999)63

X.Zhang, R.Bai, J.Colloid Interface Sci., 264(2003)30

APPENDIX A

KINETICS OF HUMIC ACID REMOVAL IN A RECYLING OPERATION MODE

In Aatmeeyata's thesis(2000), it was demonstrated that the HA removal kinetics in recycling operation mode followed first order. This result can be derived mathematically. If we assume that the mass transfer coefficient in the central chamber is k , in the steady state the concentration profile along the chamber is described as the following equation:

$$u \frac{dC}{dZ} = -kC \quad (A-1)$$

where v is the linear velocity of solution in the central chamber, C is the concentration of HA in the solution; Z is the distance from the inlet of the central chamber.

For a single pass experiment, when it reached the steady state, the HA concentration at the outlet of the central chamber can be described as the following equation:

$$C_{out} = C_{in} \exp[-k(l/v)] \quad (A-2)$$

where C_{in} and C_{out} , respectively, are the HA concentration at the inlet and outlet of the central chamber, l is the length of the central chamber.

For the recycling operation mode, we also have:

$$-V_f \frac{dC_{in}}{dt} = Q_f (C_{in} - C_{out}) \quad (A-3)$$

where Q_f is the volumetric flow rate of HA solution, V_f is the volume of feed HA solution, C_{in} is same as the HA concentration C_t in the feed tank.

It was also assumed that the removal process is reversible. From Eq.A-2, Eq.A-3 and considering that when $t=0$, $C=C_0$, $t=\infty$, $C=C_\infty$, we get:

$$C_t - C_\infty = (C_0 - C_\infty) \exp \left\{ - \frac{Q_f \left(1 - \exp \left(\frac{-kl}{v} \right) \right)}{V_f} t \right\} \quad (A-4)$$

i.e.:

$$\frac{C_t}{C_0} = \frac{C_\infty}{C_0} + \left(1 - \frac{C_\infty}{C_0} \right) \exp \left\{ - \frac{Q_f \left(1 - \exp \left(\frac{-kl}{v} \right) \right)}{V_f} t \right\} \quad (A-5)$$

In this appendix, the kinetics of HA removal for different parameters are discussed based on the above equation.

A.1 Voltage

The experimental data for five different voltages can be fitted according to Eq. A-5 and the results are shown in the Figure A.1. It shows that the final HA concentration is 0.87409, 0.56521, 0.1439, 0.22139, 0.0433 for 0 V, 20V, 40V, 50V and 60V respectively. It means that higher voltage could lead to lower C_∞ except for 50 V and

could increase the binding capacity of the system. The kinetic coefficients are 0.0203 min^{-1} , 0.0142 min^{-1} , 0.0110 min^{-1} , 0.0213 min^{-1} and 0.0184 min^{-1} respectively.

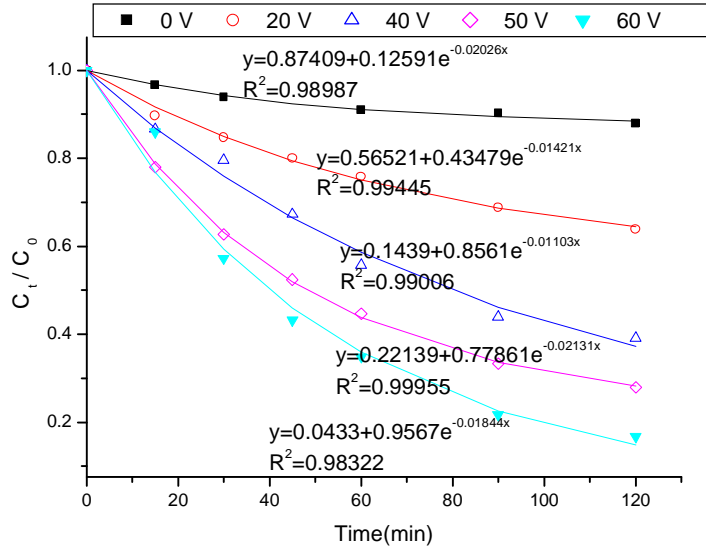


Fig.A.1 Kinetics of HA removal for different voltages in the recycling operation mode

A.2 Electrolyte concentration

The data for two different electrolyte concentrations was fitted and is shown in Figure A.2. The final HA concentration is 0.45021 and 0.41312 respectively for 0.005M and 0.025M electrolyte solution. Higher electrolyte concentration leads to higher HA removal efficiency. Simultaneously the kinetic coefficient decreased from 0.0264 min^{-1} to 0.0227 min^{-1} .

A.3 Flow rate

Two different flow rates, 96 ml/min and 192ml/min were used. The experimental results are shown in Fig. A.3. It seems that the final normalized concentration for higher flow

rate is higher and the value is 0.38108. The final concentration for lower flow rate is 0.33219. It means that lower flow rate is desirable. The kinetic coefficients are 0.01857 min^{-1} and 0.0264 min^{-1} respectively for 96ml/min and 192ml/min.

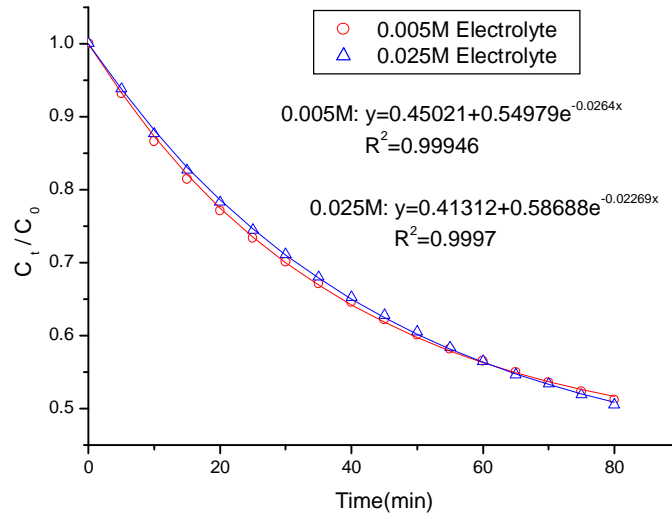


Fig.A.2 Kinetics of HA removal for different electrolyte concentrations in the recycling operation mode

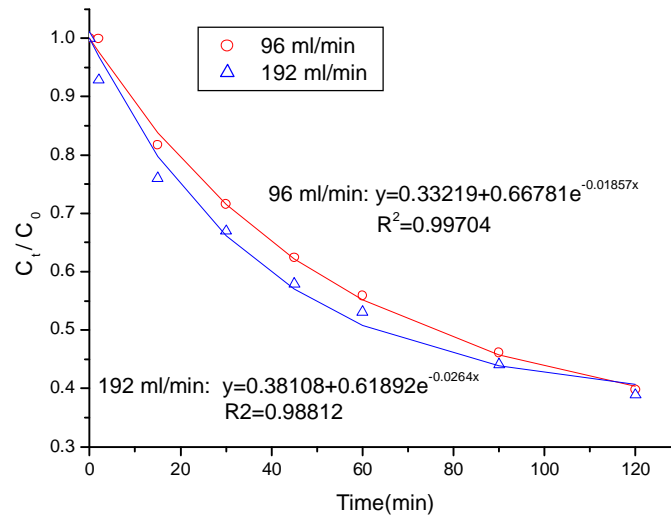


Fig.A.3 Kinetics of HA removal for different flow rates in the recycling operation mode

A.4 HA concentration

Experimental results and data fitting for four experiments with initial concentrations of HA of 7.3, 14.3, 26 and 29.2 ppm are shown in Figure A.4. The final concentrations are 0.22075, 0.22103, 0.35639, 0.43834 for initial HA concentration 7.3, 14.3, 26, 29.2ppm respectively. It is clear that higher HA concentration leads to lower HA removal efficiency. The kinetic coefficients are 0.0225 min^{-1} , 0.0174 min^{-1} , 0.0205 min^{-1} , 0.0191 min^{-1} respectively.

A.5 pH

Experimental results and the data fitting for different pH values are shown in Fig. A.5. The final HA concentrations are 0.09018, -0.04089 and -0.1108 for pH 3.68, 6.23 and 10.90 respectively. The negative sign of the concentration at high pH means that for negatively charged HA, the system can reach practically zero concentration. It also indicates that higher pH leads to a higher HA removal efficiency. The kinetic coefficients are 0.0192 min^{-1} , 0.0164 min^{-1} , 0.0164 min^{-1} for pH 3.68, 6.23 and 10.90 respectively.

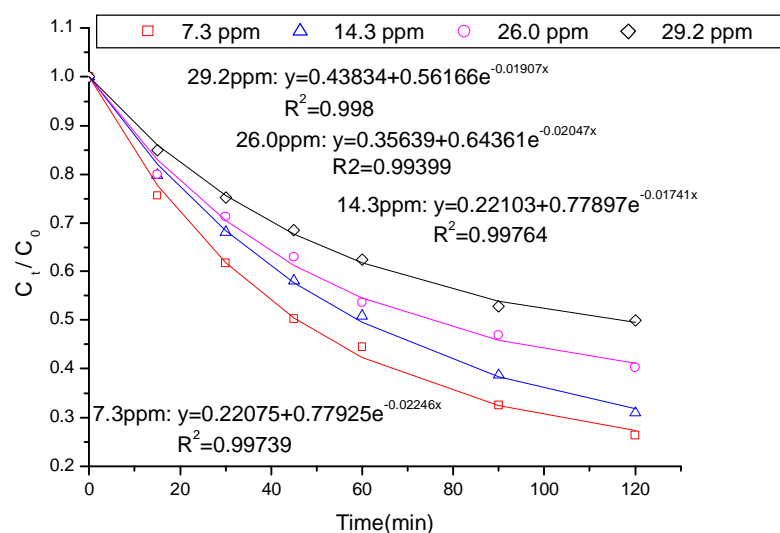


Fig.A.4 Kinetics of HA removal for different initial HA concentrations in the recycling operation mode

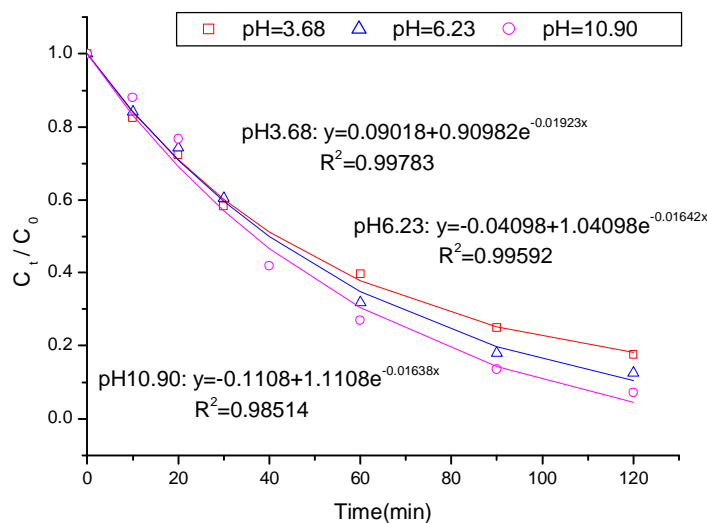


Fig.A.5 Kinetics of HA removal for different pH values in the recycling operation mode

A.6 Ionic strength

Experimental results for three different concentrations of NaCl (0.0, 0.01 or 0.05 M) and data fitting are shown in Figure A.6. The final HA concentrations are 0.63, 0.71 and 0.74 for 0.0, 0.01, 0.05M NaCl, respectively. It means that higher NaCl concentration results in

a lower HA removal efficiency. The rate coefficients are 0.0214 min^{-1} , 0.0375 min^{-1} and 0.0489 min^{-1} for 0.0, 0.01 or 0.05 M NaCl, respectively.

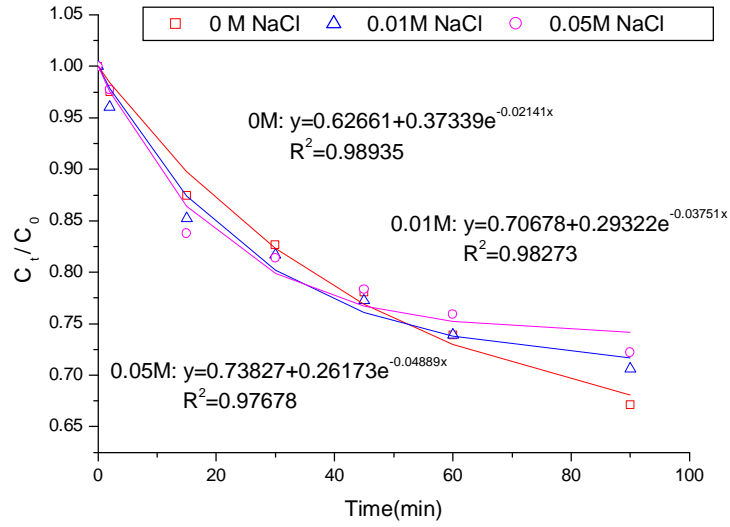


Fig.A.6 Kinetics of HA removal for different NaCl concentrations in the recycling operation mode

A.7 Conclusions

In summary, hybrid electrodialysis/ion exchange is a reversible process. It follows the first order kinetics. The equation can effectively describe the final concentration for different experiments.